

**Laser Scanning Aggregates for Real Time Property Identification**

FINAL REPORT

December 2016

Submitted by

Beena Sukumaran  
Professor  
Civil & Environmental  
Engineering  
Rowan University

Ravi Ramachandran  
Professor  
Electrical & Computer  
Engineering  
Rowan University

Michael Lim  
Professor  
Physics & Astronomy  
Rowan University



NJDOT Research Project Manager  
Pragna Shah

In cooperation with

New Jersey  
Department of Transportation  
Bureau of Research  
And

U. S. Department of Transportation  
Federal Highway Administration

## **DISCLAIMER STATEMENT**

“The contents of this report reflect the views of the authors who are responsible for the facts and the accuracy of the data presented herein. The contents do not necessarily reflect the official views or policies of the New Jersey Department of Transportation or the Federal Highway Administration. This report does not constitute a standard, specification, or regulation.”

TECHNICAL REPORT  
STANDARD TITLE PAGE

1. Report No. FHWA-NJ-2016-006	2. Government Accession No.	3. Recipient's Catalog No.	
4. Title and Subtitle Laser Scanning Aggregates for Real Time Property Identification		5. Report Date December 2016	
		6. Performing Organization Code	
7. Author(s) Beena Sukumaran Ph. D. Michael Lim Ph. D. Ravi Ramachandran Ph. D.		8. Performing Organization Report No.	
9. Performing Organization Name and Address Department of Civil Engineering, Rowan University 201 Mullica Hill Rd, Glassboro, NJ 08028		10. Work Unit No.	
		11. Contract or Grant No.	
12. Sponsoring Agency Name and Address  New Jersey Department of Transportation PO 600 Trenton, NJ 08625		13. Type of Report and Period  Final Report	
		14. Sponsoring Agency Code  Federal Highway Administration US Department of Transportation Washington, D. C. 20590	
15. Supplementary Notes			
16. Abstract The goal of this project is to develop a portable system for determining the mineralogical composition of aggregates in the field for quality control. Laser Induced Breakdown Spectroscopy (LIBS), which involves firing a laser pulse at a sample to determine its composition from light spectra emitted and interpreted using a spectrometer and a custom program, was chosen to be the basis of the portable system. Along with system development, results were analyzed via Partial Least Squares Regression (PLSR). The current analysis technique utilizes split-training and y-scaling to analyze spectra data and performs well for most samples. The results obtained from the LIBS system was compared with X-ray Fluorescence (XRF) data provided by the NJDOT.			
17. Key Words Aggregate Mineralogy, Material Testing, Laser Technology, LIBS, PLSR, Deployable MATLAB software, Real time testing, Portable equipment		18. Distribution Statement	
19. Security Classification (of this report) Unclassified	20. Security Classification. (of this page) Unclassified	21. No of Pages: 77	22. Price

## ACKNOWLEDGEMENTS

The authors wish to thank New Jersey Department of Transportation Research project manager Pragna Shah and Ed Kondrath and the Research Bureau staff for their administrative support for the duration of the research project. The authors would also like to thank the NJDOT customers, Ryan Rathbun and Paul Hanczaryk for providing the data required for calibration and valuable end-user input throughout the project. The authors would also like to extend a special thanks to the following members of the research team for their tireless efforts in ensuring the successful completion of this project. The graduate students require a special note of appreciation for their diligent and hard work on the research project.

Graduate Students, Civil and Environmental Engineering, Rowan University

*Andrew Branin, Bless Ann Varghese*

Undergraduate, Civil and Environmental Engineering, Rowan University

*Gary Liedtka-Bizuga, Jake Schwartz, Steven Buzby, Seth Wagner*

Undergraduate, Electrical and Computer Science Engineering, Rowan University

*Christine Neppel, Saima Mahmud, Josh Edwards, Traz Daczkowski, Christian Heimlich*

Undergraduate, Chemical Engineering, Rowan University

*Edward Freisinger*

Undergraduate, Physics Department, Rowan University

*Jesse Michael Kosior, Daniel John Banker*

## TABLE OF CONTENTS

	Page
EXECUTIVE SUMMARY.....	1
INTRODUCTION.....	2
OBJECTIVES.....	2
LITERATURE REVIEW.....	3
Current Chemical Testing Methods.....	3
<u>Wet Chemical Analyses</u> .....	3
<u>Inductively-Coupled Plasma – Mass Spectrometry (ICP-MS)</u> .....	3
<u>X-ray Fluorescence (XRF) Spectrometry</u> .....	3
An Introduction to LIBS.....	4
Laser Operation.....	5
Applications of LIBS.....	6
<i>NY State DOT</i> .....	7
<i>KSDOT</i> .....	7
<i>TXDOT</i> .....	7
<u>Other Noteworthy Applications</u> .....	7
Advantages and Disadvantages of Using LIBS for Geological Materials.....	8
<u>Advantages of Using LIBS for Geological Analyses</u> .....	8
<u>Disadvantages of Using Libs</u> .....	8
EXPERIMENTAL SETUP AND PROCEDURE.....	10
Experimental Laboratory Setup.....	10
Portable Laser.....	12
Laser Analysis Tool.....	13
Data Collection.....	13
<u>Calibration Set</u> .....	13
<u>Testing Set</u> .....	15
RESULTS AND DISCUSSION.....	15
Data Analysis and Interpretation.....	16
Data Preprocessing Techniques.....	17
Y Scaling.....	17
Split Training.....	18
Combined Method Model .....	18
<u>Split Training with Y-Scaling</u> .....	19
Classification Methods.....	21
<u>One-Dimensional Classification</u> .....	21
<u>Two-Dimensional Line Classification</u> .....	24
<u>Two-Dimensional Ratio Classification</u> .....	28
<u>Three Way Split Classification</u> .....	31
Accuracy of Models.....	35
<u>ANOVA (Analysis of Variance)</u> .....	36
<i>ANOVA for Various PLSR Models</i> .....	36
<i>ANOVA for Various Classifications</i> .....	38
High Pass Filter of LIBS Spectrum.....	40
<u>Moving Average Subtraction (MAS)</u> .....	40
<u>Moving Slope Analysis (MSA)</u> .....	41

	<b>Page</b>
<b><u>Frequency cut off and slope detection</u></b> .....	44
<b>Determination of a suitable sample size</b> .....	45
<b>Development of a User-Friendly Program</b> .....	45
<b>Portable Equipment Testing</b> .....	47
<b><u>Vibration/ Impact Testing</u></b> .....	47
<b><u>Temperature Testing</u></b> .....	48
<b><u>Sample Moisture Content Testing</u></b> .....	50
<b><u>Testing of Affordability of the equipment</u></b> .....	51
<b>CONCLUSIONS</b> .....	52
<b>REFERENCES</b> .....	54
<b>APPENDIX A</b> .....	55
<b>APPENDIX B</b> .....	58

## LIST OF FIGURES

	<b>Page</b>
Figure 1. Typical LIBS Setup	4
Figure 2. Laser Apparatus	6
Figure 3. Energy Graph	6
Figure 4. Experimental Setup	11
Figure 5. Experimental Setup - Sample Chamber	11
Figure 6. Portable Laser Components	12
Figure 7. Portable Laser Equipment	13
Figure 8. Y-Scaling Results	17
Figure 9. Split Training Set Results	18
Figure 10. SiO <sub>2</sub> Split Training, Y-Scaling Model Predictions	19
Figure 11. Al <sub>2</sub> O <sub>3</sub> Split Training, Y-Scaling Model Predictions	19
Figure 12. Fe <sub>2</sub> O <sub>3</sub> Split Training, Y-Scaling Model Predictions	20
Figure 13. CaO Split Training, Y-Scaling Model Predictions	20
Figure 14. MgO Split Training, Y-Scaling Model Predictions	21
Figure 15. Classification of rocks based on CaO%	22
Figure 16. Results of SiO <sub>2</sub> using Calcium Oxide classification.	22
Figure 17. Results of Al <sub>2</sub> O <sub>3</sub> using Calcium Oxide classification.	23
Figure 18. Results of Fe <sub>2</sub> O <sub>3</sub> using Calcium Oxide classification.	23
Figure 19. Results of CaO using Calcium Oxide classification.	24
Figure 20. Results of MgO using Calcium Oxide classification.	24
Figure 21. Classification of rocks based on the threshold line.	25
Figure 22. Results of SiO <sub>2</sub> using Line classification.	26
Figure 23. Results of Al <sub>2</sub> O <sub>3</sub> using Line classification.	26
Figure 24. Results of Fe <sub>2</sub> O <sub>3</sub> using Line classification.	27
Figure 25. Results of CaO using Line classification.	27
Figure 26. Results of MgO using Line classification.	28
Figure 27. The classification of rocks based on the threshold ratio of 3	29
Figure 28. Results of SiO <sub>2</sub> using Ratio classification.	29
Figure 29. Results of Al <sub>2</sub> O <sub>3</sub> using Ratio classification.	30
Figure 30. Results of Fe <sub>2</sub> O <sub>3</sub> using Ratio classification.	30
Figure 31. Results of CaO using Ratio classification.	31
Figure 32. Results of MgO using Ratio classification.	31
Figure 33. The classification of rocks based on the Ratio Square method.	32
Figure 34. Results of SiO <sub>2</sub> using Ratio Square classification.	33
Figure 35. Results of Al <sub>2</sub> O <sub>3</sub> using Ratio Square classification.	33
Figure 36. Results of Fe <sub>2</sub> O <sub>3</sub> using Ratio Square classification.	34
Figure 37. Results of CaO using Ratio Square classification.	34
Figure 38. Results of MgO of Ratio Square classification.	35
Figure 39. ANOVA results of various models for Carbonates	37
Figure 40. ANOVA results of various models for trap rocks.	37
Figure 41. ANOVA analysis of various models for non-carbonates.	38
Figure 42. ANOVA results of various split training methods for Carbonates.	39

	<b>Page</b>
Figure 43. ANOVA results of various split training methods for Trap Rocks	<b>39</b>
Figure 44. ANOVA results of split training methods for Non-Carbonates.	<b>40</b>
Figure 45. Left to right: Unfiltered Atkinson Quartzite data, moving average of data, subtraction of data, subtraction of moving average from original data, filtered data adjusted to eliminate negative values.	<b>41</b>
Figure 46. Subtraction from MAS filtration method showing the moving average N=180 to best conserve relevant information.	<b>41</b>
Figure 47. left to right: unfiltered Atkinson Quartzite data, moving slope analysis data, showing preservation of intensity information, filtered data subtracted from unfiltered data leaving only the baseline	<b>42</b>
Figure 48. left to right: unfiltered Atkinson Quartzite data, moving slope analysis preserving data with slope $\geq$ 10, moving slope analysis preserving data with slope $\geq$ 100, moving slope analysis preserving data with slope $\geq$ 1000.	<b>42</b>
Figure 49. Comparing the output of the PLSR calculation of Atkinson Quartzite, error bars showing uncertainty of data with 95% certainty	<b>43</b>
Figure 50. Comparing the output of the PLSR calculation of Carbonate Dolomite, error bars showing uncertainty of data with 95% certainty	<b>43</b>
Figure 51. Comparing the output of the PLSR calculation of EI Hamburg Gneiss, error bars showing uncertainty of data with 95% certainty	<b>43</b>
Figure 52. High Pass Filtering of LIBS spectrum	<b>44</b>
Figure 53. Results of High Pass Filtering of LIBS spectrum	<b>45</b>
Figure 54. Determination of Testing Set Size	<b>45</b>
Figure 55. Laser Data Analysis Tool	<b>46</b>
Figure 56. Update Calibration Tool	<b>47</b>
Figure 57. Vibration/ impact test results, Carbonate Dolomite	<b>47</b>
Figure 58. Vibration/ impact test results, Bechtelsville Gneiss 15179	<b>48</b>
Figure 59. Vibration/ impact test results, Plumstead Argillite Stockpile	<b>48</b>
Figure 60. Temperature Testing, Carbonate Dolomite	<b>49</b>
Figure 61. Temperature Testing Results, Plumstead Argillite Stockpile	<b>50</b>
Figure 62 LIBS spectrum obtained at 34 deg. F.	<b>50</b>
Figure 63. LIBS spectrum obtained at 68 deg. F. (laboratory condition)	<b>50</b>
Figure 64. Sample moisture content testing results, Carbonate Dolomite	<b>51</b>
Figure 65. Sample moisture content testing results, Plumstead Argillite Stockpile	<b>51</b>
Figure 66. Testing of the equipment using lower resolution spectrums	<b>52</b>

## **LIST OF TABLES**

	<b>Page</b>
Table 1. Aggregates used for calibration	<b>14</b>
Table 2. Outliers of One-Dimensional Classification	<b>21</b>
Table 3. Outliers of Two-Dimensional Line Classification	<b>25</b>
Table 4. Outliers of Two-Dimensional Ratio Classification	<b>28</b>
Table 5. Outliers of Three-Way Split Classification	<b>32</b>
Table 6. R Square values of each method against each compound	<b>35</b>
Table 7. R Square values of Carbonates, Trap Rocks and Non-Carbonates for various split training methods.	<b>36</b>



## **EXECUTIVE SUMMARY**

The contents of this report provide information regarding a study conducted for the New Jersey Department of Transportation (NJDOT) to utilize Laser-Induced Breakdown Spectroscopy (LIBS) to quantify problematic minerals in aggregate stone. LIBS is a chemical analysis technique, which involves firing a laser pulse at a sample to ablate material and excite atoms in the melted mass. The light emitted by the resulting plasma is then used to identify and quantify the sample's chemical composition. Overall, LIBS appears to be an attractive alternative to conventional chemical testing, offering accurate and relatively rapid results with little to no sample preparation. LIBS has been used to obtain typical light spectra from pure samples of metals, mica, limestone and aggregates of known composition provided by the NJDOT to properly calibrate the system for future use. The research team has developed a series of predictive models for quantifying compounds within aggregate samples. Current testing utilizes an Applied Spectra LIBS system, and data analysis is performed via Partial Least Squares Regression Analysis (PLSRA) to develop predictive models based on the spectra produced by aggregate samples with a known composition. Initially, predictive models were not accurate; however, adjustments to data collection procedures and pre-processing have significantly improved the accuracy and overall reliability of these models. A user friendly Graphical User Interface (GUI) has also been developed for visualizing the results. A portable LIBS unit has also been developed so that it can be used in the field. As a result, mineralogical composition of aggregates can be obtained in the field using the portable apparatus in a short duration.

## **INTRODUCTION**

This research project is a strong and bold partnership between three different academic departments at Rowan University namely Civil Engineering, Electrical and Computer Engineering and Physics, to address a topic of prime importance for highway design and quality control, namely the mineralogy characteristics of aggregates, which can have a significant effect on the life and performance of the roadway.

As Chesner and McMillan (2012) report in an FHWA sponsored IDEA project, Laser Induced Breakdown Spectroscopy (LIBS) can provide real time aggregate properties such as Acid Insoluble Residue (AIR), freeze-thaw cracking susceptibility (D-cracking) and Alkali Silica Reactivity (ASR). This requires bombarding aggregates with a medium to high energy laser pulse so that up to 13,000 wavelengths of subsequent optical emission can be obtained, which can then be used as a unique identifier to determine aggregate characteristics such as AIR, freeze-thaw susceptibility and ASR by determining the aggregate mineralogy. This requires significant data processing, Partial Least Squares Regression Analysis (PLS) and Principal Component Analysis (PCA). PCA aims to determine patterns in a set of large data that is obtained using the LIBS technique, to reveal similarities and differences within the data. In a multi-dimensional dataset, PCA isolates important components of the data so that the numbers of dimensions analyzed can be reduced without losing valuable information. This allows the datasets to be handled more efficiently.

The research study investigates the application of laser technology for real time aggregate property determination that can be performed in the field and laboratory to yield relevant data quickly, so that aggregate quality control can be undertaken in a timely and cost efficient manner. Laser Induced Breakdown Spectroscopy is utilized for this study in combination with data preprocessing and Partial Least Squares Regression Analysis.

## **OBJECTIVES**

This study focused on the development of a portable tool for the in-situ characterization and quality control of aggregates using laser analysis. The primary objectives of this research are as follows:

1. To obtain the characteristic laser spectra models for various aggregate sources from New Jersey and surrounding areas;
2. To calibrate the model using laser spectrums of newly added rocks to identify real time aggregate properties such as mineralogy;
3. To determine if the field and laboratory setup produce consistent results;
4. To improve the accuracy of the results with the expanded calibration dataset;
5. To develop a user friendly program for rapid analysis of laser spectra with batch capability and for future refinement of the models as new stones are added;
6. To determine the feasibility of laser technology as a portable tool for identification of real time aggregate mineralogy;
7. To determine the feasibility and affordability of laboratory based laser technology applications for field use;
8. To field test the use of lasers for real time property identification;

9. To demonstrate the use of laser technology in the field for aggregate property determination and as a means of quality control;
10. To develop a user friendly manual for operation and regular maintenance of the portable laser setup; and
11. To train New Jersey Department of Transportation (NJDOT) personnel in the use of the laser technology.

## **LITERATURE REVIEW**

This study intends to utilize LIBS to analyze the mineralogy of aggregates in the field. An overview of previous research and applications are described in the following sections, as well as an overview of conventional techniques employed by NJDOT and elsewhere for determination of mineralogy of aggregates.

### **Current Chemical Testing Methods**

Current techniques for analyzing the chemical composition of aggregate samples include Wet Chemical Analyses, Inductively Coupled Plasma – Mass Spectrometry (ICP-MS), X-ray Fluorescence (XRF) Spectrometry, and Electron Microprobe Analysis.

#### **Wet Chemical Analyses**

Wet Chemical Analyses were used exclusively prior to 1960, and each involves dissolving a powdered sample in an acid. The analyses include: Gravimetric Analyses, Volumetric Analyses, and Colorimetric Analyses. Gravimetric Analysis is a technique in which the amount of a substance is determined by reacting the dissolved sample with a chemical and measuring the mass of precipitate produced. Volumetric Analysis involve using titration to determine the amount of a chemical to be added to completely react with a certain substance in a sample, which can then be used to determine the substance's concentration in the sample. Colorimetric Analysis involves adding a solution, which will react and produce a color change in the dissolved sample, and determining the concentration based on the intensity of color. Both these techniques are still used, but both of them require sample preparation, laboratory analyses, and results will not be obtained in real-time.

#### **Inductively-Coupled Plasma – Mass Spectrometry (ICP-MS)**

ICP-MS involves injecting an acid-dissolved sample as an aerosol into Argon plasma to break the dissolved sample into separate ions, which are then extracted by a mass spectrometer in a vacuum, which separates the particles per their mass and charge. The results are determined relative to standard solutions with known concentrations. Alternatively, a small portion of the sample material may be ablated via laser before injecting it into the Argon plasma. This technique can be used but requires significant time to prepare the samples and results cannot be obtained instantaneously.

#### **X-ray Fluorescence (XRF) Spectrometry**

XRF Spectrometry is often used in the analysis of stone samples, but typically involves testing a compressed or vitrified powdered sample in solid form. This analysis is performed by directing a X-ray beam at a sample to induce dissociation of inner shell electrons. As outer shell electrons drop to the inner shell, X-ray beams of characteristic wavelengths are emitted and collected by a

variety of sensors. The intensities of a given emitted wavelength can be correlated to concentrations; however, a large number of separate standards are required to determine and account for all of the interfering effects. Electron Microprobe (EMP) Analysis operates on the same principle, but uses a focused electron beam rather than X-rays to induce electron dissociation, and requires different sample preparation. EMP analysis is generally used for very small parts of samples <sup>(5)</sup>. X-ray fluorescence can be used in many of the same fields and applications as LIBS. XRF analysis is generally complete and accurate, but measurements of elements lighter than sodium are typically very inaccurate. Its shortcoming is this form of analysis has not proven itself useful for identifying isotopes or ions in varying valence states. Throughout this research, accepted values for aggregate composition in this research are obtained from XRF analyses. XRF analyses also require sample preparation and results cannot be obtained in the field but requires that the samples be brought back to the laboratory for further analyses.

### Introduction to LIBS

The focus of this study is to develop a system which accurately determines the mineralogy of aggregates via LIBS in the field. The basic concept of LIBS involves firing a pulse laser at an aggregate sample, using a spectrometer to determine the intensities of light emitted at various wavelengths by the resulting plasma, and determining the ablated material's composition based on the results (Figure 1).

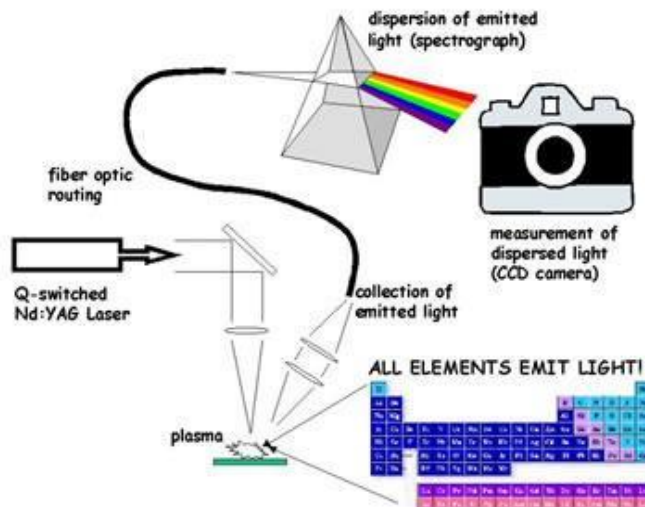


Figure 1. Typical LIBS Setup <sup>(14)</sup>

LIBS is a technique used for rapid chemical analysis. The process includes directing a short, high power laser pulse at a compound which can be either a solid, liquid, or gas. When the material is bombarded by very high intensities of light from the laser pulse, the atoms and their electrons become excited. This excitation vaporizes the material, breaks the molecular bonds in the material, and ionizes the atoms as excited electrons dissociate from the atoms, forming plasma. The free electrons will recombine with the ions after the plasma cools sufficiently. As the excited electrons drop to normal energy levels, they emit photons of wavelengths, which are specific to the element in question. Other species of the elements, i.e. ions, may emit different wavelengths of light than their neutral counterparts as their electrons drop to lower energy states. Neutral elements are stated as the element symbol, followed by a roman numeral I, once ionized atoms are denoted with a roman numeral II, and so forth. For example, neutral oxygen is denoted as O(I), while once ionized

oxygen is denoted as O(II). The light emitted by the electrons falling to their ground state is collected, and split by a spectrometer into its various wavelengths. The relative intensity of light collected for each wavelength is plotted as a spectrum for the sample. The resulting spectrum will be the sum of the spectra for all elements and species in the sample <sup>(2)</sup>. The relative quantities of each element can be determined based on the intensities of the wavelengths collected as well as the distribution of neutral atoms and various ions, as determined by various parameters <sup>(9)</sup>. However, as the light collected during this study's tests will be late in the plasma glow, the resulting light spectrum will be emitted almost entirely by neutral particles, which helps to simplify analysis, as will be discussed later.

Spectrum lines of interest for a particular element or set of elements comprising a material or mineral can be isolated and related to samples of known composition, which can then be used to predict the quantity of a material of interest in unknown samples. For the purposes of this study, Partial Least Squares Regression; which does not require the explicit identification of related peaks, will be used to determine the relative quantity of compounds within aggregates, which can be compared to mandated limits to ensure compliance with limitations. This should reduce the need for conventional chemical testing <sup>(2)</sup>.

### **Laser Operation**

This study utilizes a Nd: YAG Laser (Figure 2) for LIBS analysis of aggregate particles. The way that a pulse laser functions is described below.

1. An Ultraviolet flash lamp activates, exciting the particles in the Gain Medium. In the case of the laser used, the Gain Medium is a Neodymium ion doped Yttrium Aluminum Garnet crystal. Note that the system used in this study flashes for 8 seconds at 10 Hz before being ready to fire.
2. Stimulated Emission occurs, wherein an emitted photon from one excited particle can stimulate other excited particles to emit photons of the same wavelength.
3. The Q-Switch, or Quality Switch blocks light emitted by the Gain Medium for an adjustable delay time, which regulates the power output of the laser.
4. When the Q-Switch opens, the light is permitted to pass through a partial mirror and is emitted as a laser pulse of uniform wavelength.
5. A spectrometer is synchronized to the Q-Switch, and light is collected from the plasma glow, split into various wavelengths, and the relative intensities of light collected are output as a spectrum.

Changing the time between when the flash lamp stimulates the particles and the Q-Switch opens will change the energy of the laser pulse (Figure 3). The longer the delay time, the less energy is emitted. The resulting spectrum shows the different wavelengths emitted from the sample being struck by the laser. Note that trace elements may not be represented in the results for lower energy shots, as they may not be able to be distinguished from baseline light. Changing the Q-switch delay time gradually identifies the optimum level of energy required to identify each element clearly <sup>(6)</sup>.

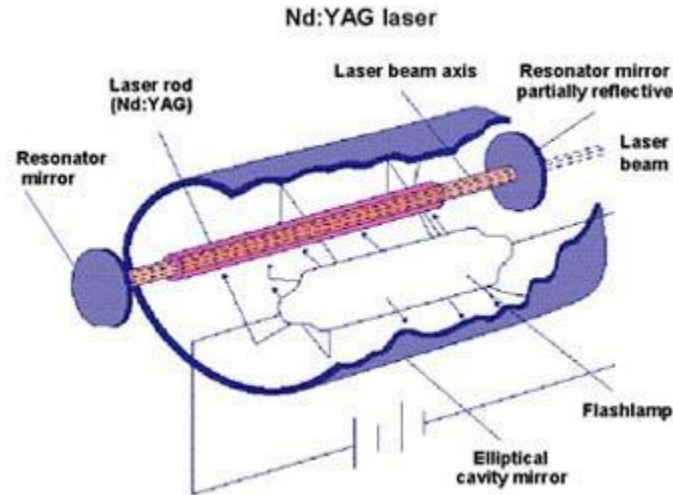


Figure 2. Laser Apparatus <sup>(15)</sup>

LIBS analysis assumes that the system is in thermal equilibrium; however real cases may not necessarily reflect this <sup>(2)</sup>. Some studies suggest that utilizing a double pulse to heat the sample and more reliably achieve local thermal equilibrium before ablating the material will help to reduce the amount of plasma formed in the air <sup>(3)</sup>.

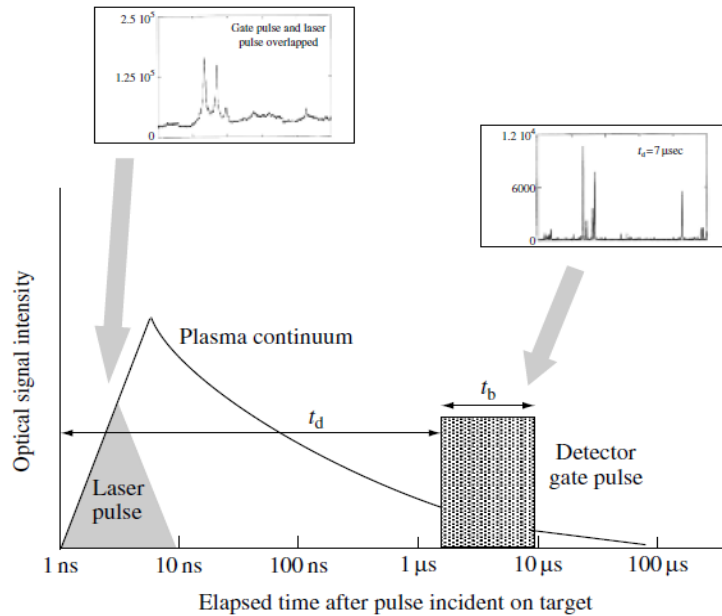


Figure 3. Energy Graph <sup>(2)</sup>

### Applications of LIBS

LIBS has been used as a means of quality control in several industries and fields, such as in the analysis of metals and alloys, analyzing water and soil contamination, archeological applications, pharmaceuticals and other medical applications, analysis of aerosols, military and forensic applications, as well as geological applications. The versatility of LIBS, from the Mars Rover to

industrial recycling, makes it a promising tool for this study. This study is limited to geological applications of LIBS.

***Previous study conducted by New York State Department of Transportation using LIBS***

The New York State Department of Transportation (NYSDOT) Materials Method 28 <sup>(1)</sup> imposes limits on the use of carbonate aggregates in asphalt and concrete; namely that a carbonate aggregate must contain at least 20% Acid Insoluble Residue (AIR), i.e. silicates, or that the aggregate must be blended into a mix containing at least 20 percent silicates. Chesner and McMillan utilized LIBS and created and calibrated a model utilizing PLSR, which predicts the AIR content of an aggregate sample <sup>(1)</sup>. Another model was created which determines the percent non-carbonated material in an aggregate blend. Both models performed reasonably well, with the percent AIR model achieving very high accuracy. It is worth noting however, that the NYSDOT models utilizes large calibration test samples.

***Previous study conducted by Kansas State Department of Transportation using LIBS***

The Kansas Department of Transportation (KSDOT) used LIBS to analyze the likelihood of D-Cracking and to identify the source quarry of an aggregate sample <sup>(1)</sup>. D-Cracking is a breakdown of aggregates, typically caused by freeze-thaw conditions. The KSDOT uses two test methods; the KTMR-21 and KTMR-22 tests, as a criterion for determining an aggregate blend. To identify a source bed, a model was developed to classify an aggregate sample based on a branching algorithm, which distinguishes an aggregate based on its spectrum meeting a unique criterion, or continuing to additional checks. A second model was generated to predict whether the aggregate would pass or fail the previously mentioned tests. The model predicted the result with perfect accuracy, indicating that a spectrum feature or features can be correlated to a susceptibility to D-Cracking.

***Previous study conducted by Texas State Department of Transportation using LIBS***

The Texas Department of Transportation (TXDOT) developed a three-model system to quantify the percent of reactive chert in an aggregate blend to classify the sample as highly reactive or not <sup>(1)</sup>. Chert is a type of silica, which is a major cause of Alkali Silica Reactive aggregates and can experience damaging expansion within the concrete. The first model resulted in very high accuracy in quantifying chert content in the testing set. Similar to the KSDOT's model, the second model was developed by regressing samples against a yes/no or pass/fail system. While the model incorrectly classified some individual spectrum, the model correctly classified aggregates when spectra were averaged. Individual sources of cherts were identified using a branching test model similar to the KSDOT, in which sources were differentiated based on a unique criterion <sup>(1)</sup>.

**Other Noteworthy Applications**

LIBS analysis can also be used for quality control of concrete. LIBS has been used to produce a depth profile of chloride and Sulphur contamination in concrete. Traditional chemical analyses are only capable of modeling such profiles with a resolution of 10 mm or more from drill dust, while LIBS analysis can be used to obtain a resolution of 1 mm. This allows one to more accurately determine the depth of these contaminants, thus mitigating the amount of acceptable concrete which is needlessly replaced; leading to more economical repairs. <sup>(8)</sup> LIBS may also be used as a means of quality control for cement powder. Calibration curves have been developed for

measuring Ca, Si, K, Mg, Al, Na, Ti, Mn, and Sr in samples of cement powder. This type of analysis is useful in cement manufacturing <sup>(4)</sup>.

LIBS has also shown to be promising for use in screening recycled concrete. LIBS could be used for three purposes: to identify large contaminants in a waste flow of demolished concrete, to control input and output flows for a system, and monitor for contaminants, such as high amounts of silicon in cement, or chloride or Sulphur contamination. This would allow such a system to reliably screen waste concrete for recycling <sup>(12)</sup>.

A study has also used LIBS in conjunction with an electron microscope to model the structure of surface micro cracks, and further research will investigate whether a similar technique can be applied to modeling the three-dimensional structure of such cracks <sup>(11)</sup>.

### **Advantages and Disadvantages of using LIBS for Geological Materials**

The use of LIBS for determining the composition of geological materials provides an alternative to time consuming chemical tests. Some studies suggest that LIBS may present a more complete analysis of a sample than can be obtained from chemical testing <sup>(7)</sup>, however the analysis also includes a number of sources of uncertainty.

#### **Advantages of using LIBS**

Using LIBS to analyze the mineral content of aggregates has several advantages over conventional chemical testing, such as XRF analysis.

- **Time Required for Analysis:** Chemical testing involves sending aggregate samples to a testing laboratory, and waiting a significant period of time to obtain results and begin working, while requiring significant sample preparation in the process, as is the case in XRF analysis. This study expects that by using LIBS to analyze the same aggregate samples, results of comparable accuracy or better can be obtained within 30 minutes, and be performed in the field with little to no sample preparation.
- **Cost of Analysis:** While a portable LIBS system will likely require a greater initial investment than conventional chemical testing, the apparatus requires only a source of electricity, as opposed to chemical testing which would incur significant testing costs.
- **Accuracy and Completeness of Results:** Because LIBS analysis represents all elements in a sample as spectrum lines, all components of a sample can be determined, including trace elements.
- **Portable LIBS systems** have previously been developed and shown to be viable for testing <sup>(7)</sup>.

#### **Disadvantages of using LIBS**

LIBS testing methodology can produce errors that an experimentalist should be aware of since it can adversely affect results; however, most of these sources of uncertainty can be corrected for or mitigated.

- **Plasma Opacity:** During the laser pulse, the plasma itself will absorb light from the laser, partially shielding the remaining material from the laser light. The plasma will also advance in the air towards the laser source, further shielding the material over the course of the laser pulse. This effect can be mitigated by utilizing a fast laser pulse (typical LIBS laser pulses are Nano- or femto-seconds in length.) The plasma will also shield part of the light emitted



by inner particles, which can skew the results. Accurate models and correct calibration curves will reduce the impact of this effect.

- **Incomplete Vaporization:** Plasma opacity, combined with the tendency for certain materials to ablate more easily than others may cause some material to be left behind after a laser pulse. This will cause inconsistency between subsequent pulses on a sample. Completely vaporized particles will also produce higher light intensities than would otherwise be observed. As in-situ testing will not be performed on powdered samples, sufficient sampling sizes will be used with short laser pulses to mitigate the impact of incomplete vaporization on the results.
- **Baseline Spectrum:** Background light will be included in the plasma spectrum, however conducting tests in a dark chamber will minimize this. The production of plasma in the air adjacent to the sample will also produce nitrogen and oxygen lines in the spectrum. During this study, these lines will be identified and subtracted from the spectra.
- **Stark Widening:** Local electric fields produced by the ionization of atoms in the plasma will cause slight variations in the wavelength of light emitted. This can be corrected by integrating a spectrum between the limiting wavelengths for a particular line to determine the total light intensity of a line. The effect of these local electric fields can also be mitigated by sampling light emitted by a cooler plasma; minimizing the presence of ionized particles in the plasma.
- **Accelerated Ionization:** The presence of free electrons can cause interactions in some particles, which will increase their likelihood of ionization. Ensuring a sufficient delay time will allow most of the free electrons to recombine with ions, so that the resulting spectrum will display lines primarily from neutral particles.
- **Chemical Matrix Effects:** Some elements ionize more readily than others, producing more free electrons to recombine with other elements, resulting in higher concentrations of neutral particles in other elements. As previously stated, collecting light from cooler plasma should mitigate these effects <sup>(2)</sup>.
- **Surface Conditions:** The roughness and pitting of a sample aggregate will affect the amount of material that is ablated by a laser pulse, which may skew results. A sufficiently large sample size should mitigate this effect. Dust or other surface contaminants may also be present on the aggregate samples. If it is determined that this significantly affects the quality of the results, the testing procedure may fire multiple pulses at a single point on each aggregate tested before reading the spectra to ensure that the majority of surface contaminants are ablated away before testing <sup>(1)</sup>.

It is also worth noting that some studies suggest that the original molecule's composition may have some influence on the wavelengths of light produced, however research on this phenomenon is still ongoing <sup>(1)</sup>.

Previous studies using LIBS have used a variety of data processing techniques, such as:

1. Artificial Neural Networks (ANN)
2. Soft Independent Modeling of Class Analogy (SIMCA)
3. Principle Component Analysis (PCA)
4. Partial Least-Squares Analysis (PLS)

From the methods provided above, ANN, PCA and Partial Least Squares Discriminant Analysis (PLS-DA) proved to be most effective when a large number of classes were analyzed. Partial Least Squares and Principle Components analyses were performed by the New York State, Kansas, and Texas Departments of Transportation to produce accurate predictive models and calibration curves for various aggregate traits and to categorize aggregates for various purposes <sup>(1)</sup>. In these analysis methods, the data projections were produced by applying linear algebraic techniques on sample data arrays. By reducing the number of data dimensions, visual relationships between the variables and quantitative analyses are simplified.

PCA can be used to visually determine whether properties in a sample can be differentiated relative to various collected data features. PLS can be used to produce a model which predicts quantities and traits in a manner similar to Multiple Linear Regression, however instead of minimizing square error, coefficients are determined by maximizing the covariance between a set of collected independent variables; in this case light intensity at various wavelengths, and known values, such as mineral concentration. Utilizing a larger number of samples and selecting samples for the training model which represent a wide range of possibilities will improve the reliability of the resulting model. Sample traits and quantities of substances in unknown samples can then be determined based on the predictive model and its reliability determined by comparing predictions to known values. This study uses PLS regression analysis to quantify the concentration of various minerals present in aggregate samples <sup>(1)</sup>. This method was selected due to its relative simplicity in calculating predicted values from input data and an established model, as well as due to the success of other state Departments of Transportation in applying this technique to similar applications. As each prediction can be made as a linear combination of normalized light intensities and coefficients, a predicted value for each compound or mineral can be calculated independently. As the procedure for developing a model using PLS is quite involved, it will not be explored in detail in this report.

## **EXPERIMENTAL SETUP AND PROCEDURE**

### **Experimental Laboratory Setup**

The experimental setup is shown in Figures 4 and 5. Additionally, a modified procedure was developed and is explained below. After the flashlamp is activated, the system will trigger and the laser is fired. When the laser's Q-switch opens, an electric pulse is sent along a Bayonet Neill–Concelman (BNC) cable to the spectrometer (4 on Figure 4(a)). When triggered, a laser pulse will exit the laser (1 in Figure 4(a)), and pass through a series of optics. To mitigate shot to shot variation, a relatively intense laser pulse is fired, and about 95 percent of the laser energy is then split off via a beam splitter (4 on Figure 4(b)) and directed to an energy sink (5 in Figure 4(b)).

The remaining light is directed through a series of optics within the sample chamber, which refocuses the laser and directs it downward at a steep angle toward the sample on the tray (3 in Figure 5), which has been previously positioned so that the sample is at the appropriate location and height. The Beam Splitter (Label 4 in Figure 5) rotates such that its tip will be positioned at the focal point, and the sample stage height is adjusted such that a sample comes in contact with the tip before it is moved away from the sample tray. Light emitted by the ablated mass reflects off the mirror (Label 2 in Figure 5) and is collected by a fiber optic cable, which is connected to each of the spectrometer's channel ports. The spectrometer then transfers the data it collects to the software in the laptop via a USB cable.

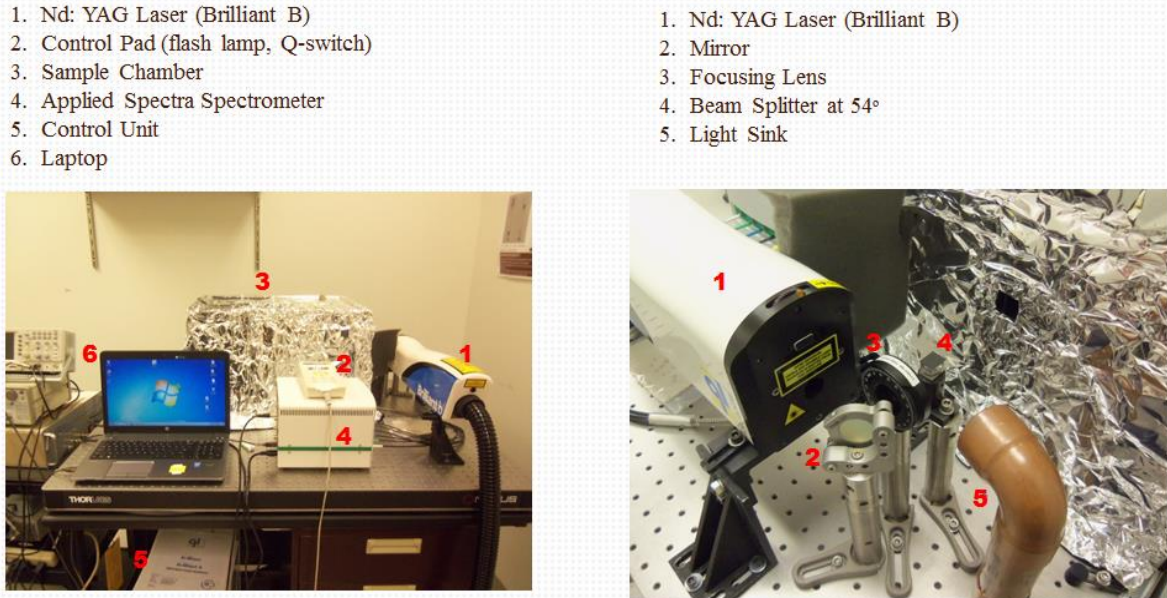


Figure 4. Experimental Setup

(a) Overall view of laser setup

(b) Close-up view of laser optics

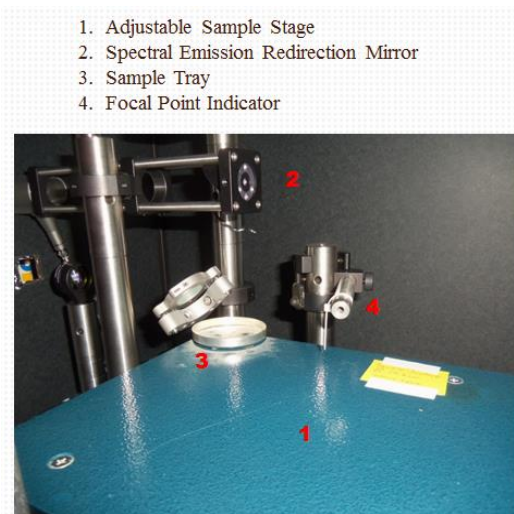


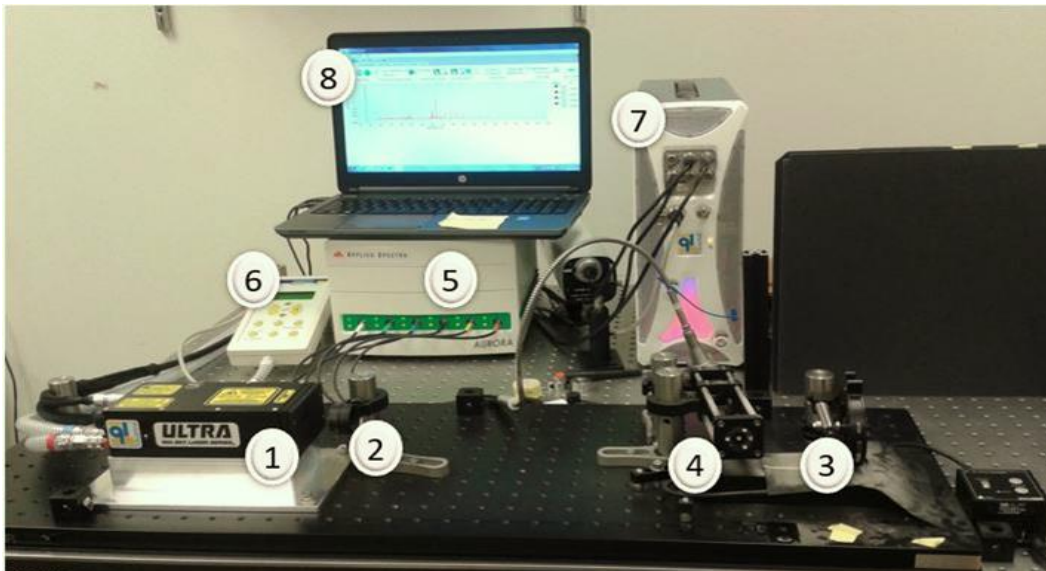
Figure 5. Experimental Setup - Sample Chamber

After the appropriate number of shots has been fired, the software will automatically prompt the user to save the data. An appropriate naming convention should be selected for the data files. Previous test files have names which include the date, type of stone sample, and the test number.

Previous tests have been conducted as a series of independent tests, to mitigate the effect of shot to shot variation, the 'Accumulate Data' option in the software is checked, and 100 shots are fired per sample, per location. This results in a single output spectrum per location which is the sum of the spectra from 100 shots. In the event of a low-emission shot, this additive data collection ensures that the overall trends and peaks in the output data remain largely unaffected. To conduct these tests in a timely manner, the *continuous fire* option on the laser is utilized rather than the single shot option. It was found that the software does not encounter issues when this option is utilized.

### Portable Laser

The portable system consists of several noteworthy components as shown in Figures 6 and 7. The Quantel ULTRA Laser emits laser light focused on the sample aggregate, which creates plasma at the surface of the material. The focusing lens concentrates the light from the laser onto a spot on the sample. This creates plasma that emits light that can be analyzed to determine the composition of the sample. The automatic adjustable sample holder keeps the sample aggregate in place and ensures that the sample can be placed exactly at the focal point of the laser. The input optical-fiber collects the wavelengths of light emitted by the plasma and transmits it to the spectrometer. The spectrometer resolves the collected light into spectra with a wavelength resolution of 190 to 1040 nm.



Labels:

- |                                       |                                |
|---------------------------------------|--------------------------------|
| 1. Quantel Laser                      | 5. Spectrometer                |
| 2. Focal lens                         | 6. Remote Control              |
| 3. Automatic adjustable sample holder | 7. Power Unit                  |
| 4. Receiver                           | 8. Laptop with Aurora software |

Figure 6. Portable Laser Components

The detector controller is used to start and stop the laser using a delay generator, as well as modify laser timing parameters. The laser power supply unit supplies power to the laser and also provides a lockout mechanism so that unauthorized individuals cannot operate the laser, if the key is removed. The Aurora software is used to analyze and graph the collected light data. It can output data tables to be used for percent composition analysis, which is described later.



Figure 7. Portable Laser Equipment

### **Laser Analysis Tool**

The software code, named the “Laser Analysis Tool” has been constantly updated to make it more efficient and user friendly. The final version consists of a more professional Graphical User Interface and proper titles for every screen including progress bars. An Excel file is created for ease of analysis. The code is also efficient and reduces the size of the laser analysis program while making it faster. This version of the code contains no known bugs and functions to meet all expectations.

### **Data Collection**

#### **Calibration Set**

A standard set of data is collected to calibrate the model using PLSR. 35 rock types are used for calibration. For each rock type, 10 rock samples are randomly selected. Each rock is tested at 5 different locations. 200 shots are fired to ablate the surface contaminants and stabilize the light intensity collected for the next 100 shots. This calibration set consists of 35 rock types as mentioned earlier with 10 carbonates, 17 non-carbonates and 8 trap rocks as shown in Table 1.

Each spectrum collected is the accumulated light data of 100 shots which is averaged to minimize the shot to shot variations. For each rock type, 50 spectrums are collected so as to capture the heterogeneity in the rocks.

Table 1 - Aggregates used for calibration

	<b>Name of the aggregate</b>	<b>Type of rock</b>
1	Allen Myers Carbonate	Carbonate
2	Andreas Lehigh Carbonate	Carbonate
3	Bechtelsville Gneiss	Non-Carbonate
4	Braen Franklin Carbonate	Carbonate
5	Carbonate Dolomite	Carbonate
6	Dyer Quarry Diabase	Trap Rock
7	EI Hamburg Gneiss	Non-Carbonate
8	Eureka Milford Quartzite	Non-Carbonate
9	Fanwood Trap rock	Trap Rock
10	Hanson Glen Gneiss	Non-Carbonate
11	Kingston Argillite	Non-Carbonate
12	Kingston Trap Rock	Trap Rock
13	Lehigh Asphalt Carbonate	Carbonate
14	New Hope Crushed Stone Carbonate	Carbonate
15	OW Trap rock Orange Basalt	Trap Rock
16	Westfield Trap rock	Trap Rock
17	Pioneer Laflin Quartzite	Non-Carbonate
18	Temple Quartzite	Non-Carbonate
19	Atkinson Quartzite	Non-Carbonate
20	Woodboro Carbonate	Carbonate
21	Plumstead Argillite Belt	Non-Carbonate
22	Plumstead Argillite Stockpile	Non-Carbonate
23	Tilcon Diabase	Trap Rock
24	New hope Carbonate	Carbonate
25	Eastern Wantage Carbonate	Carbonate
26	Tilcon Oxford Carbonate	Carbonate
27	Plumstead Argillite Lockatong	Non-Carbonate
28	Tilcon Oxford Gneiss	Non-Carbonate
29	Eastern Hamburg Gneiss Losee	Non-Carbonate
30	Moore's Argillite Trap rock Ind	Trap Rock
31	Bechtelsville Gneiss 15179	Non-Carbonate
32	Plumstead Argillite 15165	Non-Carbonate
33	Tarheel Quartzite	Non-Carbonate
34	Kingston Trap rock 15219	Trap Rock
35	Pyramid Gneiss	Non-Carbonate

## **Testing Set**

A separate set of data is collected to validate the model and test the accuracy of each model. Initially, 5 samples were selected randomly and tested at 3 locations on each sample. Later, it was found that 30 data points were required to obtain a more representative dataset. Hence, the testing set size was increased to 10 samples and 3 locations each on each sample.

## **RESULTS AND DISCUSSION**

Initial tests were performed on pure metal samples to demonstrate how effectively LIBS can be used to identify the elemental composition of a sample. The peak wavelengths were compared to the NIST atomic spectral database to demonstrate how certain spectra lines can be used to qualitatively identify elements in a sample. Samples of pure mica and limestone were then tested to obtain typical output spectra corresponding to each of these minerals which are used in the future analysis of the different aggregates. Following these pure sample tests, a PLS model was developed based on a simplified case; identifying the amount of copper and zinc present in pennies minted in various years with varying chemical composition. The results of testing this model appeared to be quite accurate, showing that the PLS method of analysis has promise for aggregate analysis.

Testing was then performed on aggregate stone samples, with much more complex compositions. The results of XRF testing for each sample provided by the NJDOT provide a set of known compositions to aid in calibrating the models. Output spectra for a given type of aggregate stone typically show very similar trends, with slight variation and rare outliers likely caused by the innate inhomogeneity of the solid stone samples.

Data from several separate shots for each type of stone were input into the model as a testing set, and the results were averaged to help mitigate the effects of variation and possible outliers. The resulting outputs and deviation from 'known' values were then compared to the results of inputting the data from outside the calibration data. Models were generated using calibration sets of various sizes, and as expected, it was found that increasing the size of the calibration set generally improved the accuracy of the models.

At this point in time, it was considered possible that the data set itself was the source of the error. To test this hypothesis, an entire new set of data was collected for future models. This averaging testing was repeated on this new data using the original center clipping threshold of 200, however as before, results were inconsistent and in most cases did not outperform the original calibration technique or data set. These results led the research group to the conclusion that this error was caused by excessive variation in spectrum data or variation in accepted values which had not been represented. To address this, future tests used a modified testing procedure. These samples were tested such that the output spectrum was the sum of the emissions from 100 shots, and tests were conducted on five separate locations per sample. Once new data had been collected using this new procedure, new models were developed.

The results showed that while variable, an increase in calibration set size typically improves the accuracy of predictions overall. This general trend is evident regardless of the number of PLS components used to calibrate the model. It was also determined that a larger testing set may be necessary to produce reasonable predictions.

## Data Analysis and Interpretation

Before any type of analysis can be performed, the raw data must be adjusted to a useable form. Over the course of this research various techniques have been used, including:

- Discarding “bad shots;” i.e. data sets from laser pulses which, due to randomness in the system, produce abnormally low light emission from the sample, where relative light intensities cannot be properly represented. The experimental procedure has since been changed so that each collected spectrum is the sum of the emissions from 100 laser shots; mitigating the effect of low emission shots and rendering this step unnecessary.
- Subtracting baseline light intensity from the spectrum (the Data Analysis software used with the current spectrometer does this automatically, and the enclosed sample chamber minimizes external light contamination).
- Reducing spectral amplitudes. Following the first procedure modification, resulting spectra amplitudes were reduced by a factor of 100 to produce an effective average for each testing location. This is not strictly necessary, but the practice was continuing for consistency of results.
- Removing remaining variation along baseline via center clipping; in which light intensities below a certain value are assumed to be noise and are set to be zero. The threshold for center clipping was varied in previous tests, and the model response considered, however modern models merely use this technique with a 0 threshold to remove negative values caused by noise in the system.
- Normalizing light intensities for a given spectrum to the total amount of light emitted by the sample in said spectrum to account for shot to shot variation in total light emission. Several different normalization techniques have been used, but this method has been shown to be the most effective.

To ensure that the XRF data provided for calibration are reproducible, additional XRF tests were performed by both the Rowan research team and NJDOT staff. The Rowan research team tested on solid samples while the NJDOT staff tested on powdered samples. Given this difference in procedure, it was expected that the Rowan research team’s results would be less consistent as these tests examined various points on an inherently inhomogeneous sample, whereas the NJDOT staff’s powdered samples were expected to produce more consistent results given the fact that the samples effectively blended the solid samples into a more homogeneous mass. As per the XRF testing procedure, all elements were assumed to be bound in oxides, which may or may not actually be the case in real samples. These tests confirmed that the XRF results provided by the NJDOT were more reliable and reproducible, and the provided XRF results continued to be used as known values for calibration.

Each model was calibrated using an optimized number of PLS components determined through the MATLAB code’s built-in mean square error output. In each case, the model was generated using 15 to 20 PLS components which had been determined to be excessive, and examining the amount of variation explained by each component and the residuals remaining after each. No additional PLS components were used after the addition of another would explain less than another one percent of the variation in the known values, but an approximate point of diminishing returns for reduction of residuals was also considered.



## Data Preprocessing Techniques

Before any alternative pre-processing options were explored, a Base Model was developed for comparison. In the Base Model, the 100 shot total spectra were reduced in amplitude as previously described, negative values were removed through applying center clipping with a 0 threshold, and spectra were normalized to the total light emission. The performance of other methods were visually compared to the Base Model in Figures 10 through Figure 14. Each case is shown with two bars, representing the upper and lower bounds of a 90 percent confidence interval so as to show the overall variability of predictions. In each case the results for two carbonate rocks, the Carbonate Dolomite and Woodboro Carbonate, and two non-carbonate rocks, the original Gneiss and Argillite samples, are reported as these generally represent the trends for samples of the same designation. Only the five most significant compounds are reported for sake of visual clarity. Unless otherwise noted, each method described below includes these Base Model steps before applying other data preprocessing techniques.

## Y-Scaling Method

One method explored in Tucker et al. (2010) research is scaling the Y-variables, thereby forcing the PLS algorithm to consider the concentrations of all compounds equally rather than prioritizing compounds with high variability in the calibration set<sup>(10)</sup>. This is done in two ways. One method is to divide the value of each compounds by the maximum value of the same compound among all the aggregates in the calibration set, thereby reducing each concentration to the ratio of the smallest to the largest value, to one for each compound being considered (Y-scaling Ratio:1). The other method involves first subtracting the minimum value for each case before dividing all remainders by the range for that compound, thereby reducing each to a value between 0 and 1 (Y-scaling 0:1). Regardless of which method is used, the reverse adjustments must be applied to predicted values to convert them to actual predictions. The predicted ranges for each case are shown in Figure 8. Note that both methods of Y-scaling produce nearly identical predictions.

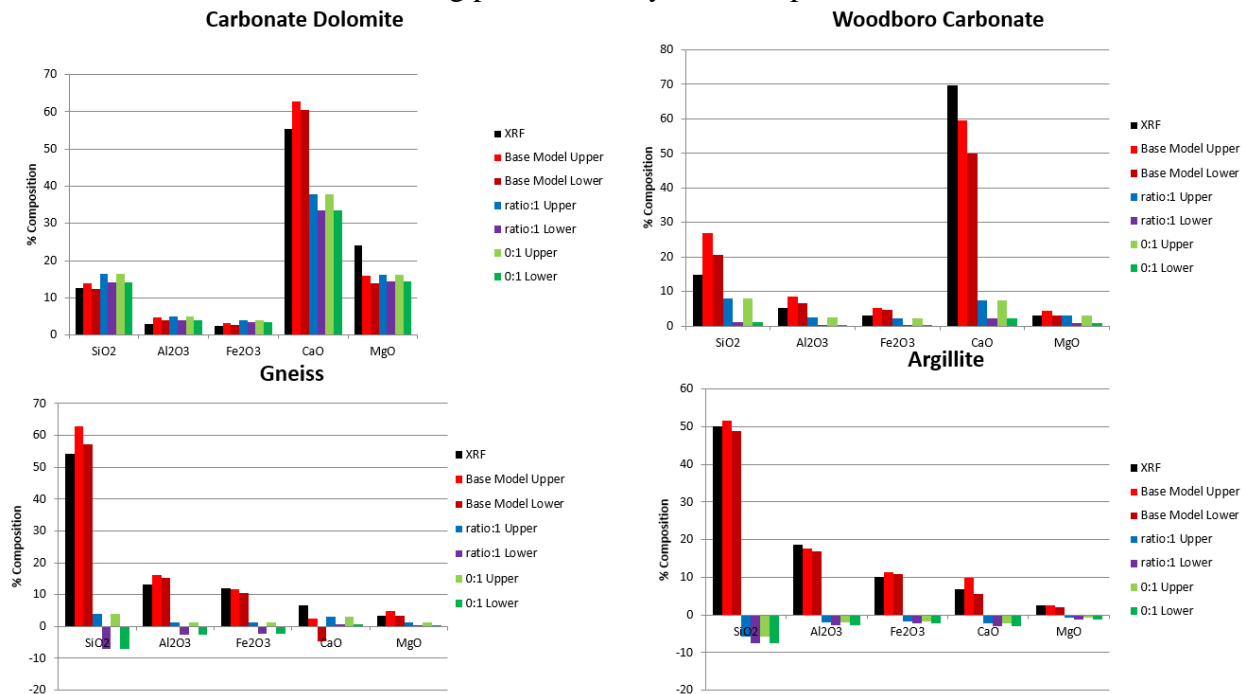


Figure 8. Y-Scaling Results

The above result show that this method tends to underestimate the composition and often produces unreasonable predictions for the given data set. This method has therefore been rejected.

### Split Training Method

The final method explored was inspired by the work by Tucker et al <sup>(10)</sup>. This technique involved reducing the range of values presented in the calibration set by training two or more separate models as opposed to a broad base one. Tucker et al. suggested that by applying a broad base model to obtain a ‘first guess’ of a stone’s composition and then applying an appropriately specialized model for a more precise prediction, individual models can become more accurate. This is because they consider a narrower range of possibilities. In this case samples were divided into carbonate and non-carbonate rocks for the sake of providing an intuitive classification of samples. Figure 9 shows the results for the model corresponding to the stone’s classification: carbonate or non-carbonate.

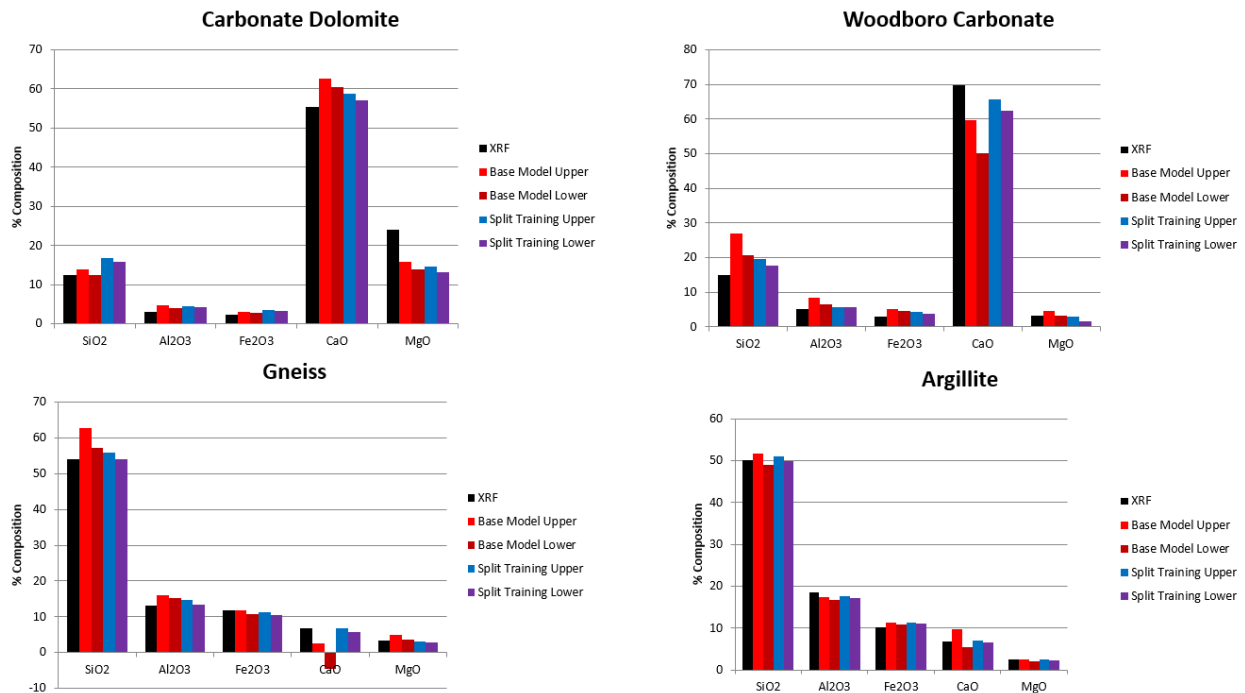


Figure 9. Split Training Set Results

This technique shows real promise. While still imperfect, using this split training set method has shown to be an improvement over the base model in terms of accuracy and precision. Models will be further refined by building on this technique by applying other methods in conjunction with this. Future model testing will also be performed using larger testing sets to produce more reliable results with greater confidence, and to establish an appropriate standard testing set size to obtain a reliable prediction.

### Combination Model

The above methods such as Split Training and Y-Scaling were combined. Based on the initial guess using a Y-Scaled model, the aggregates are classified and send to the specified precise model of Y-scaling.

### Split Training with Y-Scaling

The results from combining the split training model and Y-Scaling are shown in Figures 10 through 14. Through the use of Y-scaling coupled with split training, better results were produced. Split training combined with a Y Scaling Ratio:1 produced similar results as before. This suggests that this method is subject to variability of samples or an error during analysis. Split training combined with Y-scaling 0:1 produce accurate results and was selected for final use.

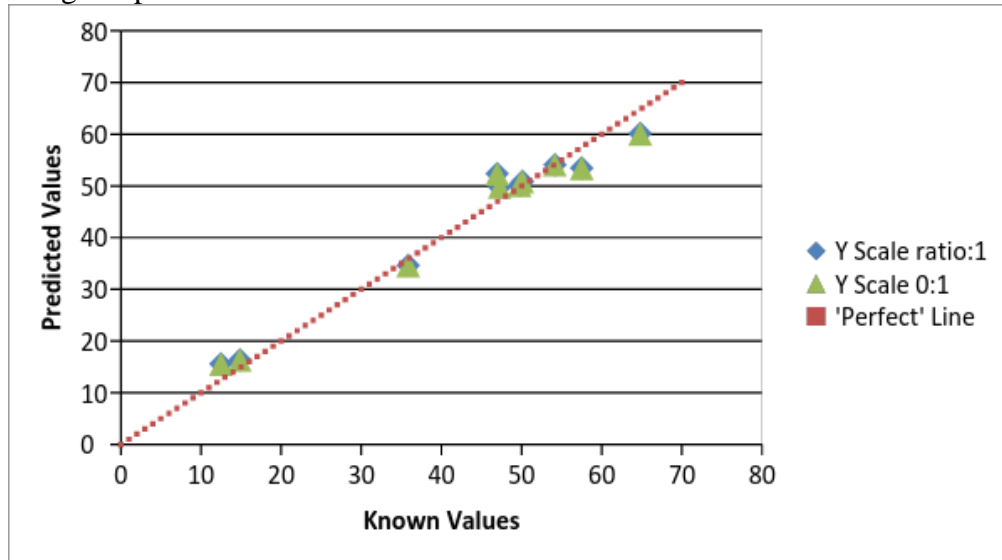


Figure 10. SiO<sub>2</sub> Split Training, Y-Scaling Model Predictions

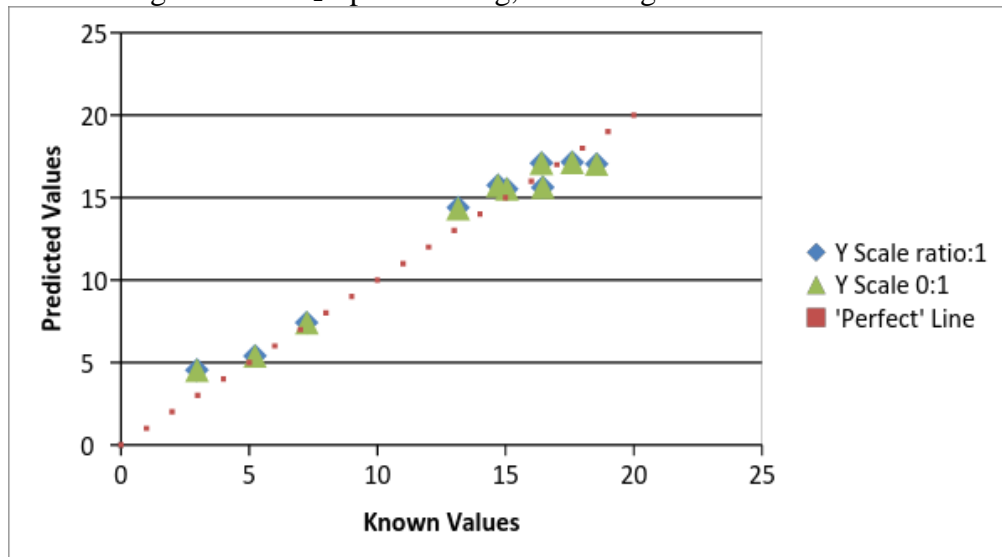


Figure 11. Al<sub>2</sub>O<sub>3</sub> Split Training, Y-Scaling Model Predictions

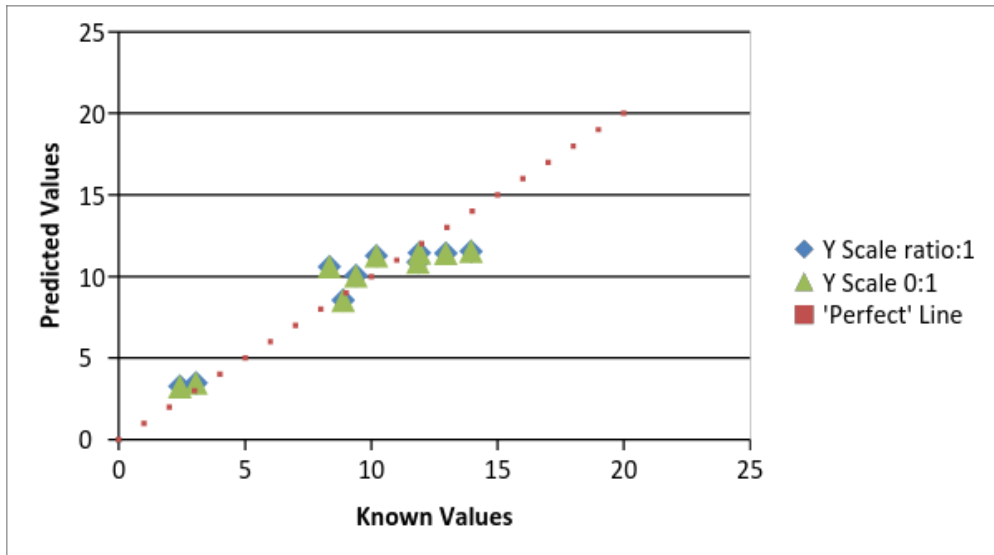


Figure 12. Fe<sub>2</sub>O<sub>3</sub> Split Training, Y-Scaling Model Predictions

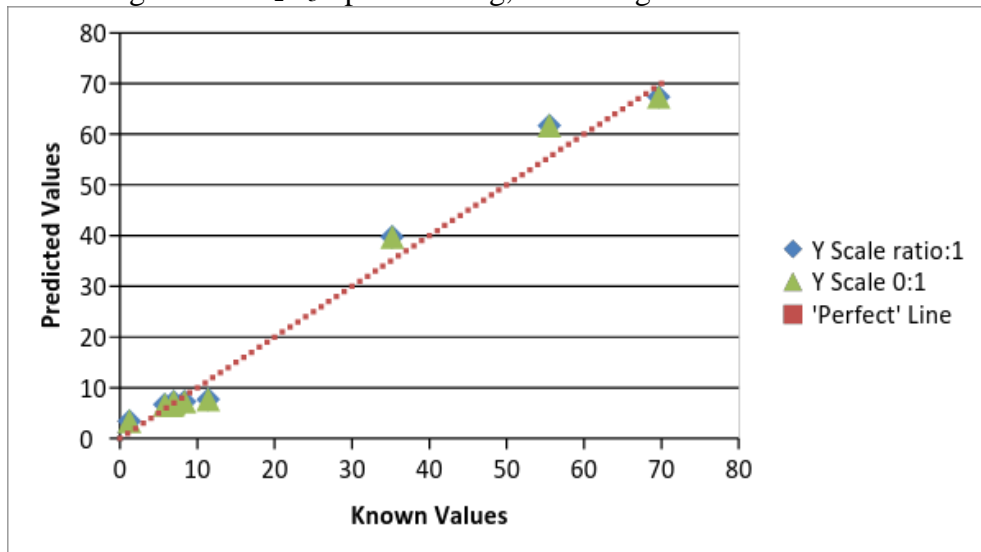


Figure 13. CaO Split Training, Y-Scaling Model Predictions

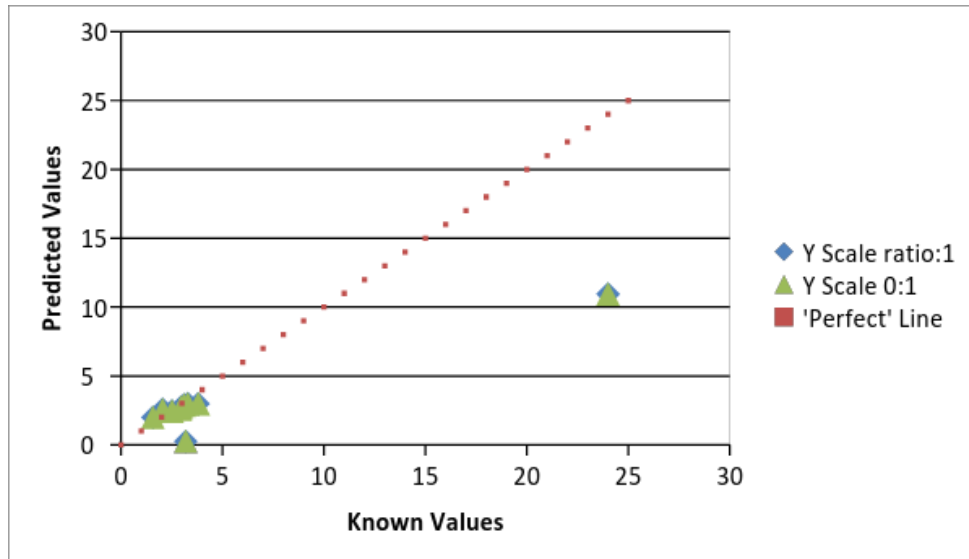


Figure 14. MgO Split Training, Y-Scaling Model Predictions

### Classification Methods

The chosen method for analysis of the data for classification was Split Training with Y-scaling 0:1 based on the fact that this method produced the most accurate results. But before deciding on how to classify the aggregates, various methods for split training were analyzed, which are detailed below.

### One-Dimensional Classification

One-Dimensional Classification uses the initial guess from a Broad-Based model and classifies the samples based on percent calcium oxide into two categories. If the composition of CaO is below 25 percent, the sample is classed as a non-carbonate rock, but if the composition of CaO in the sample is above 25 percent, then the rock is classified as a carbonate rock. The rocks will be classified and sent into more precise models, 'Carbonate' or 'Non-carbonate' to produce more accurate results. This threshold is chosen based on the percentage of Calcium Oxide from the XRF analysis of each rock. Figure 15 shows the percent of CaO present in various rocks that are used for calibration and their rock classification. Figure 16 through 20 shows the results of Calcium Oxide classification method for each compound. For simplicity, the major five compounds are shown here. This method has not been selected since it is less effective in classifying rocks. The initial prediction values of the percentage of CaO in Andreas Lehigh Carbonate is 16.83% and of Lehigh Asphalt Carbonate is 11.12%, which are less than the threshold ratio (25%) as shown in Table 2. Because of the low CaO content in Andreas Lehigh Carbonate and Lehigh Asphalt Carbonate, these rocks are not correctly identified as Carbonates demonstrating that this method was not very effective in identifying the split models.

Table 2 - Outliers of One-Dimensional Classification

Outlier	Threshold Value	Classified as:
Lehigh Asphalt Carbonate	11.12	Non Carbonate
Andreas Lehigh Carbonate	16.83	Non Carbonate

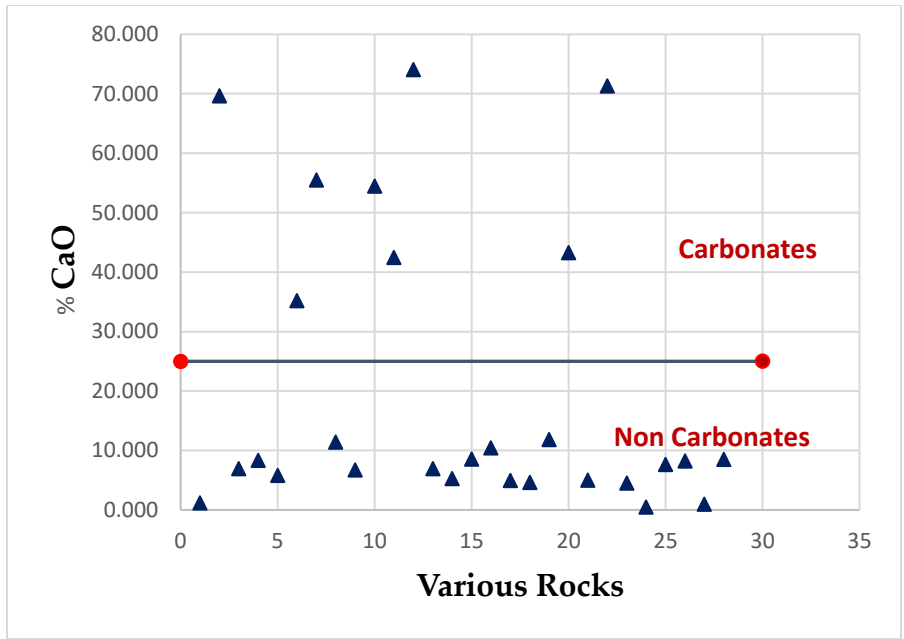


Figure 15. Classification of rocks based on CaO%

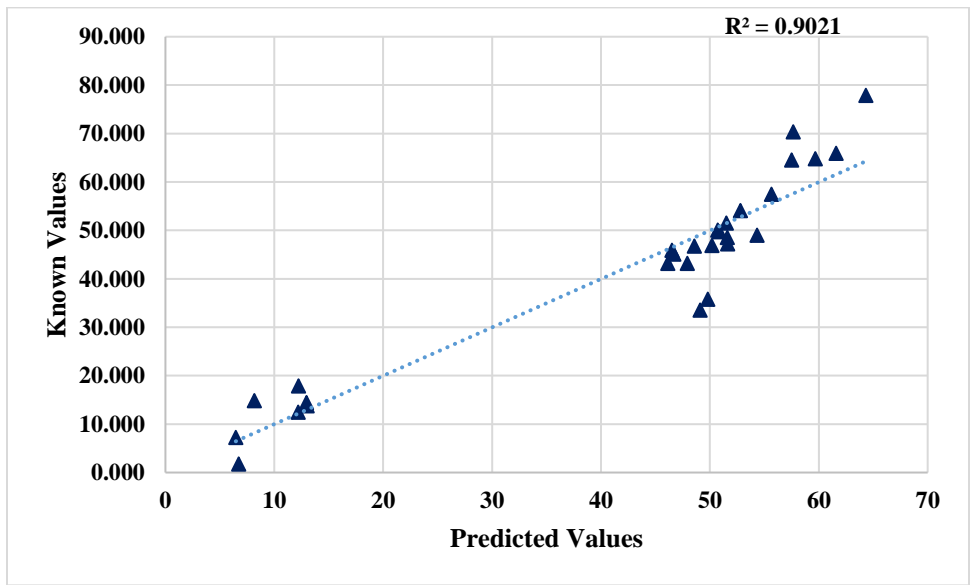


Figure 16. Results of SiO<sub>2</sub> using Calcium Oxide classification.

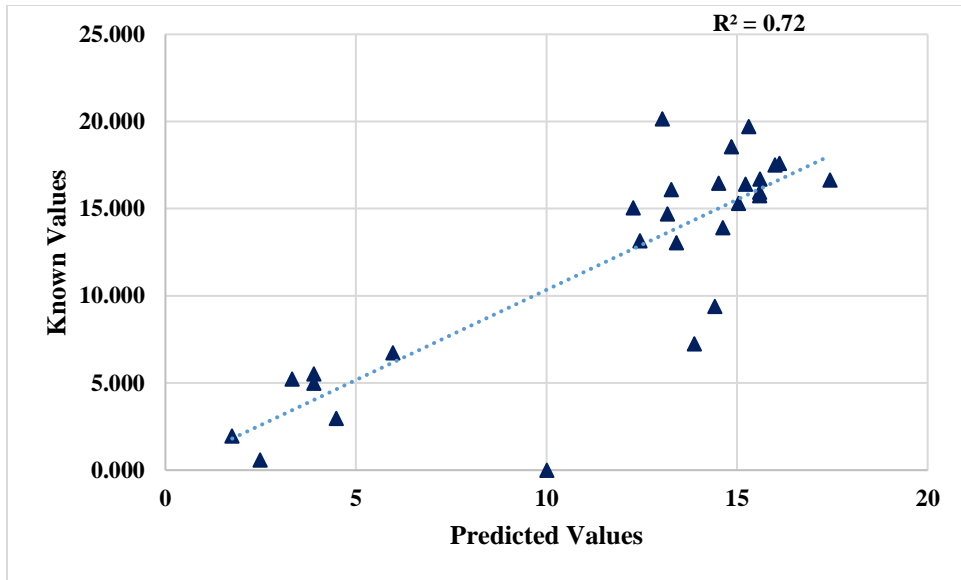


Figure 17. Results of Al<sub>2</sub>O<sub>3</sub> using Calcium Oxide classification.

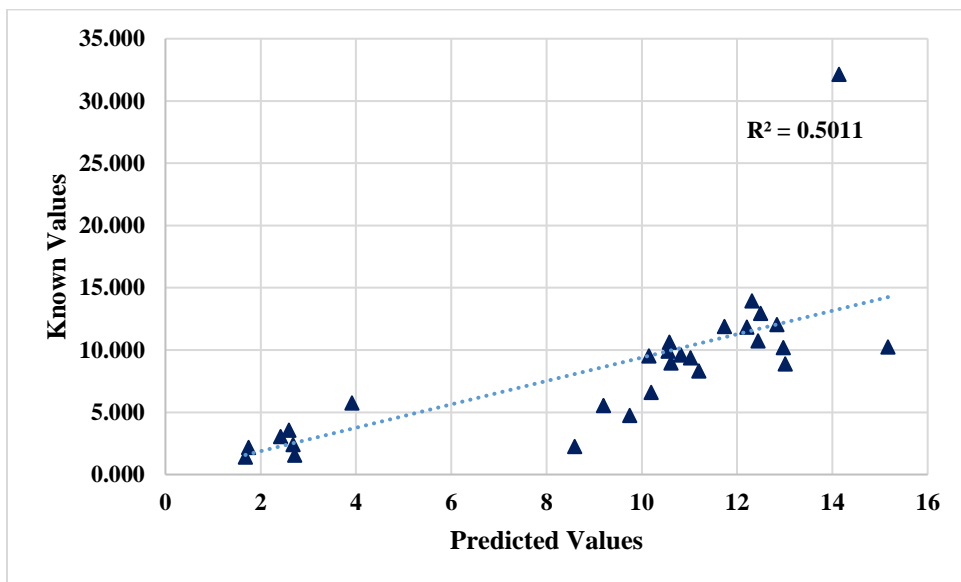


Figure 18. Results of Fe<sub>2</sub>O<sub>3</sub> using Calcium Oxide classification.

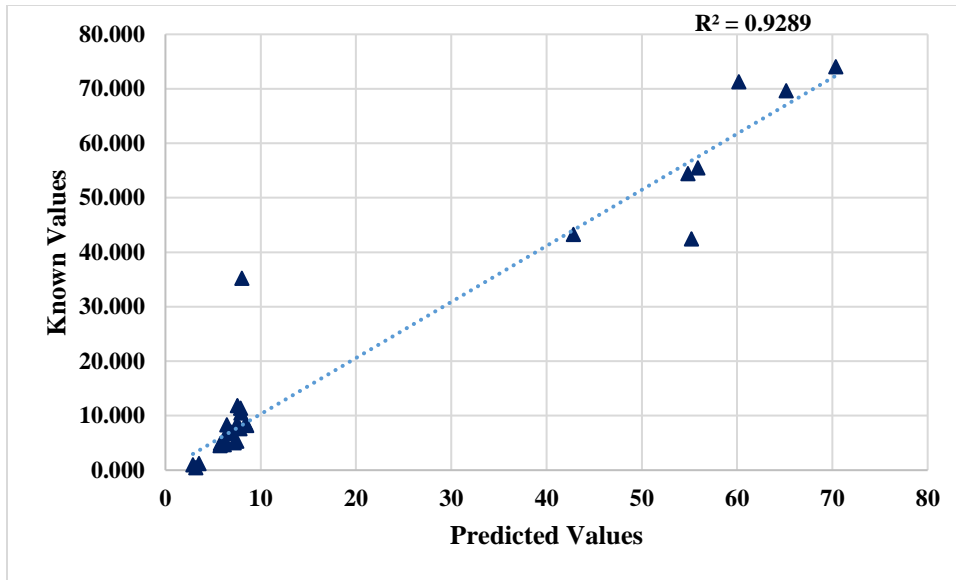


Figure 19. Results of CaO using Calcium Oxide classification.

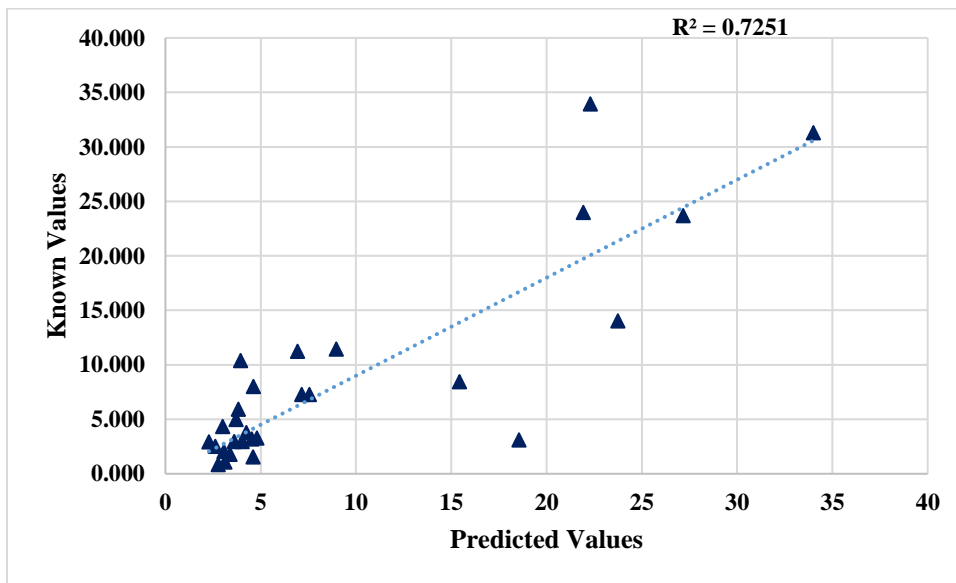


Figure 20. Results of MgO using Calcium Oxide classification.

### Two-Dimensional Line Classification

This method is based on a graphical pattern observed by plotting the percentage of Ferrous Oxide and the ratio of percentages of Silica to Calcium Oxide ( $\text{SiO}_2/\text{CaO}$ ) present in the aggregate. Carbonate with lower  $\text{SiO}_2$  and  $\text{Fe}_2\text{O}_3$  values tend to move closer to zero and non-carbonates with higher  $\text{Fe}_2\text{O}_3$  values tend to move away from both axes. A threshold line separating both carbonates and non-carbonates is found using trial and error maximizing the space between the line and each data point. The second method used was with a line classification referred to as a Two Way Split, which uses an equation to determine the classification of the rock. The equation is derived from Figure 21, with ferrous oxide on the x-axis and Silica/Calcium oxide ratio on the y-axis.



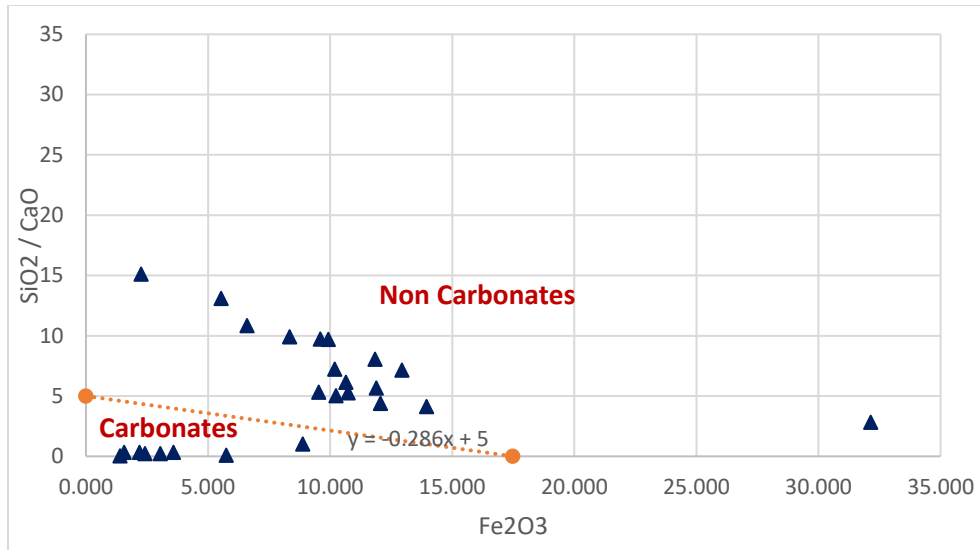


Figure 21. Classification of rocks based on the threshold line.

$$Y + 0.286X - 5 = 0 \quad (1)$$

where,  $X$  is the percentage of Fe<sub>2</sub>O<sub>3</sub> and  $Y$  is the ratio of percentages of SiO<sub>2</sub> and CaO.

When  $Y + 0.286X - 5$  is less than zero, it is classified as carbonate and when it is greater than zero, it is classified as a non-carbonate. Based on the initial prediction, the rocks will be classified accordingly and split into corresponding model. Figure 22 through 26 shows the results of line classification method. This method fails to classify the Lehigh Asphalt Carbonate as a carbonate and most of the trap rocks are incorrectly classified as carbonates as shown in Table 3. This method also gives the lowest R Square value; hence it is no longer used.

Table 3 - Outliers of Two-Dimensional Line Classification.

Outlier	Threshold Value	Classified as:
Bechtelsville Gneiss 15179	-0.53705	Carbonates
Dyer Quarry Diabase	-8.788	Carbonates
Hanson Glen Gneiss	-13.379	Carbonates
Kingston Argillite	-52.283	Carbonates
Kingston Trap Rock	-4.78	Carbonates
Plumstead Argillite Stockpile	-12.371	Carbonates
Temple Quartzite	-4.1864	Carbonates
Tilcon Diabase	-7.0635	Carbonates

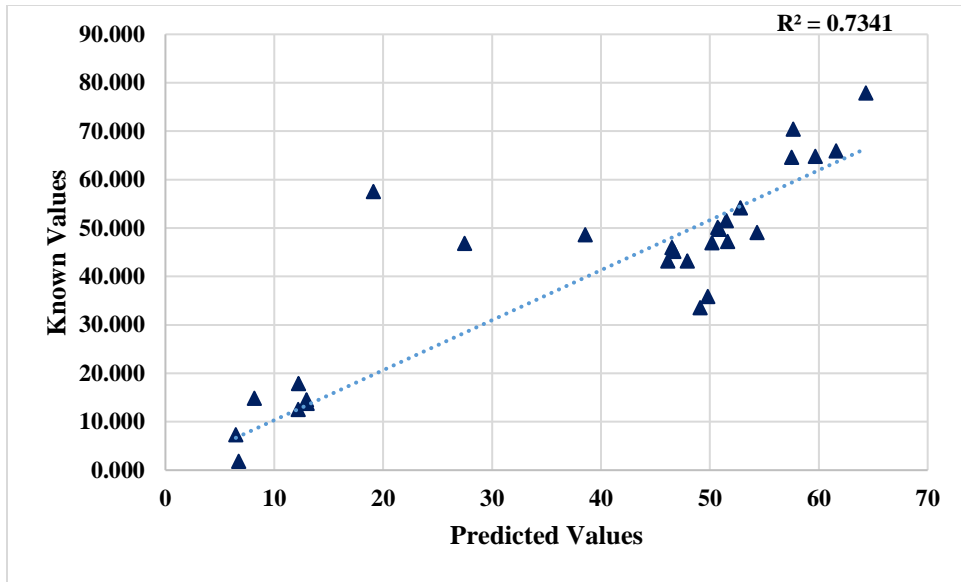


Figure 22. Results of SiO<sub>2</sub> using Line classification.

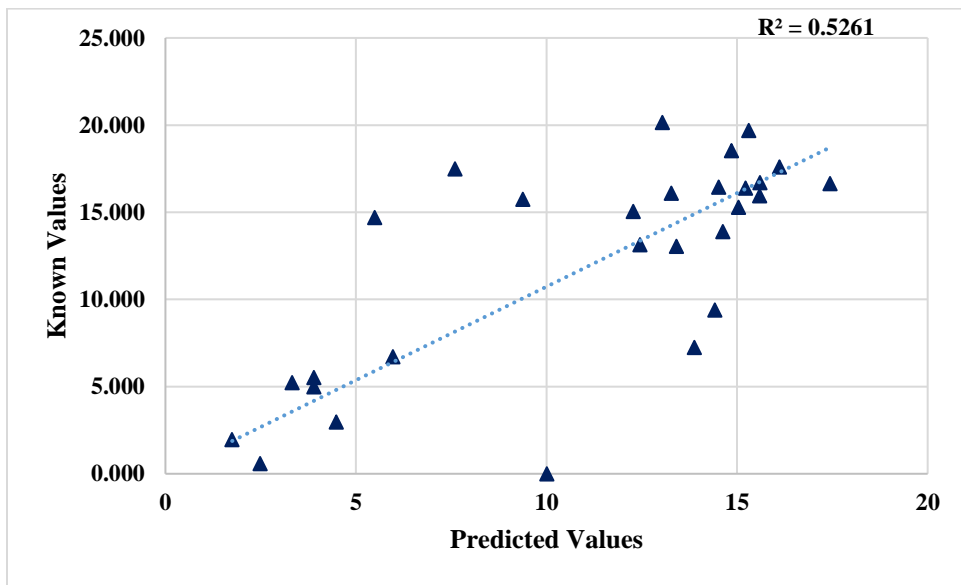


Figure 23. Results of Al<sub>2</sub>O<sub>3</sub> using Line classification.

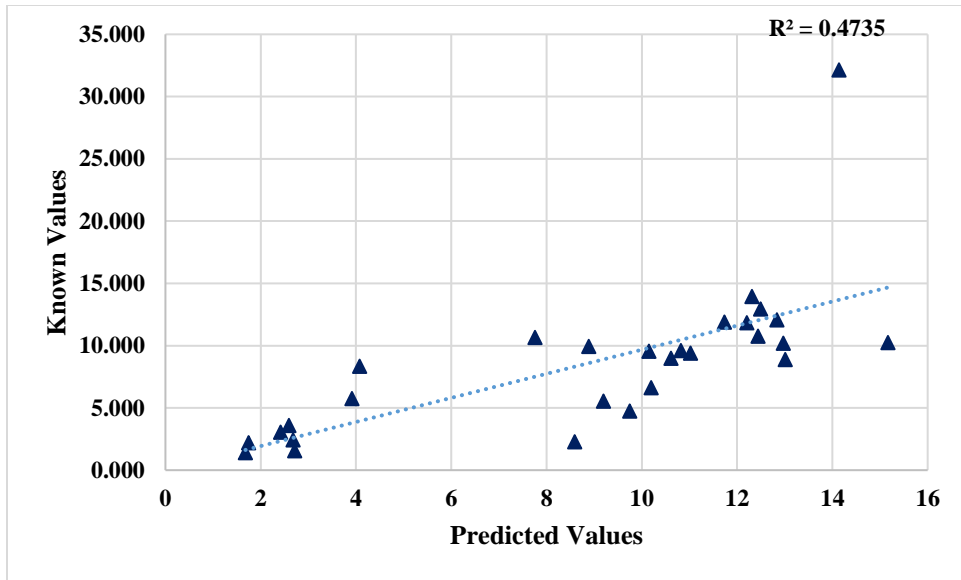


Figure 24. Results of Fe<sub>2</sub>O<sub>3</sub> using Line classification.

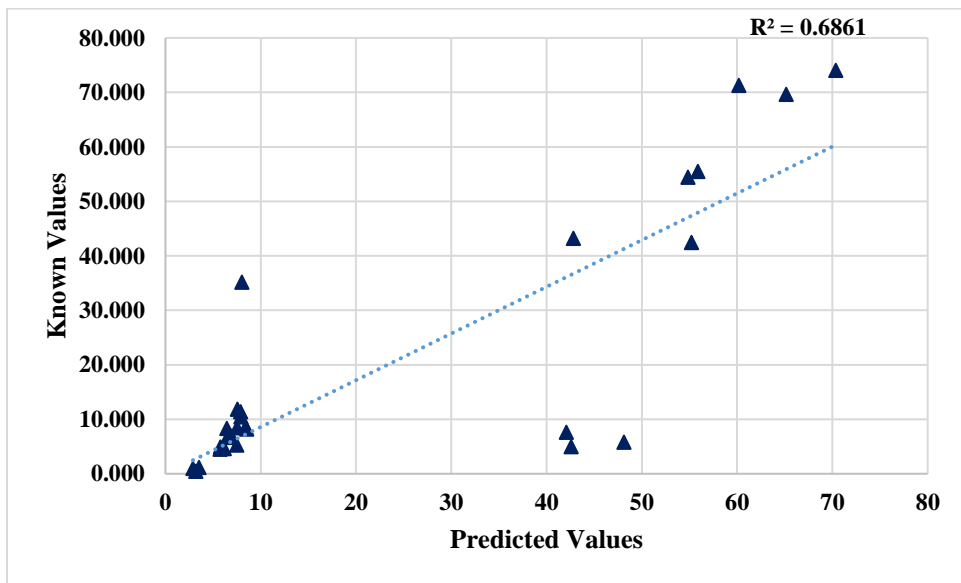


Figure 25. Results of CaO using Line classification.

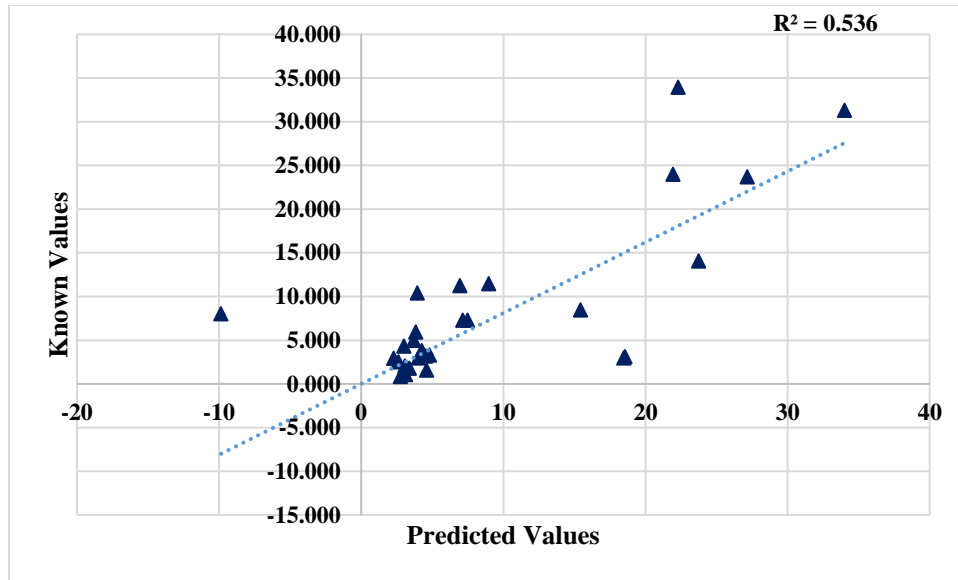


Figure 26. Results of MgO using Line classification.

### Two-Dimensional Ratio Classification

A Two-Dimensional Ratio classification method is implemented considering two compounds, calcium oxide and silica. Carbonates tend to have higher percentages of Calcium Oxides (CaO) and non-carbonates tend to have higher percentage of SiO<sub>2</sub>. Classification is done using a ratio of SiO<sub>2</sub> to CaO. If this ratio is below 3 the aggregate is considered carbonate, otherwise it is considered a non-carbonate as shown in Figure 27. The ratio classification method resulted in an effective classification of carbonates and non-carbonate rocks. Figure 28 through 32 shows the results for the Ratio Classification Method. The percentage of rocks going to the right bin has been increased compared to the Calcium Oxide classification method. Even then, most of the trap rocks which are near the threshold value is incorrectly classified. Carbonates except Lehigh Asphalt Carbonate are classified correctly for split training purposes compared to the Two-Dimensional Line classification method as shown in Table 4. However, the accuracy of prediction of trap rocks and non-carbonates are yet to be improved. An improvement has been made on this classification and is discussed in the next session.

Table 4 - Outliers of Two-Dimensional Ratio Classification

Outlier	Threshold Value	Classified as:
Lehigh Asphalt Carbonate	17.668	Non-Carbonate

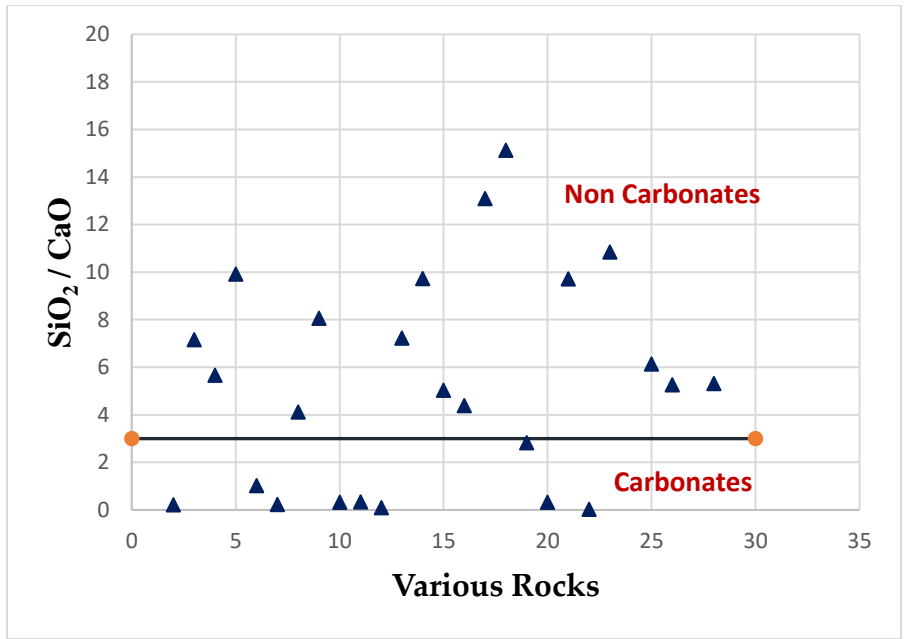


Figure 27. The classification of rocks based on the threshold ratio of 3

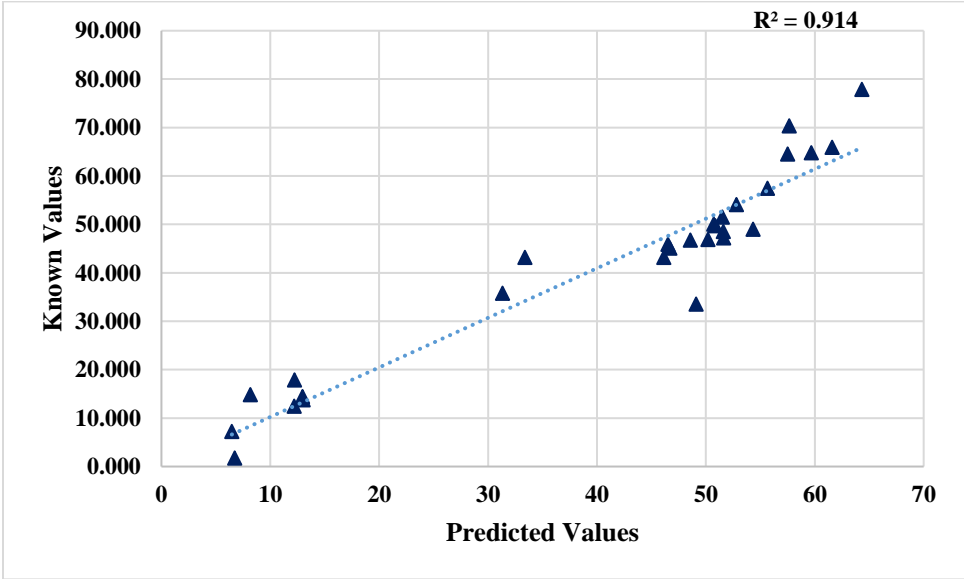


Figure 28. Results of SiO<sub>2</sub> using Ratio classification.

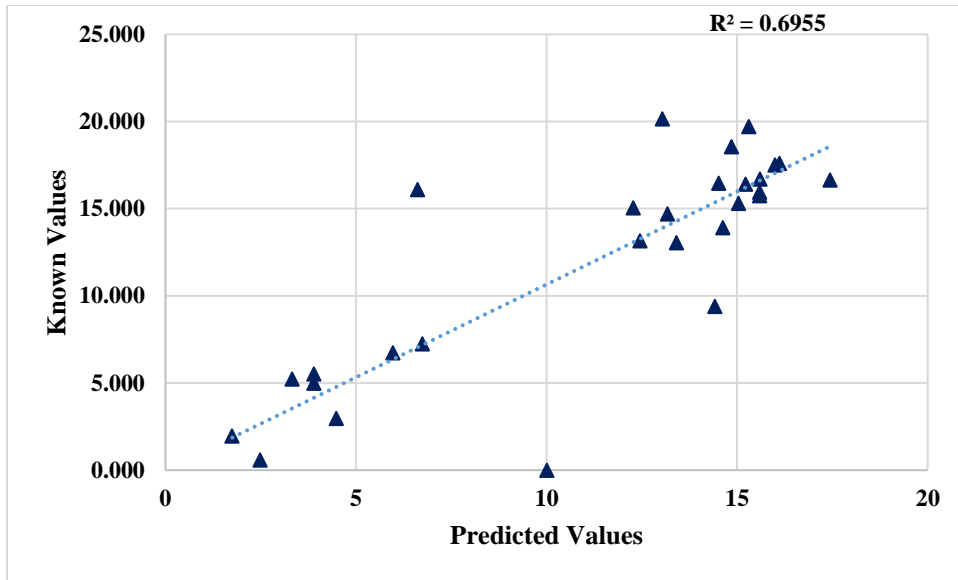


Figure 29. Results of Al<sub>2</sub>O<sub>3</sub> using Ratio classification.

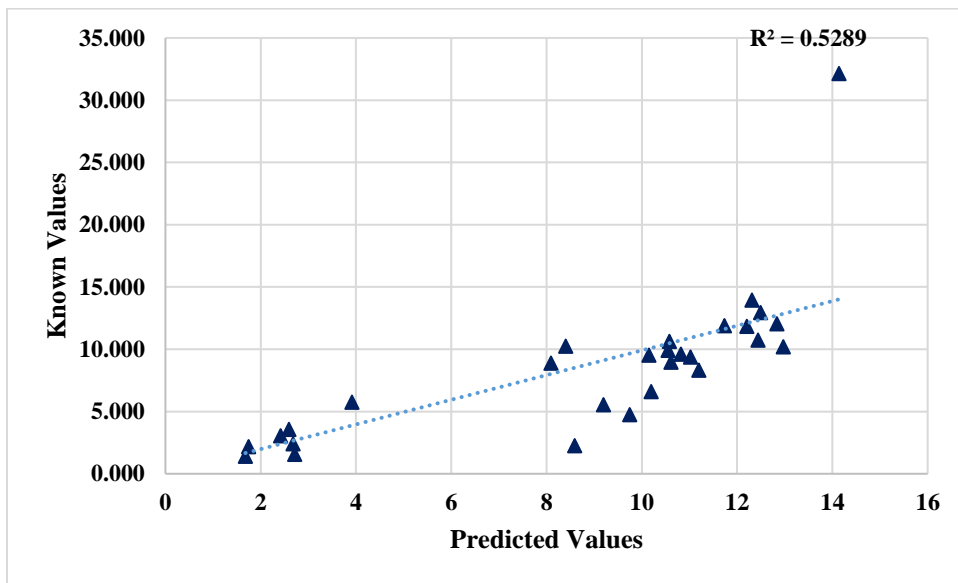


Figure 30. Results of Fe<sub>2</sub>O<sub>3</sub> using Ratio classification.

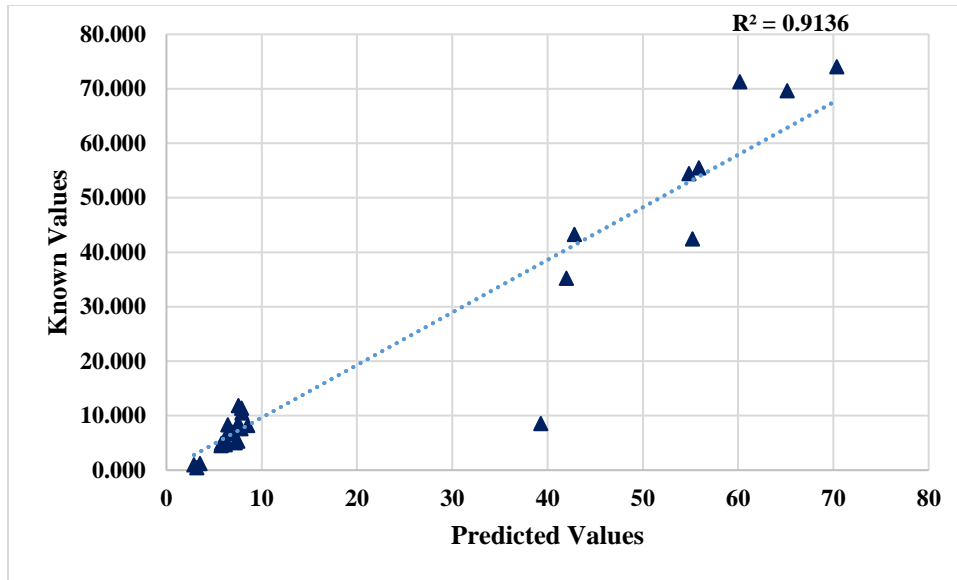


Figure 31. Results of CaO using Ratio classification.

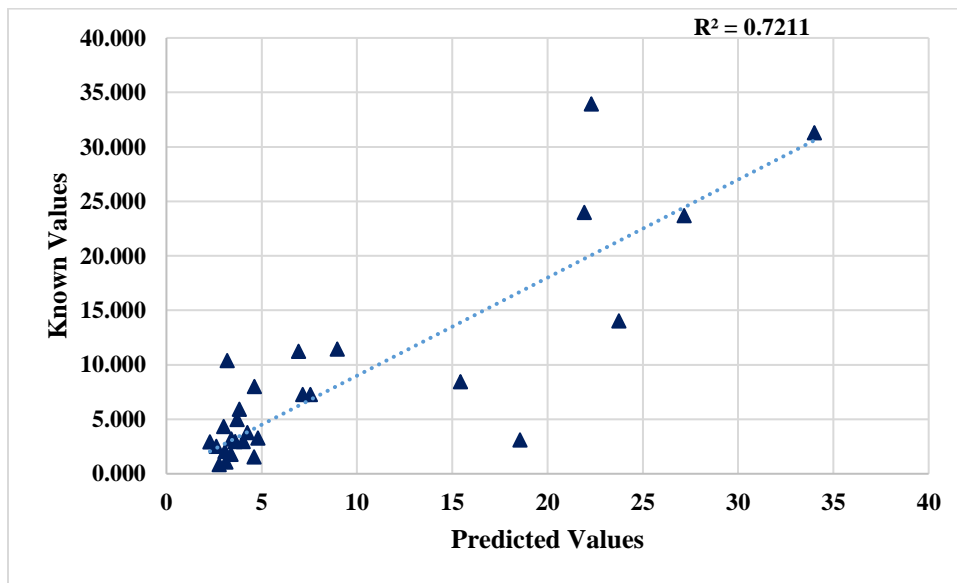


Figure 32. Results of MgO using Ratio classification.

### Three Way Split Classification

A Three-Way Split was finally decided to be the best way to classify the aggregate rocks. Based on the initial prediction of composition using a Broad-Based Model, the rocks are classified into three categories namely Carbonates, Trap Rocks and Non-Carbonates. The ratio classification gives a clear demarcation between Carbonates and Non-carbonates. To amplify this demarcation between two categories,  $SiO_2/CaO$  ratio is squared. Trap rocks seems to have higher percentage of  $Fe_2O_3$  compared to other non-carbonates (other than trap rocks), hence  $Fe_2O_3$  is used to distinguish between Trap Rocks and Non-carbonates. The following formula is how this method classifies the sample into one of three categories.

$$\frac{SiO_2^2}{CaO} * Fe_2O_3 < 150 = Carbonates \quad (2)$$

$$150 < \frac{SiO_2^2}{CaO} * Fe_2O_3 < 500 = \text{Trap Rocks} \quad (3)$$

$$500 < \frac{SiO_2^2}{CaO} * Fe_2O_3 = \text{Non - Carbonates} \quad (4)$$

If the value of  $(SiO_2/CaO)^2 \times Fe_2O_3$  is less than 150, it is a Carbonate. If it is between 150 and 500, then it is a trap rock; otherwise it is a non-carbonate as shown in Figure 33. The threshold values are chosen based on XRF values and further modified based on the initial guess values. Lehigh Asphalt Carbonate is again classified as Non-Carbonate, which is later identified as a contaminated rock by NJDOT. Some trap rocks are classified as non-carbonates as shown in Table 5. This can be explained by the metamorphism of trap rocks due to the weathering process where the CaO and  $Fe_2O_3$  contents are washed away. Three-Way Split classification is found to be the best method for an accurate prediction of chemical composition. Figure 34 through 38 shows the results for the split training using the Three Way Split Classification technique.

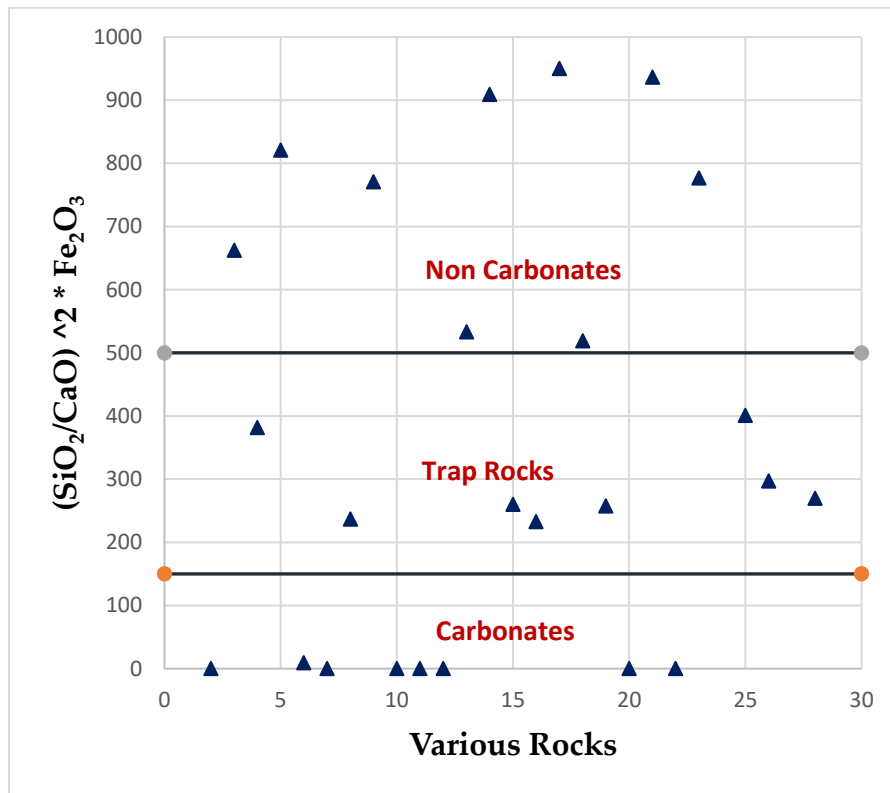


Figure 33. The classification of rocks based on the Ratio Square method.

Table 5 - Outliers of Three-Way Split Classification

Outlier	Threshold Value	Classified as:
Fanwood Trap Rock	6539.836	Non-Carbonate
Kingston Trap Rock	8052.592	Non-Carbonate
Kingston Trap Rock 15219	991.4638	Non-Carbonate
OWT Orange Basalt	1744.469	Non-Carbonate
Lehigh Asphalt Carbonate	8411.455	Non-Carbonate



Tilson Diabase	18852.28	Non-Carbonate
Westfield Trap Rock	1189.668	Non-Carbonate

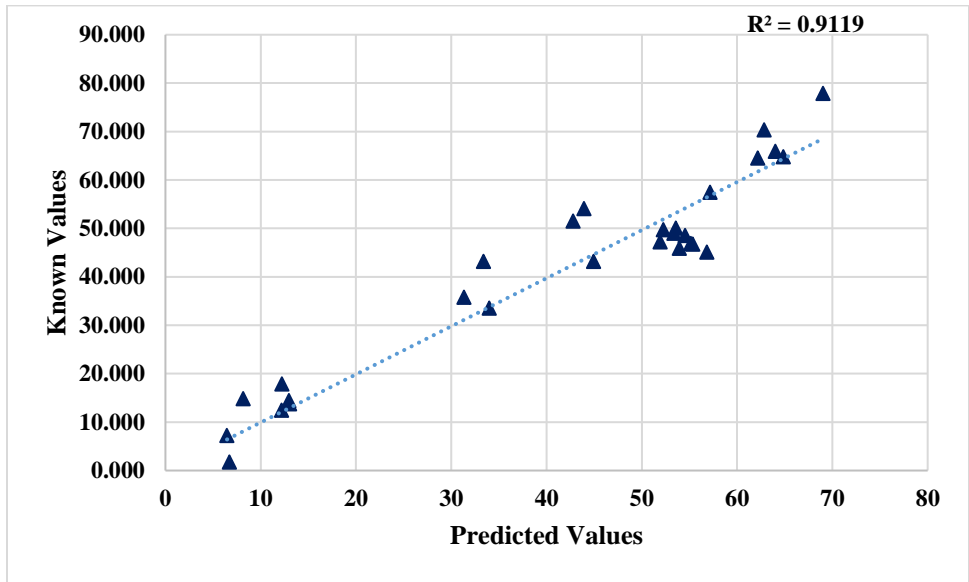


Figure 34. Results of SiO<sub>2</sub> using Ratio Square classification.

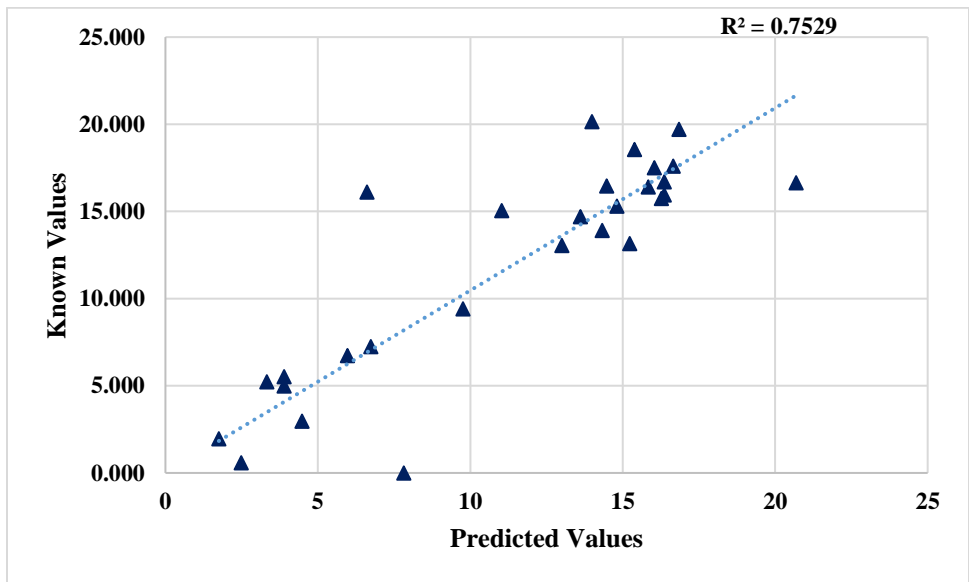


Figure 35. Results of Al<sub>2</sub>O<sub>3</sub> using Ratio Square classification.

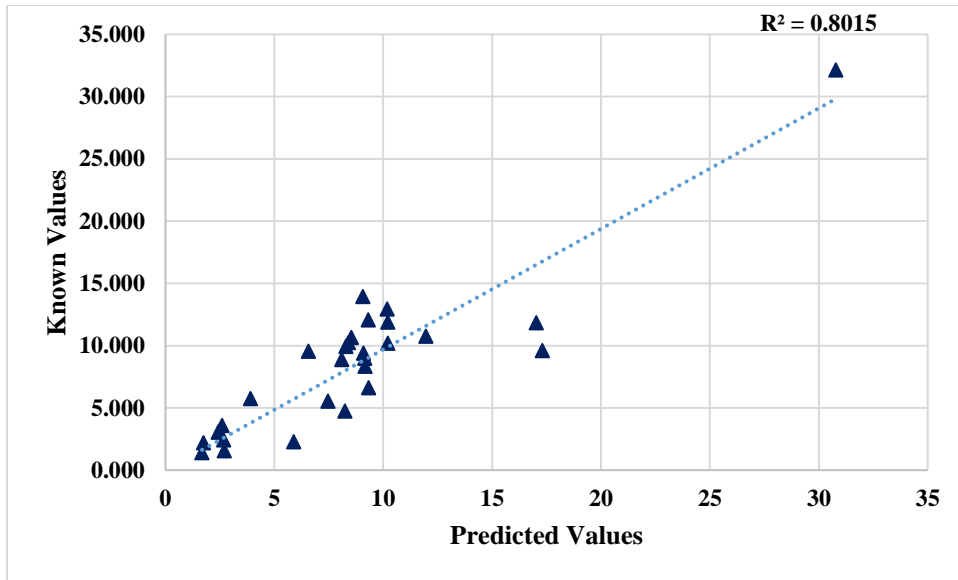


Figure 36: Results of Fe<sub>2</sub>O<sub>3</sub> using Ratio Square classification.

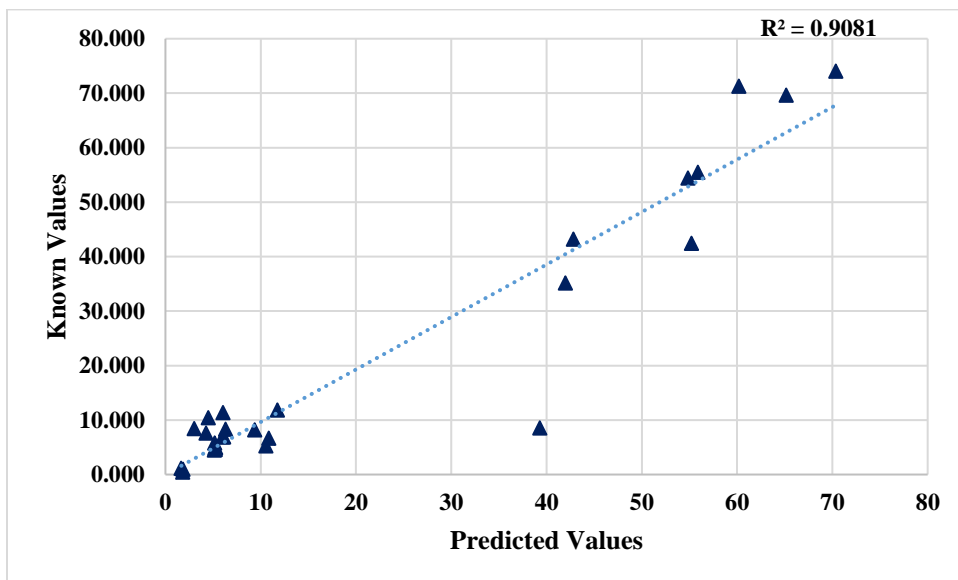


Figure 37: Results of CaO using Ratio Square classification.

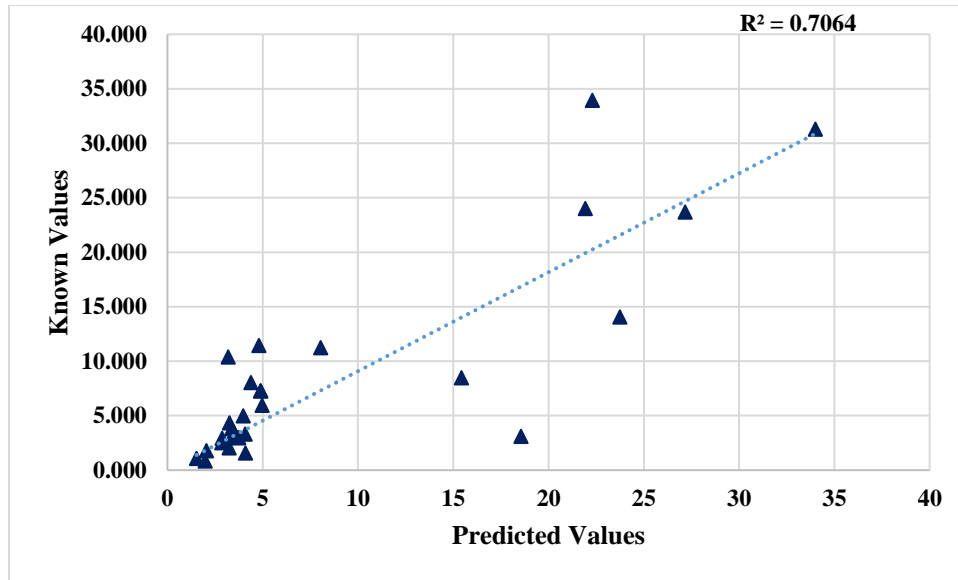


Figure 38. Results of MgO of Ratio Square classification.

### Accuracy of Models

The accuracy of each model is determined using R square values and ANOVA analysis.

### Statistical Analyses

$R^2$  values show the percentage of variation of the predicted results. When the  $R^2$  value is higher, the model fits the data better. Table 6 shows the  $R^2$  values for each model compared for each compound and Table 7 shows the  $R^2$  values for carbonates, trap rocks and non-carbonates for each split training classification method. Split Training with Y-Scaling combined with the Three Way Split Classification shows the highest  $R^2$  values. Y-Scaling improved the accuracy of minor compound predictions since this method considered all compounds with equal priority.

Table 6 –  $R^2$  values of each method against each compound

<b><math>R^2</math> Value</b>	<b>SiO<sub>2</sub></b>	<b>Fe<sub>2</sub>O<sub>3</sub></b>	<b>Al<sub>2</sub>O<sub>3</sub></b>	<b>CaO</b>	<b>MgO</b>
<b>Base Model</b>	.8589	.6103	.3691	.8421	.4914
<b>Y-Scaling</b>	.8722	.6956	.4924	.8469	.6178
<b>Split Training</b>	.9109	.753	.5276	.9271	.7123
<b>Split Training with Y Scale One-Dimensional Classification</b>	.9021	.72	.5011	.9829	.7251
<b>Split Training with Y Scale Two-Dimensional Line Classification</b>	.7341	.5261	.4735	.6861	.536
<b>Split Training with Y Scale Two-Dimensional Ratio Classification</b>	.914	.6955	.5289	.9136	.7211

<b>Split Training with Y Scale Three-Way Split Classification</b>	.9119	.7529	.8015	.9081	.7064
---	-------	-------	-------	-------	-------

Table 7 – R<sup>2</sup> values of Carbonates, Trap Rocks and Non-Carbonates for various split training methods.

<b>R<sup>2</sup> Value</b>	<b>Carbonates</b>	<b>Trap Rocks</b>	<b>Non-Carbonates</b>
<b>One-Dimensional Classification</b>	.806	.873	.983
<b>Two-Dimensional Line Classification</b>	.819	.687	.710
<b>Two-Dimensional Ratio Classification</b>	.932	.713	.978
<b>Three-Way Split Classification</b>	.932	.747	.969

### **ANOVA (Analysis of Variance)**

ANOVA is a statistical method developed by Ronald Fisher in 1918<sup>(13)</sup> to analyze the variance of more than two groups. This is also called the Fisher analysis of variance. This is an extended version of the t- and z-test. The assumptions considered while running ANOVA for the prediction results are as follows:

1. The weighted average errors of each compound of aggregates are normally distributed.
2. Independence of cases: Each LIBS test at various locations and on different samples are independent of each other.
3. Homogeneity: The variance between the aggregate groups are approximately equal.

A two-way ANOVA analysis is conducted on the average weighted error of each compound for all aggregates.

### **ANOVA for Various PLSR Models**

The two-way ANOVA analysis is conducted on the results for the various spectrum analysis methods. Figure 39 through 41 shows the results of the ANOVA analysis to assess the accuracy of the different spectrum pre-processing techniques and split training strategies. X-axis represents the P-value associated with each analysis method, which is the significance level of the interaction term. Y-axis represents each method of analysis as follows:

- 1- Base Model
- 2- Y-Scaling
- 3- Split Training
- 4- Split Training with Y-Scaling

When the P-value on the X-axis is lower this indicates that the method is successful. Figure 39 shows that Split Training with Y-Scaling (#4 in Figure 39) is the best method because it has the lowest error for carbonates. Figure 40 for trap rock and Figure 41 for non-carbonates also indicates that method #4 is the most accurate.

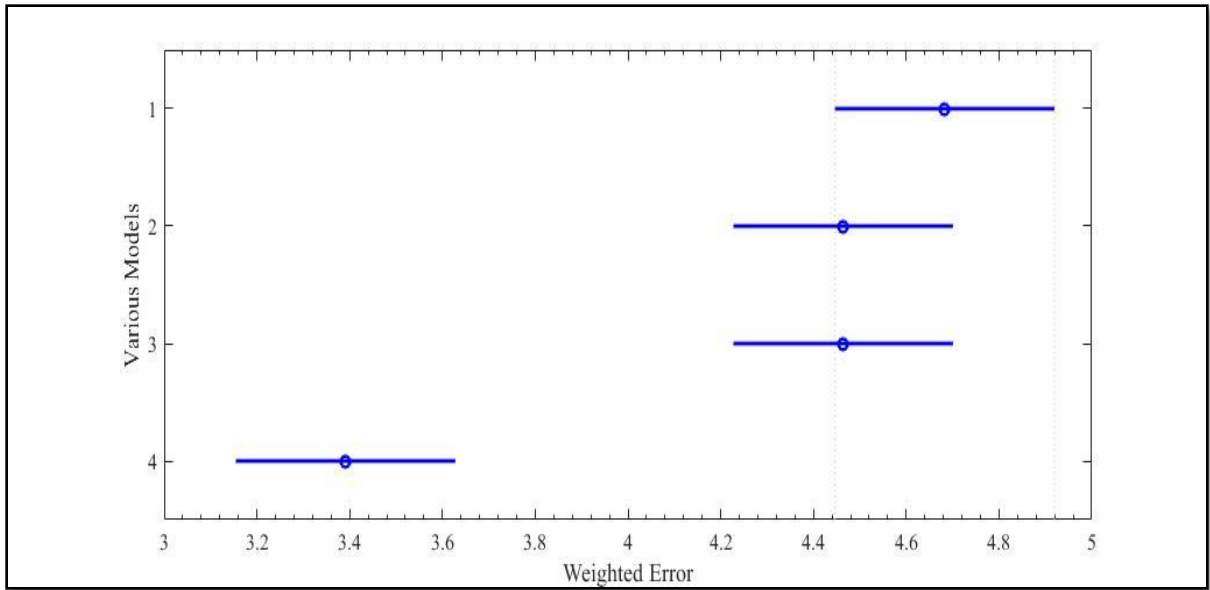


Figure 39. ANOVA results of various models for Carbonates

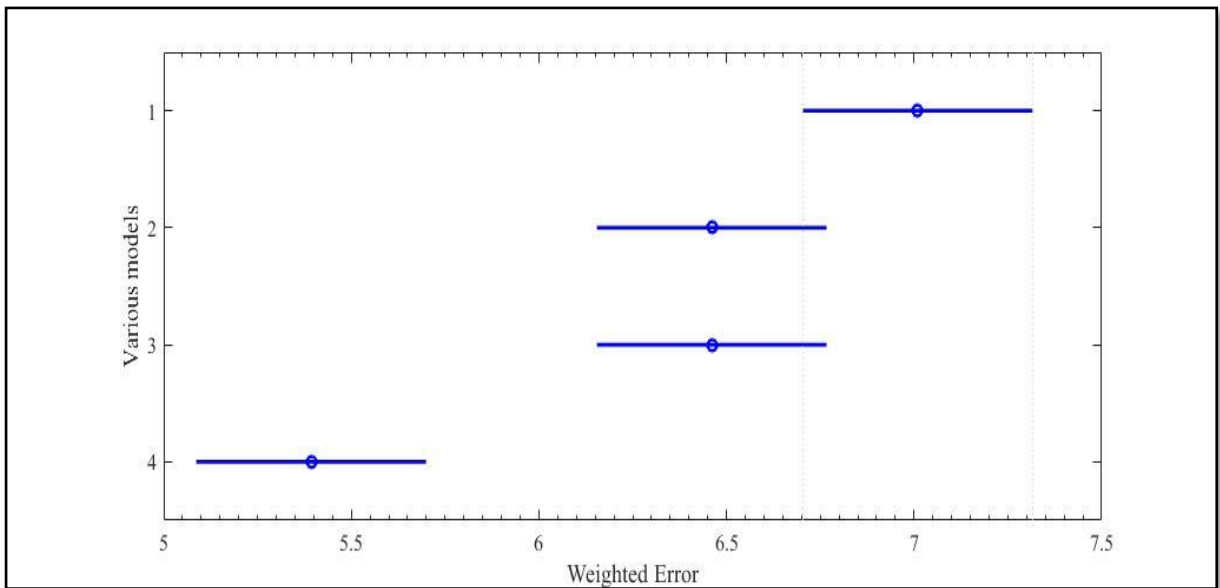


Figure 40. ANOVA results of various models for trap rocks.

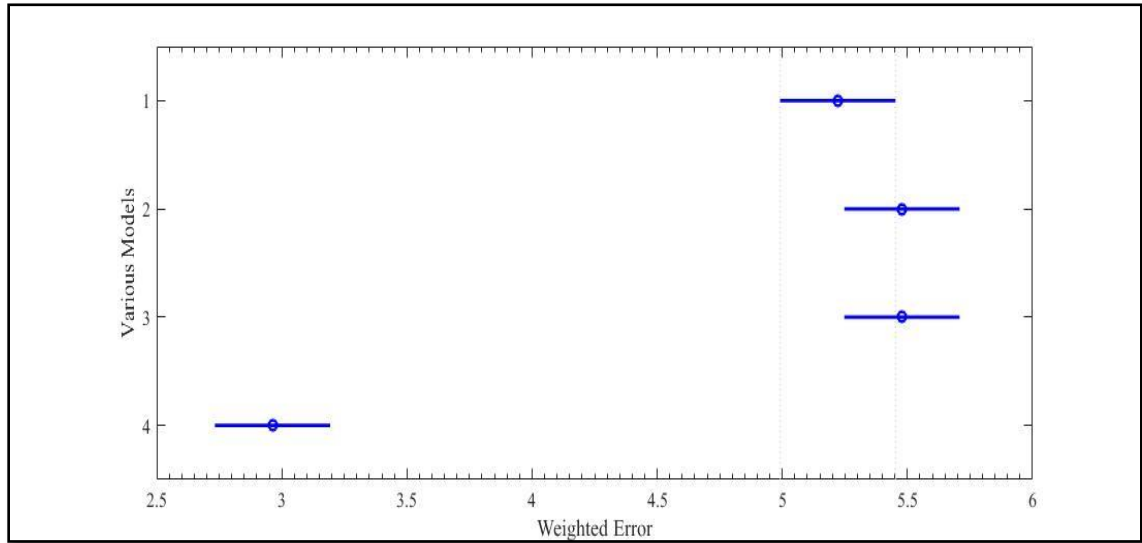


Figure 41. ANOVA analysis of various models for non-carbonates.

### **ANOVA for Various Classifications**

Two-way ANOVA is also conducted to determine the relative accuracy of the various classification methods. Figures 42 through 45 show the results from the ANOVA analysis for various split training classification methods. X-axis represents the error of each classification method. Y-axis represents each method of classification as follows:

- 1- One-Dimensional Classification
- 2- Two-Dimensional Line Classification
- 3- Two-Dimensional Ratio Classification
- 4- Three-Way Split Classification

Figure 42 displays the results of the ANOVA analysis for carbonates. Methods #3 and #4 are equally accurate with the lowest error. ANOVA analysis on trap rocks (Figure 43) shows that method #1 is more accurate compared to the other three methods. ANOVA analysis on non-carbonates (Figure 44) shows that methods #1, #3 and #4 are significantly different from method #2. However, method 4 is selected because it has slightly less error than methods #1 and #3.

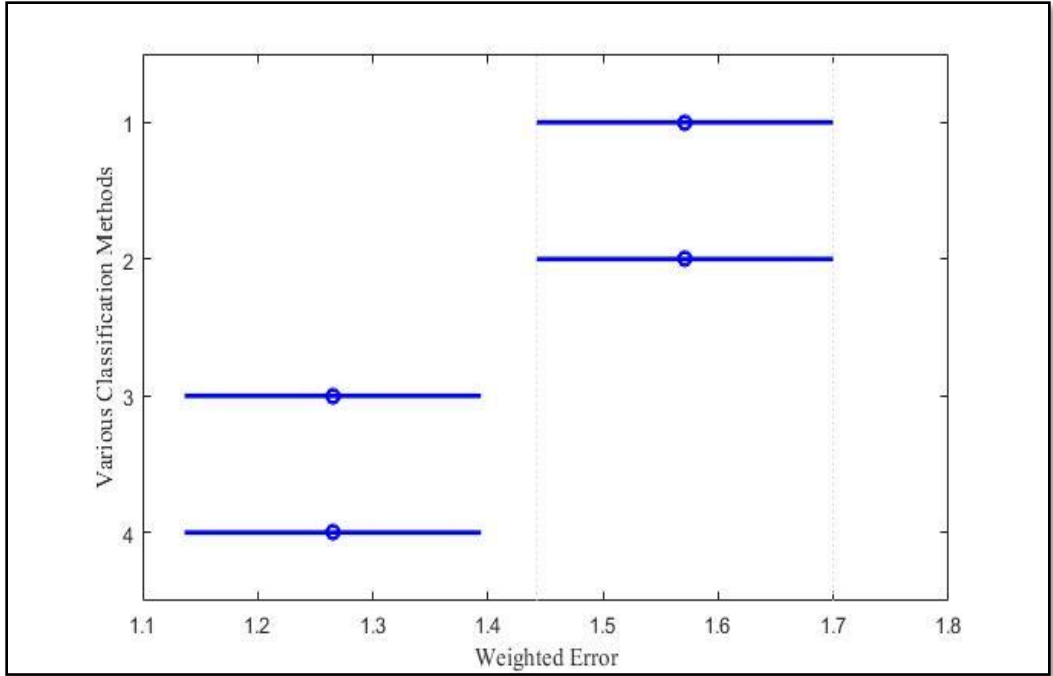


Figure 42. ANOVA results of various split training methods for Carbonates

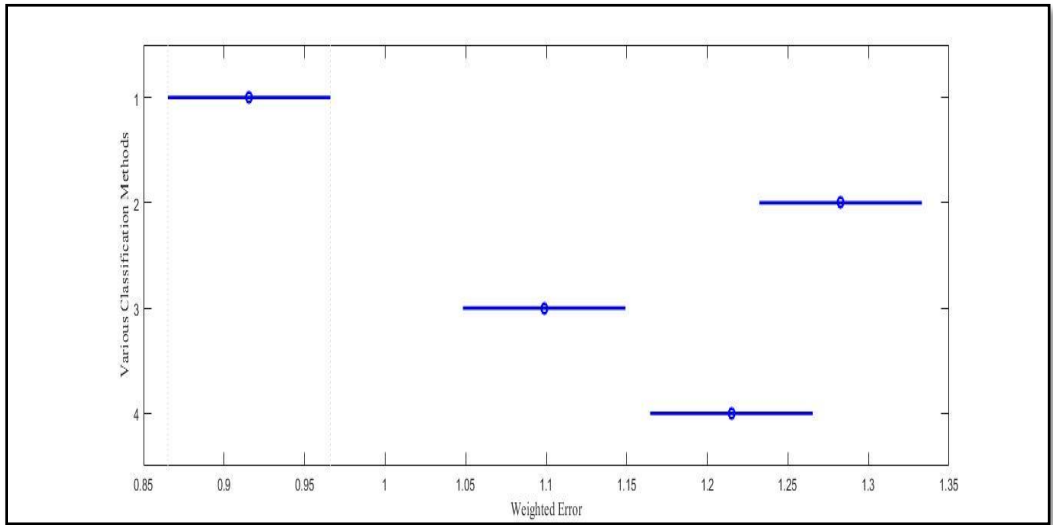


Figure 43. ANOVA results of various split training methods for Trap Rocks

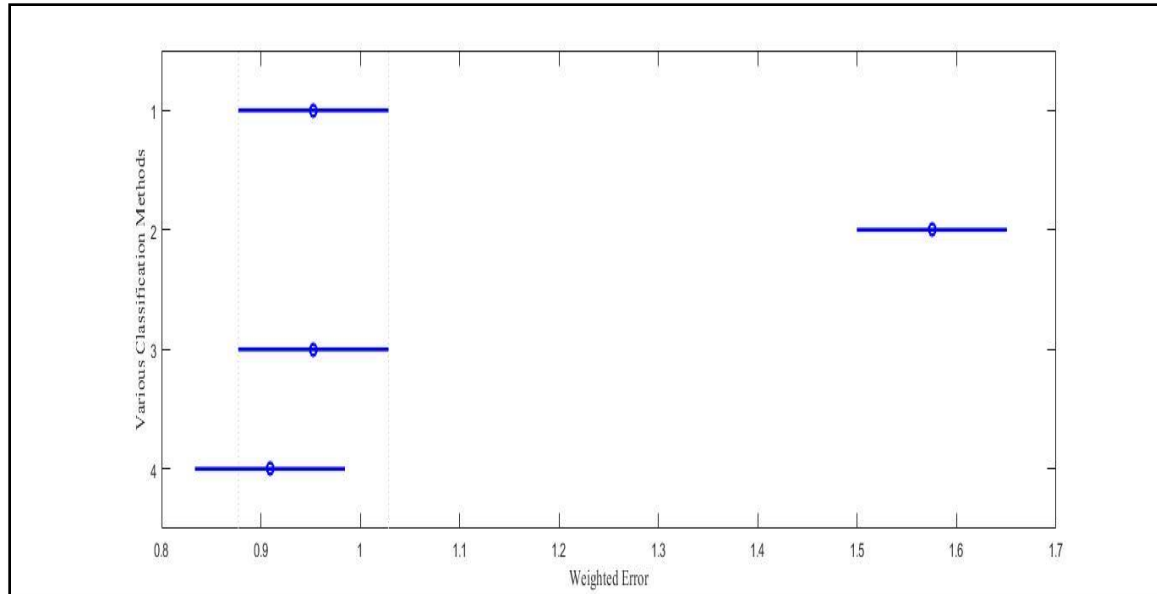


Figure 44. ANOVA results of split training methods for Non-Carbonates

### **High Pass Filter of LIBS Spectrum**

To improve the accuracy of the LIBS-PLSR analysis model, a filtering technique was developed to eliminate the Bremsstrahlung baseline, while preserving the remaining information. This called for the development of a code that could filter both the rock data used for training the PLSR model and the rock data to be tested. A filtering technique was developed in MATLAB as a preliminary step to the future integration of the filter method into the PLSR code, creating an easy-to-use graphical interface.

### **Moving Average Subtraction (MAS)**

To remove the baseline of the LIBS data, a moving average of the data was created with an adjustable value,  $N$ , which would take the average of the  $N$  values before and after each data point between  $N:(12,288-N)$ . Values 1:  $N$  and  $(12,288-N)$ : 12,288 were assigned as zero. By adjusting the  $N$  value, the peaks of the original data were eliminated, leaving only the baseline. This resulting baseline was then subtracted from the original data, and all negative values of intensity were set to zero intensity. This method removes the baseline height from the maximum intensity of the peaks with the assumption that the relevant data is shifted in intensity by the baseline. Figures 45 and 46 shows the effect of moving average subtraction.



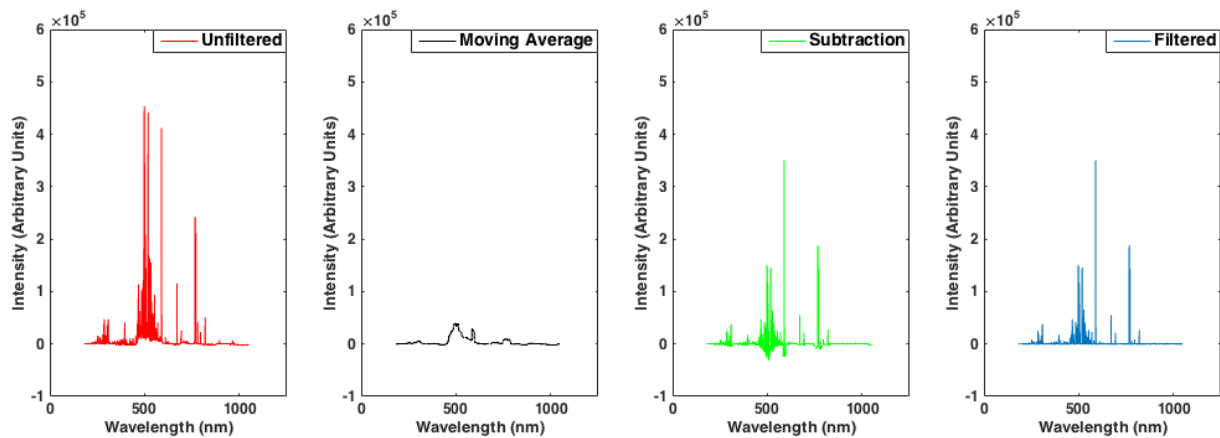


Figure 45. Left to right: Unfiltered Atkinson Quartzite data, moving average of data, subtraction of data, subtraction of moving average from original data, filtered data adjusted to eliminate negative values.

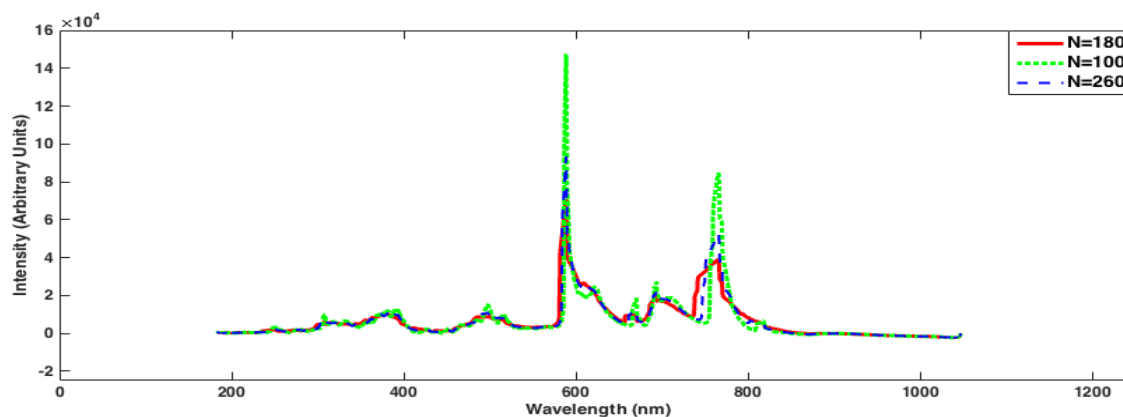


Figure 46. Subtraction from MAS filtration method showing the moving average N=180 to best conserve relevant information.

### Moving Slope Analysis (MSA)

An array consisting of 12,288 zero points was created. The original data was then scanned point to point to determine slope. If the slope,  $((J+1)-J)/1$ , was greater than or equal to 100, the corresponding J point in the zero array was assigned the value. By adjusting the slope value, the original peak data was preserved. This method preserved relative intensity when removing the baseline, with the assumption that the baseline overshadows relevant information.

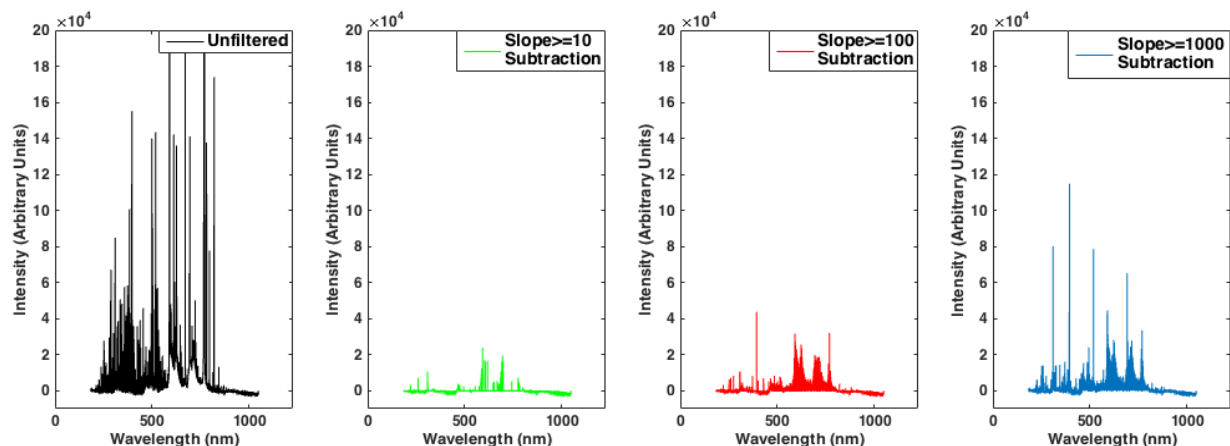


Figure 47. From Left to Right - Unfiltered Atkinson Quartzite data, moving slope analysis data, showing preservation of intensity information, filtered data subtracted from unfiltered data leaving only the baseline

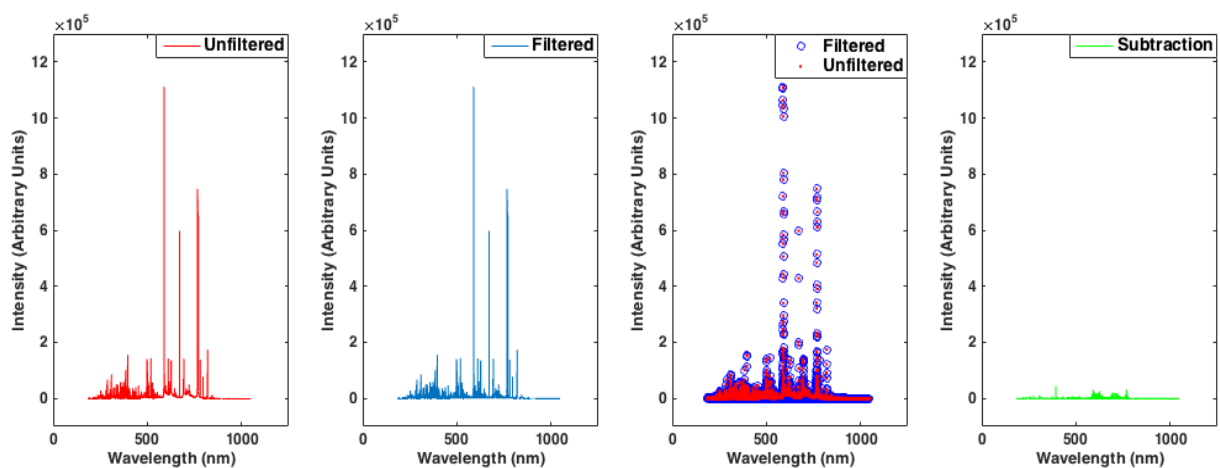


Figure 48. From left to right - Unfiltered Atkinson Quartzite data, moving slope analysis preserving data with slope $\geq 10$ , moving slope analysis preserving data with slope $\geq 100$ , moving slope analysis preserving data with slope $\geq 1000$ .

The effectiveness of the MAS filtering technique was maximized by varying the N value used for the average to determine which value would result in the greatest preservation of intensity peak data. An average of 361 data points surrounding each individual point, N=180 value, was shown to best preserve the data while still eliminating the baseline as shown in Figure 47. The MSA filtering technique was maximized similarly by determining the slope value that resulted in best conservation of the sharp intensity peak data as shown in Figure 48. The effectiveness of the filters was determined by comparing the results of the filtered model to the XRF values and the results of the unfiltered model. A student's t-test was performed with 95% confidence that the true value lies within the uncertainty of the mean. Figures 49 through 51 show the results of MSA and MAS filtering methods.

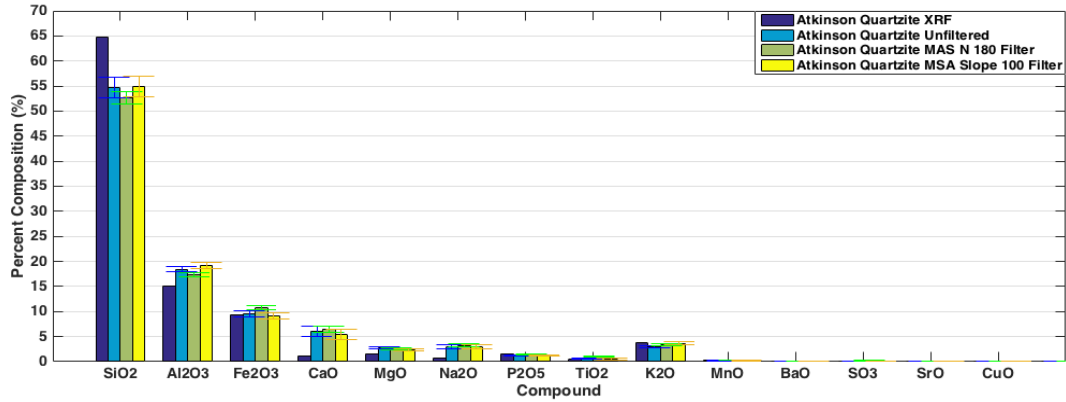


Figure 49. Comparing the output of the PLSR calculation of Atkinson Quartzite, error bars showing uncertainty of data with 95% certainty

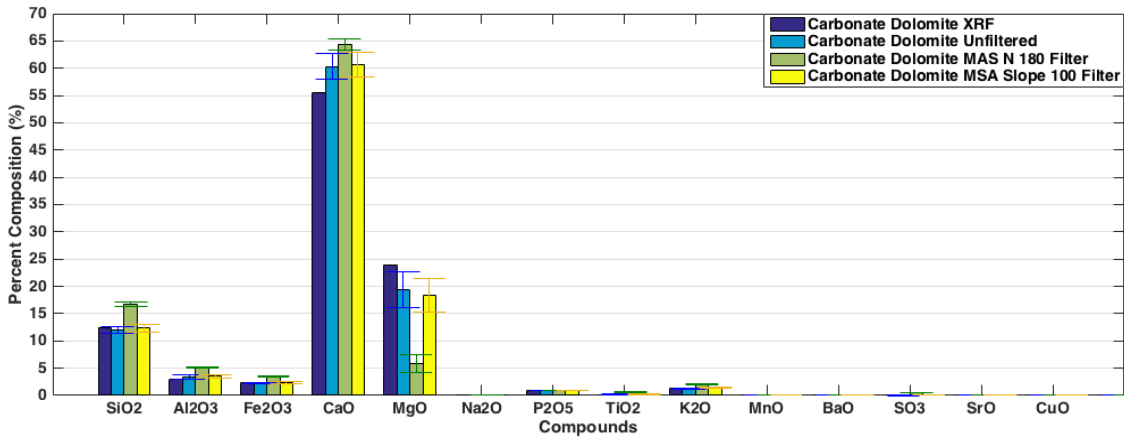


Figure 50. Comparing the output of the PLSR calculation of Carbonate Dolomite, error bars showing uncertainty of data with 95% certainty

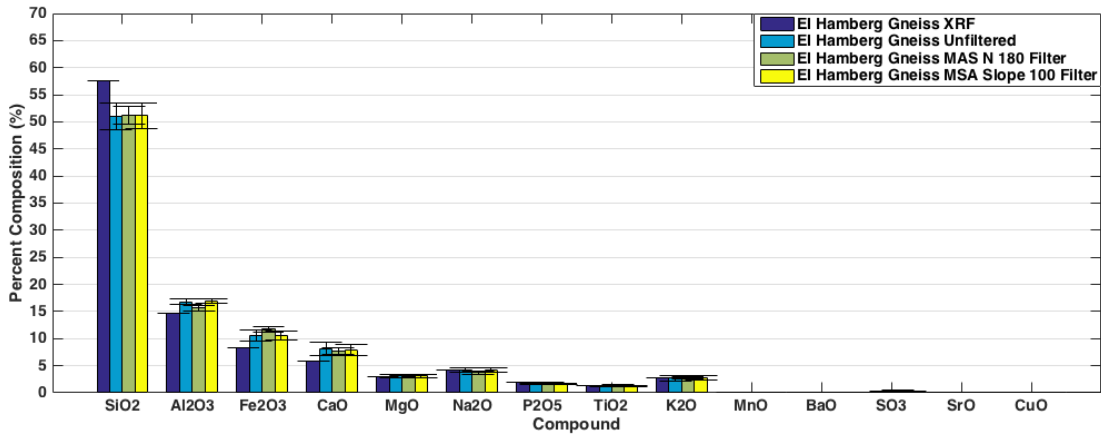


Figure 51. Comparing the output of the PLSR calculation of EI Hamburg Gneiss, error bars showing uncertainty of data with 95% certainty

### **Frequency cut off and slope detection**

This method uses a high-pass filter, in which each laser pulse reading had an associated cutoff frequency selected and values lower than this cutoff would be removed from the data. The hope was that this technique would remove any noise in the data generated by these frequencies. The ultimate goal of this was that the identified broadening would be removed.

This method was to find the standard deviation of the derivative of the laser system's readings. Using the standard deviation and a chosen slope threshold an edge detection system was developed that could differentiate the quick spikes in the data from the small, gradual raises. All rises in the 'Y' direction that were not equal to or greater than the chosen slope were filtered out, as any tiny or slow changes in the 'Y' direction of the data were considered to be noise. Figure 52 shows the filtered and unfiltered spectrums after high pass filtering.

Both methods worked with various samples. Although the broadening was successfully removed the filtered data seemed to have no significant effect on the accuracy of the results after tested in the analysis program. Due to fear of the filtering negatively effecting data in the future, it was removed from the process and deemed unnecessary. Figure 53 shows the comparison of results using filtered and unfiltered spectrums. Although the high pass filter removed the broadening of the spectrum, there is no improvements in the model predictions. Hence, the idea of removing the broadening of spectrum is not considered anymore.

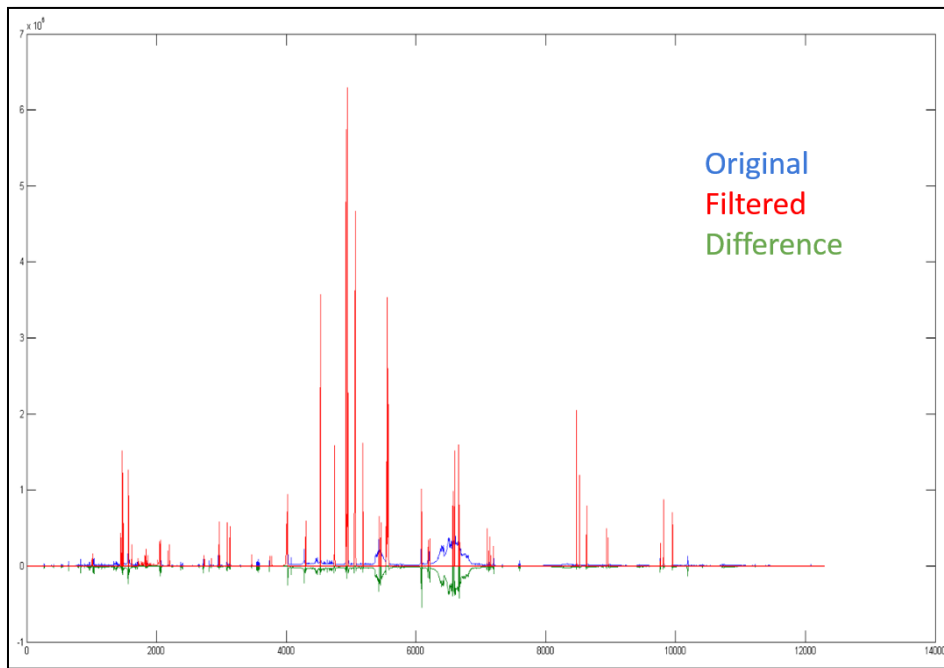


Figure 52. High Pass Filtering of LIBS spectrum

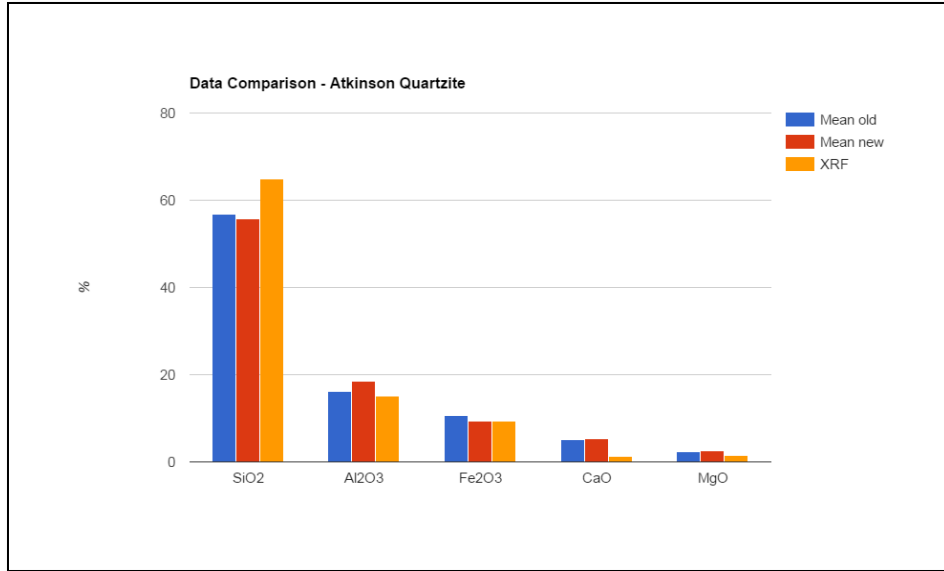


Figure 53. Results of High Pass Filtering of LIBS spectrum

#### Determination of a suitable sample size

Testing set size is determined based on the number of samples required for a stabilized prediction. Figure 54 shows predictions of Woodboro Carbonate for various testing set size. X-axis shows the total number of testing data used for each prediction and Y-axis shows the predicted values for the percentage of SiO<sub>2</sub>. As per the figure, a minimum of 30 data points is recommended. The number of samples tested is of greater importance than the number of locations tested per sample. Thus, a testing set size of 10 samples with 3 locations per sample is selected.

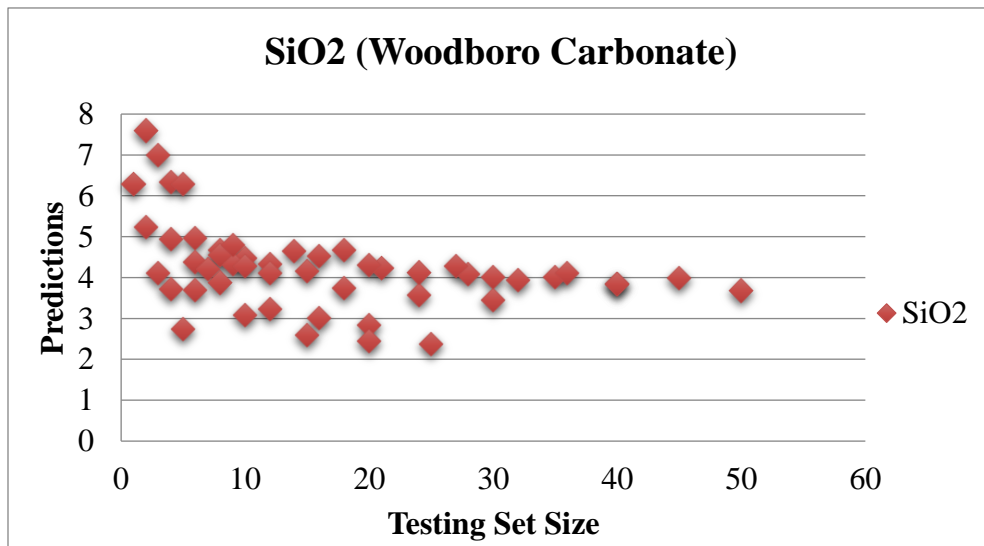


Figure 54. Determination of Testing Set Size

### Development of a User-Friendly Program

A Graphic User Interface (GUI) program is developed using MATLAB to analyze the LIBS spectrum. Figure 55 shows the GUI for the Laser Data Analysis Tool. It gives options for the various operating modes such as training the model, testing single aggregates at a time and testing a set of aggregates. In the training mode, number of PLS components are calculated by default or by manual input. For each testing mode, testing threshold defaults are 150 for carbonate and 500 for non-carbonate. Carbonate threshold classifies rocks into Carbonates and Non-Carbonates while non-carbonate threshold classifies rocks between Non-Carbonates and Trap Rocks. A custom threshold option is also provided. The user can select the input data and run the program. A *help* option is also provided to address any questions users would have about running the program. The directory to which results will be saved can be changed using *Settings*.

A GUI for updating the calibration data is also provided. Figure 56 shows the interface of the updated calibration tool. It provides the options to input the laser calibration data as a folder and the corresponding XRF data as an excel spreadsheet.

A stand-alone deployable software for these programs has been developed, which could be installed and used in any system without MATLAB. This software program will not allow users to make changes to the code or available features.

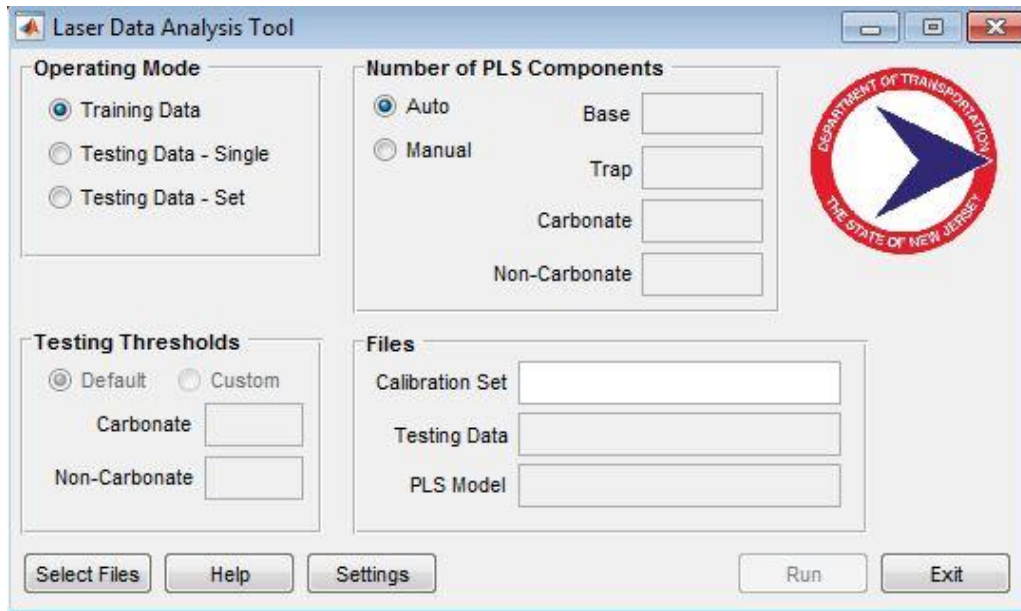


Figure 55. Laser Data Analysis Tool

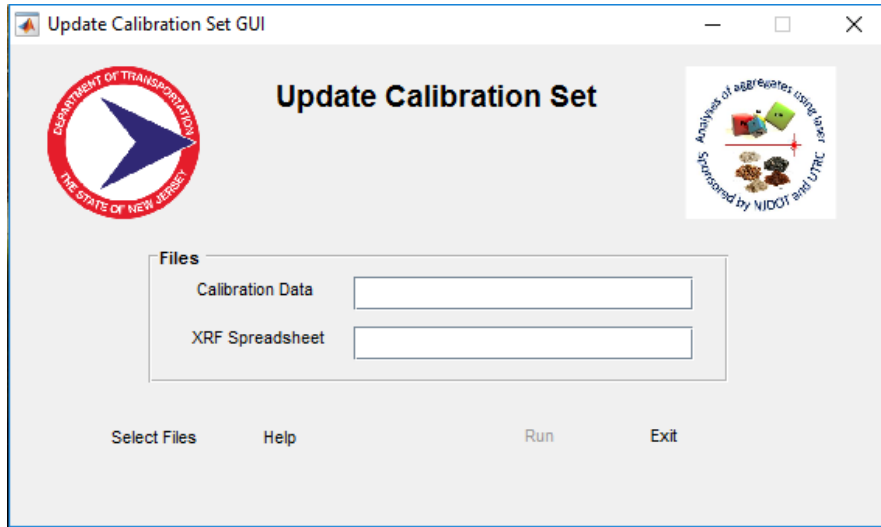


Figure 56. Update Calibration Tool

## Portable Equipment Testing

### Vibration/ Impact Testing

To test the durability and the resiliency of the portable laser system, the equipment was loaded into the back of a truck which was then subjected to high speeds and roadways with poor driving conditions. Sudden jerks and rigorous impacts due to pot holes, rutting, and overall inconsistencies in the roadway, as well as sudden application of the vehicle's brakes were applied to simulate an idealized worst case scenario for future customer use. The following tests were conducted on the same samples of the same batch of aggregates before and after the ride. Figures 57 through 59 depict the results for the vibration and impact testing.

The results look more or less the same before and after field test. The small variations can be attributed the typical shot-to-shot variations within the aggregate samples which has been experienced before and is to be expected.

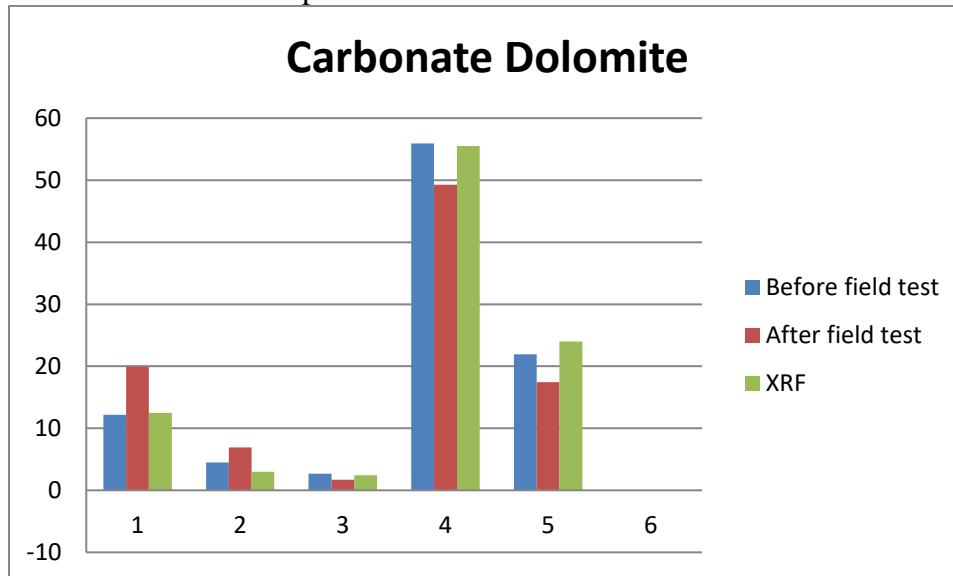


Figure 57. Vibration/ impact test results, Carbonate Dolomite

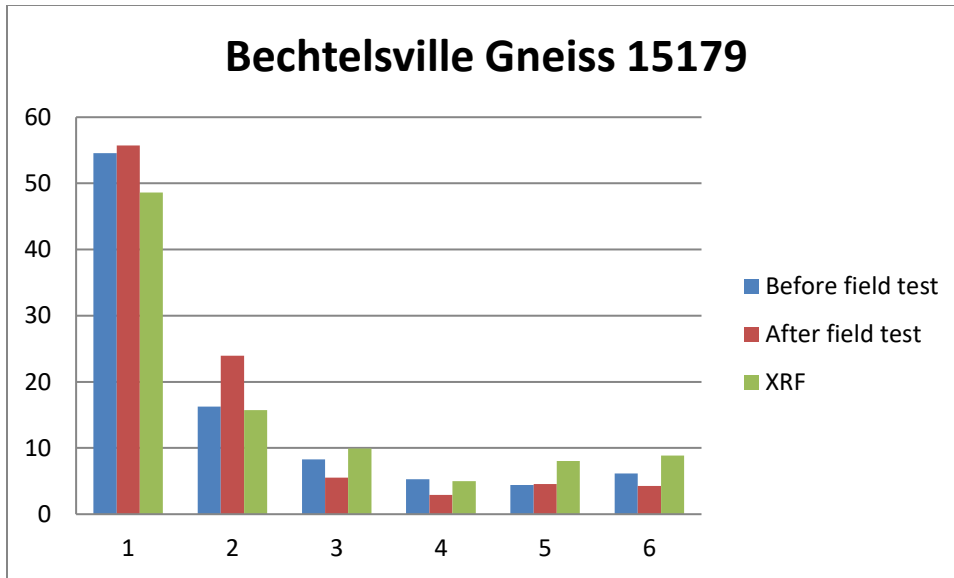


Figure 58. Vibration/ impact test results, Bechtelsville Gneiss 15179

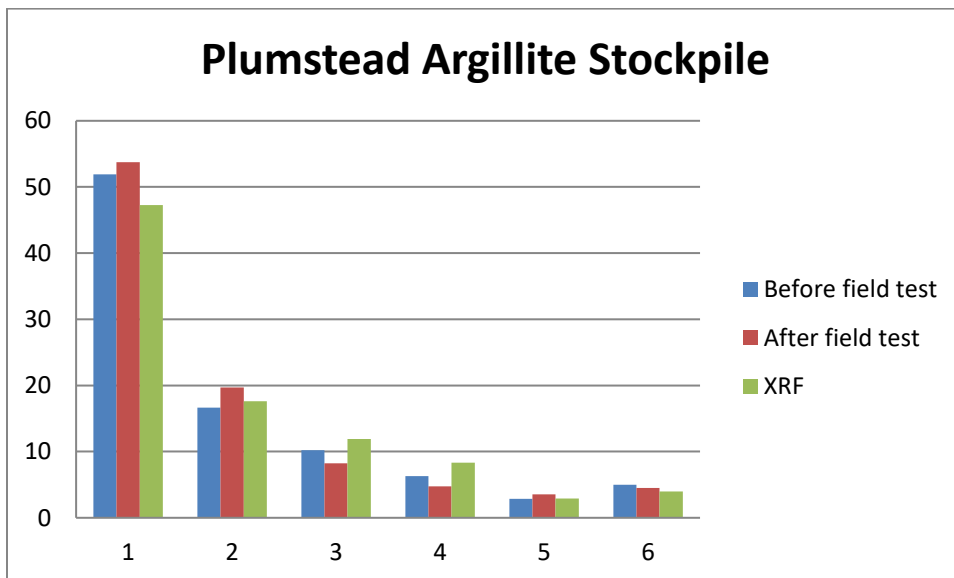


Figure 59. Vibration/ impact test results, Plumstead Argillite Stockpile

### Temperature Testing

The equipment was kept in the field and allowed to cool off and heat up to the atmospheric temperature within a 4-hour time frame. It was then tested on the same sample of aggregates from the same stockpile of rocks at various temperatures to depict the field conditions. Finally, these were compared with the results obtained in the laboratory conditions at a room temperature of 68 °F.

Figure 60 and 61 shows the results of temperature testing for Carbonate Dolomite and Plumstead Argillite Stockpile. The results show a wide variation of results at the various temperatures. Testing at the temperature of approximately 79 °F and room temperature with an average of 68 °F gives results close to the XRF values. This has been deemed acceptable while testing at 54 °F and



32 °F had a wide variation from acceptable values and therefore it has been concluded that this equipment should be utilized with temperatures above 60 °F and on less humid days.

The poor performance of the equipment is explained by the spectrums obtained at different temperatures 34 °F and 68 °F as shown in Figures 62 and 63. The first and third fiber optic channels of the spectrometer give negative light intensities. Since the Aurora module of spectrometer is not rugged to test outside of the laboratory freezing temperatures and humidity can affect the data collection which in turn affect the results. The ultra Quantel laser has been manufactured for harsh environments and an anti-freeze cooling reagent is used as coolant. This minimizes the effect of laser on the poor data collection. Some spectrum processing was done to uplift the negative values of the spectrum, but it doesn't make improvements and hence neglected.

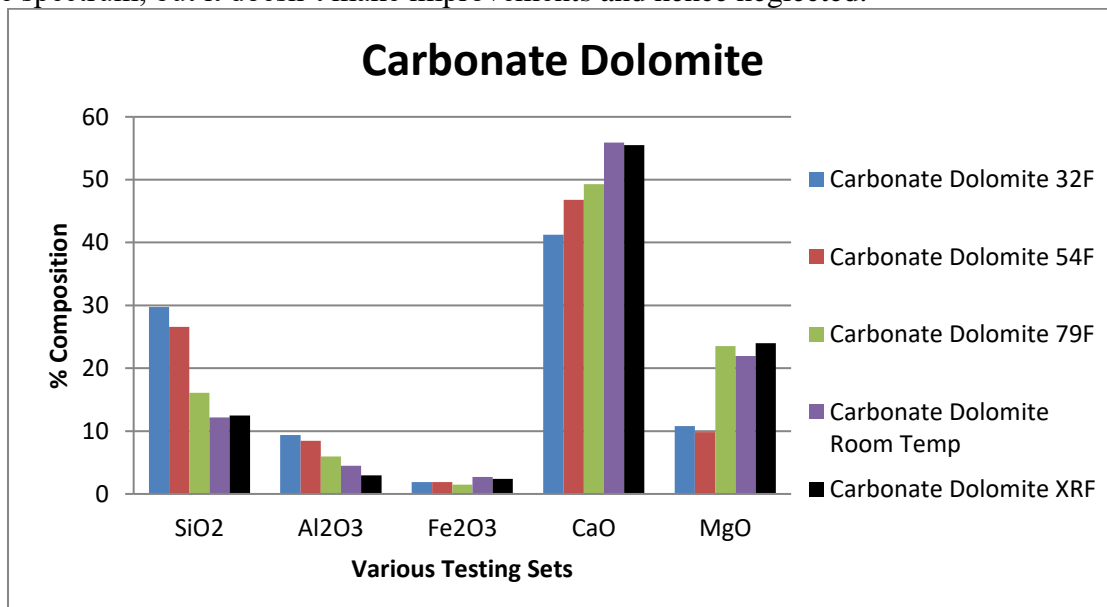


Figure 60. Temperature Testing, Carbonate Dolomite

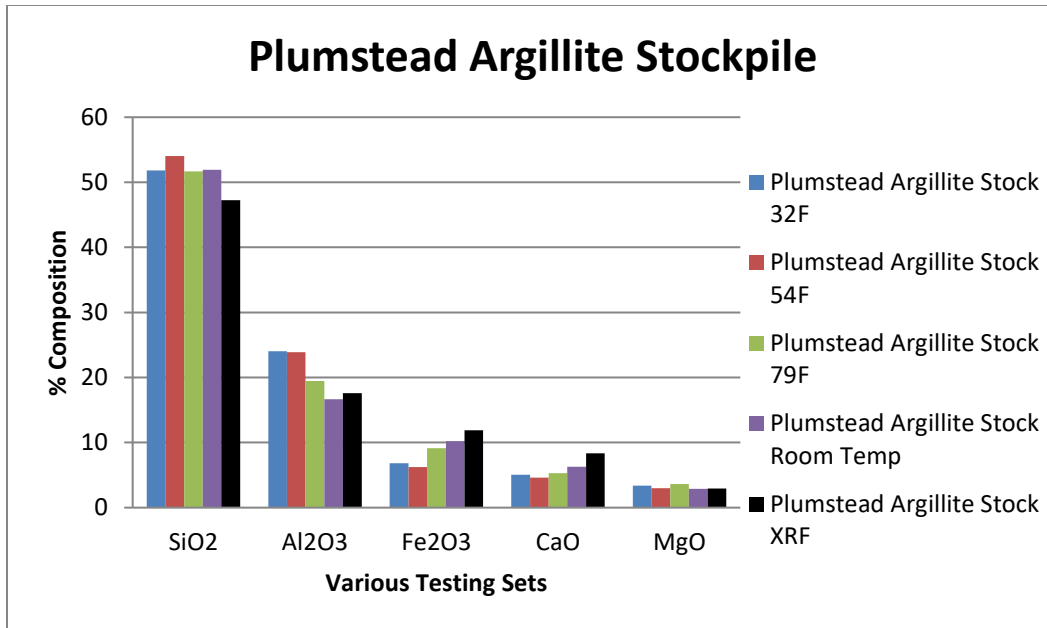


Figure 61. Temperature Testing Results, Plumstead Argillite Stockpile

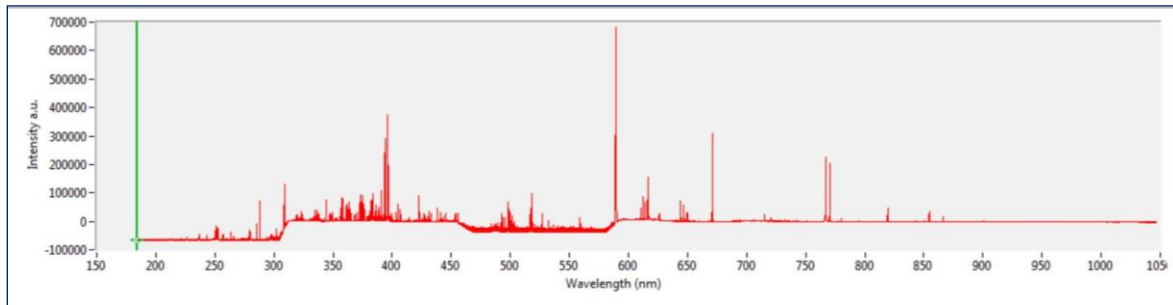


Figure 62. LIBS spectrum obtained at 34 deg. F

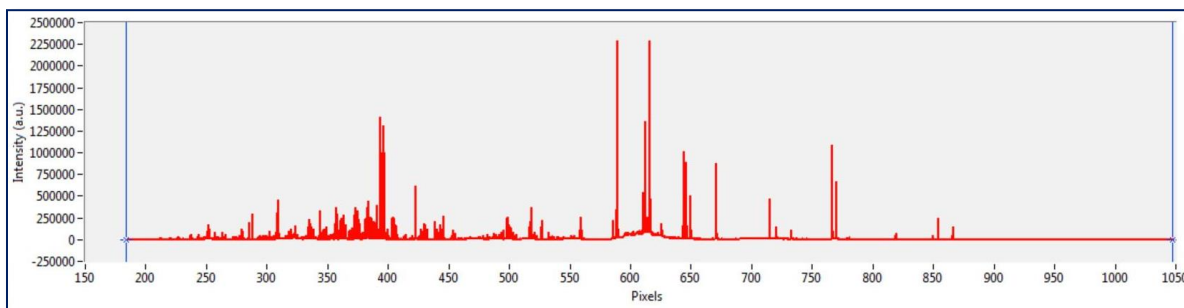


Figure 63. LIBS spectrum obtained at 68 deg. F. (laboratory condition)

**Sample Moisture Content Testing**

To understand the effect of moisture content of the sample on the results the samples were soaked in water for 24 hours. They were then wiped with a damp cloth and no other sample preparation had been done. These samples were tested before and after soaking. Figures 64 and 65 show the

results of sample moisture content testing. The testing depicts the samples collected after a rainy day and the results show that there does not appear to have any effect on LIBS testing.

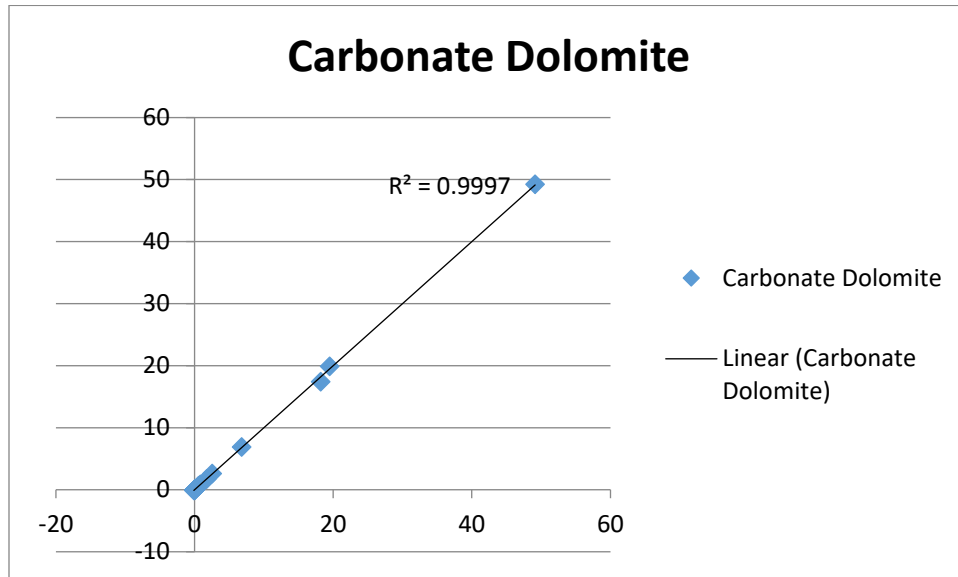


Figure 64. Sample moisture content testing results, Carbonate Dolomite

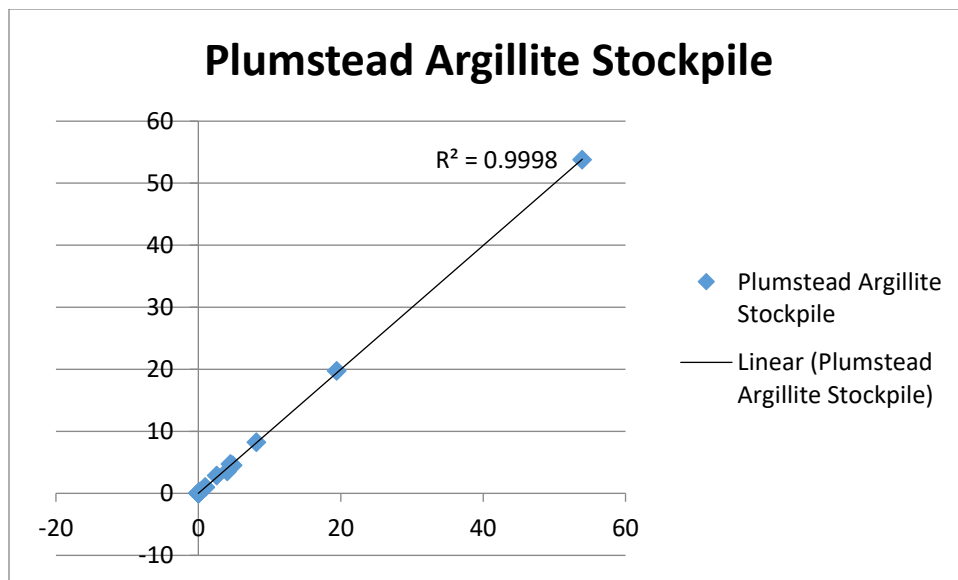


Figure 65. Sample moisture content testing results, Plumstead Argillite Stockpile

### **Testing of Affordability of the equipment**

Testing was done through LIBS spectrum using a high as well as a low-resolution spectrometer. Data was collected from the same sample and same location of an aggregate of Atkinson Quartzite. The Aurora module of high resolution spectrometer has a resolution of 12288 points. Figure 66 shows the results for lower resolution spectrometer. Although various resolutions give the same result as that of the higher resolution spectrometer, the results are slightly better for lowest resolution (1/20<sup>th</sup>). This may be due to the reduced sensitivity of the low-resolution spectrometer to the signal noises.

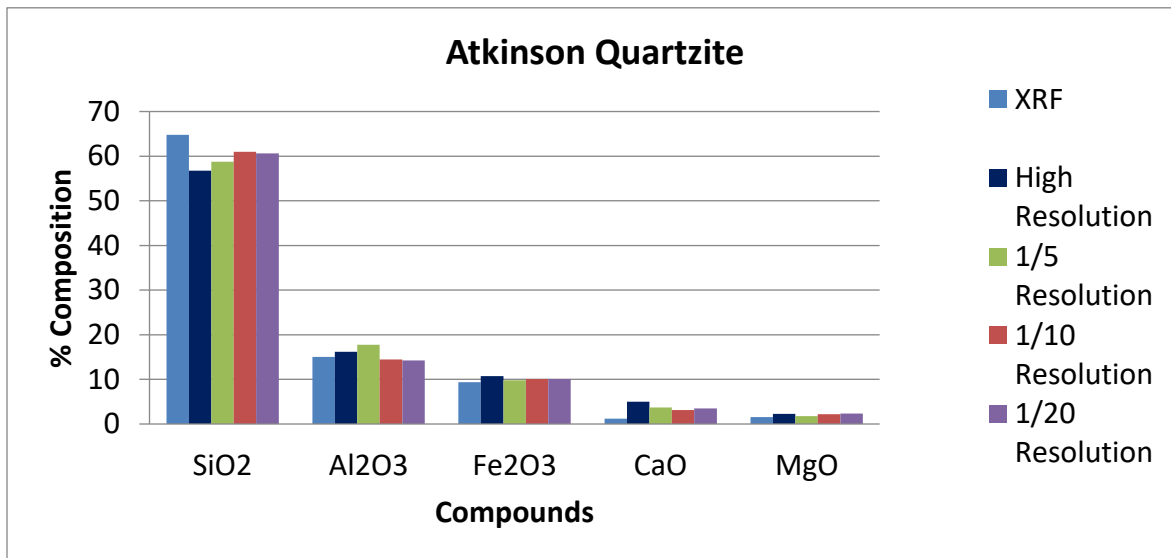


Figure 66. Testing of the equipment using lower resolution spectrums

## CONCLUSIONS

The purpose of this project is to utilize LIBS to analyze the mineral composition of aggregates in the field, and ensure said aggregate samples meet NJDOT standards. A review of previous literature and applications of LIBS has shown the system to be an attractive alternative to conventional chemical testing procedures. LIBS involves the use of a pulse laser to ablate and excite particles in a mass. As these particles return to normal energy states they emit photons of characteristic wavelengths which can be collected and fed into a spectrometer to obtain a spectrum of emitted light. The corresponding elements for wavelengths of light can be determined from the NIST atomic spectra database. Previous applications by other state DOTs using LIBS to analyze the composition and characteristics of aggregate samples have generally met with success. These analyses generally utilized PLSR analysis to develop predictive models by relating variation in spectrum traits to variation in a mineral concentration or other aggregate properties using known samples. Such models can then be used to determine the mineral concentrations or traits in an unknown sample from the light spectrum it produces. A number of models have been generated using Partial Least Squares Regression and subsequently tested. While preliminary models were inaccurate and unreliable, after several iterations of testing procedure modifications and numerous variations of data preprocessing and calibration parameter adjustments, reasonably accurate and consistent predictive models have been created using a split training set strategy. Split Training with Y-Scaling is found to have more accurate predictions with three way split classification system. The conclusions from the model testing are the following.

- Split Training with Y-Scaling using a Three-Way Split classification is found to be the best model with an overall accuracy of 90%.
- 35 rocks were used to calibrate the model with 10 Carbonates, 8 Trap Rocks and 17 Non-Carbonates.
- A standard testing set size is determined as 10 samples with 3 locations per sample to represent the aggregate stockpile. The initial 200 laser shots are neglected to eliminate the

surface dust contamination and also to stabilize the peak light intensity collected. The accumulated data of succeeding 100 shots are saved per locations.

- No sample preparation is needed for this testing. Brush the sample with a damp cloth to remove the surface dust.
- Testing for a single stone type takes less than an hour to collect the LIBS spectrum, analyze the data and predict the result.
- Various high pass filtering methods are considered to remove the broadening of the spectrum. This idea of smoothing the spectrum is not pursued further in this study as it did not produce significant improvement in test results.
- A user-friendly GUI program is developed for easy analysis of LIBS data. The user can browse the data needed to be analyzed. Manual input options are also provided for the number of PLS components and also for the carbonate, non-carbonate threshold values. A stand-alone software for the data analysis program is developed, named “Laser Analysis Tool,” which can be installed and used in any system without MATLAB. A program for expanding the calibration set in future is developed, which will automatically create the analysis input file needed for the model training.
- The portable equipment is built to handle the vibrations and the impact caused by poor roadway and driving conditions.
- The portable equipment is tested for various atmospheric temperatures by allowing it to cool/heat to the atmospheric temperature in 4hrs. It is found that the portable equipment gives reliable test results at 60<sup>0</sup>F or above. The equipment should be stored in a temperature controlled room during winter to avoid the damage to the spectrometer caused by the freezing weather.
- The aggregate samples with high moisture content were also tested with no impact on the accuracy of the results obtained.
- This equipment is also tested with a low cost, temperature controlled, lower resolution spectrometer (Flame Miniature Spectrometer from Ocean Optics) and found producing similar results with the same accuracy. Thus the equipment can be made 50% more affordable in the future.
- A manual is developed for the end users that includes the safety precautions, operation and maintenance of the equipment and trained the NJDOT personnel to equip them to use the equipment.

In conclusion,

1. Laser Induced Breakdown Spectroscopy can be used to quantify the chemical composition of aggregate stone samples.
2. Partial Least Square Regression Analysis can be used to develop predictive models to predict the aggregate composition.
3. Split Training with Y Scaling with a Three-Way Split classification produce accurate results.
4. A Graphical User Interface program facilitates rapid model testing and future refining of the models.
5. The equipment is feasible and affordable as a portable tool for field use and is efficient in terms of time and cost compared to XRF.

## REFERENCES

1. Chesner, Warren and McMillan, Nancy. "Automated Laser Spectrographic Pattern Matching For Aggregate Identification." *Highway IDEA Project 150*, 2012, pp 38.
2. Cremers, D. A. and Radziemski, L. J, Handbook of Laser-Induced Breakdown Spectroscopy. John Wiley & Sons, Ltd, 2006.
3. Giacomo, A. De et. al. "Experimental and theoretical comparison of single-pulse and double-pulse laser induced breakdown spectroscopy on metallic samples" *Spectrochimica Acta Part B*, Vol. 63, (2008), pp 805–816.
4. Mansoori, A. et. al. "Quantitative analysis of cement powder by laser induced breakdown spectroscopy" *Optics and Lasers in Engineering*, Vol. 49, (2011), Issue 3, pp 318-323.
5. Nelson, Stephen. (2013). "Mineral Chemistry." *Tulane University*. <[http://www.tulane.edu/~sanelson/eens211/mineral\\_chemistry.htm](http://www.tulane.edu/~sanelson/eens211/mineral_chemistry.htm)> (Oct. 25, 2013)
6. Celio Pasquini, Juliana Cortez, Lucas M. C. Silva and Fabiano B. Gonzaga, "Laser Induced Breakdown Spectroscopy" *J. Braz. Chem. Soc.*, Vol. 18, (2007), No. 3, 463-512.
7. Warren H. Chesner and Nancy J. McMillan "Automated Laser Spectrographic Pattern Matching for Aggregate Identification." *Highway IDEA Project 150*, 2012, pp 35.
8. A. Taffe, D. Schaurich & G. Wilsch *Concrete Repair, Rehabilitation and Retrofitting II*. Taylor and Francis Group, London, 2009.
9. E. Tognoni, Cristoforetti G., Legnaioli S., & Palleschi V. "Calibration-Free Laser-Induced Breakdown Spectroscopy: State of the art" *Spectrochimica Acta Part B*, Vol. 65, pp 1–14, 2009.
10. Tucker, J.M., Dyar M. D., Schaefer M. W., Clegg S.M., Wiens R. C., "Optimization of laser-induced breakdown spectroscopy for rapid geochemical analysis" *Chemical Geology*, Vol. 277, Issues 1-2, 2010, pp 137-148.
11. W. Wessel, A Brueckner-Foit, J. Mildner, L. Englert, L. Haag, A. Horn, M. Wollenhaupt, T. Baumert "Use of femtosecond laser-induced breakdown spectroscopy for micro-crack analysis on the surface" *Engineering Fracture Mechanics*, Vol. 77, (2010), pp 1874-1883.
12. Xia, H. and M.C.M. Bakker. "Online Sensor System Based on Laser Induced Breakdown Spectroscopy in Quality Inspection of Demolition Concrete," *27th International Conference on Solid Waste Technology and Management*, (2012).
13. Ronald A. Fisher, *Statistical Methods for Research Workers*. Oliver and Boyd, Edinburgh, 1925.
14. <http://www.arl.army.mil/www/default.cfm?page=247>
15. <http://industrial-lasers.net/yag.html>

## APPENDIX A

Below is a summary of XRF results provided by the NJDOT. Note that this list only includes samples used for model calibration. Additional samples and chemical composition results have recently been received and will be incorporated into future models.

Rock Names	SiO <sub>2</sub>	Al <sub>2</sub> O <sub>3</sub>	Fe <sub>2</sub> O <sub>3</sub>	CaO	MgO	Na <sub>2</sub> O	P <sub>2</sub> O <sub>5</sub>	TiO <sub>2</sub>	K <sub>2</sub> O	MnO
Allen Myers Carbonate	13.8	6.725	2.195	43.25	31.3	0	0.7485	0.2265	1.235	0.0918
Andreas Lehigh Carbonate	42.75	19.8	5.485	20.8	4.985	0.5855	0.687	0.8165	3.185	0.072
Bechtessville Gneiss	51.55	15.3	9.61	5.3	5.945	8.275	1.135	1.435	1.02	0.1155
Braen Franklin Carbonate	1.81	0.581	1.405	71.3	23.7	0	0.5725	0	0.05845	0.2
Carbonate Dolomite	12.5	2.97	2.42	55.5	24	0	0.8705	0.1795	1.3	0.06685
Dyer Quarry Diabase	46.8	17.5	10.65	7.625	7.285	6.795	0.9015	1.455	0.5945	0.1645
EI Hamburg Gneiss	57.5	14.7	8.34	5.795	2.975	4.115	1.9	1.25	2.86	0.09225
Eureka Milford Quartzite	65.95	20.15	4.75	0.99	2.98	1.355	0.474	0.6405	2.285	0.0999
Fanwood Traprock	43.2	15.95	10.75	8.22	11.25	8.45	0.7115	0.889	0.247	0.167
Hanson Glen Gneiss	54.15	13.15	11.85	6.715	3.295	3.205	2.185	1.9	2.215	0.178
Kingston Argillite	41.45	17.8	12.1	7.32	8.17	8.595	1.003	0.7935	2.11	0.238
Kingston Trap Rock	45.95	16.7	12.065	10.465	7.275	4.235	0.985	1.161	0.65	0.202
Lehigh Asphalt Carbonate	35.85	7.25	8.885	35.2	3.195	0.775	1.27	1.41	3.965	0.124
New Hope Crushed	17	6.065	2.05	44.15	26.7	1.445	0.3336	0.3395	1.475	0.0858

Stone Carbonate										
OW Traprock Orange Basalt	43.2	16.1	10.25	8.575	10.4	9.41	0.6765	0.8265	0.2545	0.188
Westfield Traprock	45.3	17.1	12.25	7.88	7.215	7.625	0.728	0.7815	0.786	0.1965
Pioneer Laflin Quartzite	66.2	24.35	3.145	0.3775	1.265	0.5595	0.3795	0.654	2.795	0.0666
Temple Quartzite	87.8	8.87	0.2575	0.1365	0.469	0	0.378	0.904	0.931	0
Atkinson Quartzite	64.8	15.05	9.39	1.21	1.575	0.756	1.64	0.545	3.79	0.245
Woodboro Carbonate	14.85	5.23	3.055	69.65	3.11	0	0.932	0.5775	1.865	0
Plumstead Argillite Belt	49.75	16.4	12.95	6.955	2.055	3.585	1.795	1.345	4.015	0.2345
Plumstead Argillite Stockpile	47.25	17.6	11.9	8.34	2.93	3.98	1.57	1.17	4.17	0.2195
Tilcon Diabase	46.95	16.45	13.95	11.4	3.805	3.435	1.53	1.325	0.7145	0.195
Newhope Carbonate	17.9	5.52	3.585	54.45	14.05	0.7885	0.943	0.574	1.71	0.118
Eastern Wantage Carbonate	14.5	4.99	1.565	42.45	33.95	0	0.574	0.1875	1.55	0.0295
Tilcon Oxford Carbonate	7.29	1.96	5.755	74.05	8.47	0	0.742	0.356	0.301	0.336
Plumstead Argillite Lockatong	50.1	18.55	10.2	6.93	2.52	4.55	1.48	1.165	3.645	0.186
Tilcon Oxford Gneiss	64.6	13.05	5.545	4.935	1.79	4.98	1.38	0.697	1.83	0.1085
Eastern Hamburg Gneiss Losee	70.4	13.9	2.27	4.655	0.8475	4.33	1.31	0.255	1.77	0.04575
Moores Argillite	33.55	9.4	32.15	11.85	1.08	0.2355	1.27	2.35	6.135	0.516



Traprock Ind										
Bechtelsville Gneiss 15179	48.6	15.7 5	9.93	5.005	8.025	8.84	0.605	1.115	1.53	0.1075
Plumstead Argillite 15165	49.0 5	19.7	6.61	4.525	4.995	10.15	0.908	0.6985	2.64	0.1285
Tarheel Quartzite	77.9	0	8.98	0.461	4.34	1.09	1.505	1.37	3.86	0.186
Kingston Traprock 15219	45.1 5	16.6 5	9.54	8.49	11.45	6.125	0.803	1.095	0.426 5	0.165
Pyramid Gneiss	45.7 5	0	33	4.985	0.622 5	0.099	1.33	3.875	7.95	0.439

## APPENDIX B

### Algorithm, for Split Training and Y-Scaling Model

#### plsregress function as per MATLAB 2015 (Copyright 2007-2010 The MathWorks, Inc.)

```
%%%%%%%%%%%%%%%%%%%%%%%%%%%%%%%%%%%%%%%%%%%%%%%%%%%%%%%%%%%%%%%%%%%%%%%%
% function laseranalysis(rock_data, PLS, ncomp_in, mode_custom_thresh)
%
% This function handles the training and testing of a PLS model to predict
% the chemical components of an observed data set. In training mode, this
% function will take the observed X data and known Y data as well as the
% number of PLS components to use and train a PLS model, saving the beta
% matrix for use in testing. In testing mode, the function loads the saved
% beta matrix and creates a predicted chemical composition for the observed
% data set.
%
% Inputs:
%   rock_data - struct containing X and Y data with same number of
%   observations and corresponding rows aligned (training) or a matrix
%   containing all of the X data (testing)
% (X - observed data set. In training this contains the spectrometer data
%   for all aggregate stones. In testing, this contains the spectrometer
%   data for just one aggregate stone.
%
%   Y - known data set. In training, this contains the known composition
%   of all aggregate stones. For testing, enter 0 for this input.)
%
%   PLS - struct containing PLS generated in training mode. Only used in
%   testing mode. For training mode, this input will be null.
%
%   ncomp - number of PLS components to be used in training the PLS model.
%   In training mode enter the number of PLS components to use or enter a
%   number <= 0 to automatically use the maximum PLS components. In testing
%   mode, enter 0 for this input.
%
%   mode - 'train' or 'test' (obtained from GUI)
%
% Outputs:
%   Training mode - Saves the PLS model in a struct; contains beta matrix
%   necessary for testing.
%   Testing mode - Saves the predicted chemical composition for the input
%   observed spectrometer data.
%%%%%%%%%%%%%%%%%%%%%%%%%%%%%%%%%%%%%%%%%%%%%%%%%%%%%%%%%%%%%%%%%%%%%%%%

function laseranalysis(rock_data, PLS, ncomp_in, mode, thresholds,
resultsFigName, settingsSave_dir, TStamp)
% TRAINING MODE %
if(strcmp(mode, 'train'))
    w = waitbar(0, 'Generating PLS Model...', 'Name', 'Please Wait...');
    try
        frames = java.awt.Frame.getFrames();
        frames(end).setAlwaysOnTop(1);
    catch
```

```

end

% LOAD DATA IF FUNCTION IS CALLED FROM GUI
if(ischar(rock_data))
    disp('Loading Rock Data.')
    rock_data = load(rock_data);
    rock_data = rock_data.rock_data;
    X = rock_data.X;

    disp('Loading Y Data.')
    Y = rock_data.Y;
    classer = rock_data.C;
end

%%%%%%%%%%%%%%%%%%%%%%%%%%%%%%%%%%%%%%%%%%%%%%%%%%%%%%%%%%%%%%%%%%%%%%%%
% PREPROCESSING STAGE %
%%%%%%%%%%%%%%%%%%%%%%%%%%%%%%%%%%%%%%%%%%%%%%%%%%%%%%%%%%%%%%%%%%%%%%%%
% NOTE %
%%%%%%%%%%%%%%%%%%%%%%%%%%%%%%%%%%%%%%%%%%%%%%%%%%%%%%%%%%%%%%%%%%%%%%%%
% This stage can eventually contain all of the different types of
% preprocessing techniques we want to test. This includes the split
% training technique, Y-scaling, and normalizing the data to total
% light emission.
%%%%%%%%%%%%%%%%%%%%%%%%%%%%%%%%%%%%%%%%%%%%%%%%%%%%%%%%%%%%%%%%%%%%%%%%

waitbar(1/10,w);
% Remove light intensity values less than 0.
[m,n]=size(X);

disp('Removing negative light intensity values.')
for i=1:m
    for j=1:n
        if X(i,j)<0
            X(i,j)=0;
        end
    end
end
waitbar(3/10,w);
% Normalizing Data to Total Light Emission
disp('Normalizing spectra to total light emissions.')

% Initializing total light intensity.
total_light_int=zeros(m,1);

for i=1:m
    for j=1:n
        total_light_int(i) = total_light_int(i) + X(i,j);
    end
end

% Determine Xnorm
Xnorm = zeros(m,n);
for i=1:m
    for j=1:n
        Xnorm(i,j) = X(i,j)/total_light_int(i);
    end
end

```

```

    end
end
waitbar(4/10,w);
% Perform Y Scaling
numCol= size(Y,2);

% Initialize minmax matrix. Currently 2x24, but it can be of varying
% size.
minmax_base = zeros(2, numCol);
for i = 1:numCol

    maxVal = max(Y(:,i));
    minVal = min(Y(:,i));
    minmax_base(2,i) = minVal;
    minmax_base(1,i) = maxVal;
    val_range = maxVal-minVal;
    if(val_range == 0)
        Yscaled(:,i) = 0;
    else
        Yscaled(:,i) = (Y(:,i) - minVal)/val_range;
    end

end

waitbar(5/10,w);
% NOTE: Do Y scaling for Carb and Nonc models after splitting into
% separate matrices

% Determine pls components if set to 'Auto'
% THIS NEEDS TO BE DONE SEPARATELY FOR EACH OF THE SPLIT TRAINING
% MODELS

ncomp_base_in = ncomp_in.Base;
if ncomp_base_in<=0;
    disp('Determining optimal number of PLS components for Base model.')
    ncomp = 25;

    % Find PLS regression for starting number of ncomp
    [~,~,~,~,~,PCTVAR] = plsregress(Xnorm,Yscaled,ncomp);
    pctvar_count = 0;
    PCTVAR = 100*PCTVAR;

    % Set ncomp to max number that explains >1% of variation
    for i = 1:ncomp
        if (PCTVAR(2,i) >= 1)
            pctvar_count = pctvar_count + 1;
        else
            break;
        end
    end
    ncomp = i - 1;
    disp(['Number of Base PLS components automatically set to ',
num2str(ncomp), '.']);
else
    ncomp = ncomp_base_in;
end

```

```

waitbar(7/10,w);
% PLS REGRESSION
disp('Generating Broad Base PLS Model.')
[~,~,~,~,betamat,PCTVAR] = plsregress(Xnorm,Yscaled,ncomp);

% Creates a structure with all of the PLS Model variables to be saved as
a
% .mat file.
PLS_Model_base = struct('Date', date, 'PercentVariation', PCTVAR, 'Beta',
betamat, 'MinMax', minmax_base);
PLS_Model_base.NComp = ncomp;

% SPLIT TRAINING
Ycarb = [];
Xcarb = [];
Ynonc = [];
Xnonc = [];
Ytrap = [];
Xtrap = [];
for i = 1:size(Y,1)
    switch classer(i)
        case 'c'
            Ycarb = cat(1,Ycarb,Y(i,:));
            Xcarb = cat(1,Xcarb,Xnorm(i,:));
        case 'n'
            Ynonc = cat(1,Ynonc,Y(i,:));
            Xnonc = cat(1,Xnonc,Xnorm(i,:));
        case 't'
            Ytrap = cat(1,Ytrap,Y(i,:));
            Xtrap = cat(1,Xtrap,Xnorm(i,:));
        otherwise
            error('Error in XRF Sheet used in Calibration. Unknown
classification')
    end
end

% Calculate ncomp for carbonate rocks
ncomp_carb_in = ncomp_in.Carbonate;
if ncomp_carb_in<=0;
    disp('Determining optimal number of PLS components for Carbonate
model.')
    ncomp_carb = 25;

% Find PLS regression for maximum number of ncomp
[~,~,~,~,~,PCTVAR] = plsregress(Xcarb,Ycarb,ncomp_carb);
pctvar_count = 0;
PCTVAR = 100*PCTVAR;
% Set ncomp to max number that explains >1% of variation
% Stop searching if two components in a row are found to explain
% less than 1%.
for i = 1:ncomp_carb
    if (PCTVAR(2,i) >= 1)
        pctvar_count = pctvar_count + 1;
    else

```

```

        break;
    end
    end
    ncomp_carb = i - 1;
    disp(['Number of Carbonate PLS Model components automatically set to
', num2str(ncomp_carb), '.']);
    else
        ncomp_carb = ncomp_carb_in;
    end

% Perform Y scaling for Carbonate rocks
minmax_carb = zeros(2, numCol);
for i = 1:numCol

    maxVal = max(Ycarb(:,i));
    minVal = min(Ycarb(:,i));
    minmax_carb(2,i) = minVal;
    minmax_carb(1,i) = maxVal;
    val_range = maxVal-minVal;
    if(val_range == 0)
        Yscaled_carb(:,i) = 0;
    else
        Yscaled_carb(:,i) = (Ycarb(:,i) - minVal)/val_range;
    end

end

%-----
% Calculate ncomp for noncarbonate rocks
ncomp_nonc_in = ncomp_in.Carbonate;
if ncomp_nonc_in<=0;
    disp('Determining optimal number of PLS components for Non-Carbonate
model.')
```

```

    ncomp_nonc = 25;

% Find PLS regression for maximum number of ncomp
[~,~,~,~,~,PCTVAR] = plsregress(Xnonc,Ynonc,ncomp_nonc);
pctvar_count = 0;
PCTVAR = 100*PCTVAR;
% Set ncomp to max number that explains >1% of variation
% Stop searching if two components in a row are found to explain
% less than 1%.
for i = 1:ncomp_nonc
    if (PCTVAR(2,i) >= 1)
        pctvar_count = pctvar_count + 1;
    else
        break;
    end
end
ncomp_nonc = i - 1;
disp(['Number of Non-Carbonate PLS Model components automatically set
to ', num2str(ncomp_nonc), '.']);
else
    ncomp_nonc = ncomp_nonc_in;
end

```

```

% Perform Y scaling for NonCarbonate rocks
minmax_nonc = zeros(2, numCol);
for i = 1:numCol

    maxVal = max(Ynonc(:,i));
    minVal = min(Ynonc(:,i));
    minmax_nonc(2,i) = minVal;
    minmax_nonc(1,i) = maxVal;
    val_range = maxVal-minVal;
    if(val_range == 0)
        Yscaled_nonc(:,i) = 0;
    else
        Yscaled_nonc(:,i) = (Ynonc(:,i) - minVal)/val_range;
    end

end

%-----
ncomp_trap_in = ncomp_in.Trap;
if ncomp_trap_in<=0;
    disp('Determining optimal number of PLS components for Traprock
model.')
```

ncomp\_trap = 25;

```

    % Find PLS regression for maximum number of ncomp
    [~,~,~,~,~,PCTVAR] = plsregress(Xcarb,Ycarb,ncomp_trap);
    pctvar_count = 0;
    PCTVAR = 100*PCTVAR;
    % Set ncomp to max number that explains >1% of variation
    % Stop searching if two components in a row are found to explain
    % less than 1%.
    for i = 1:ncomp_trap
        if (PCTVAR(2,i) >= 1)
            pctvar_count = pctvar_count + 1;
        else
            break;
        end
    end
    ncomp_trap = i - 1;
    disp(['Number of Traprock PLS Model components automatically set to
', num2str(ncomp_trap), '.']);
else
    ncomp_trap = ncomp_trap_in;
end

% Perform Y scaling for Traprocks
minmax_trap = zeros(2, numCol);
for i = 1:numCol

    maxVal = max(Ytrap(:,i));
    minVal = min(Ytrap(:,i));
    minmax_trap(2,i) = minVal;
    minmax_trap(1,i) = maxVal;
    val_range = maxVal-minVal;
    if(val_range == 0)
        Yscaled_trap(:,i) = 0;
    end
end

```

```

        else
            Yscaled_trap(:,i) = (Ytrap(:,i) - minVal)/val_range;
        end
    end

end

waitbar(8/10,w);

% PLS REGRESSION Trap
disp('Generating Trap Rock PLS Model.')
[~,~,~,~,betamat,PCTVAR] = plsregress(Xtrap,Yscaled_trap,ncomp_trap);

% Creates a structure with all of the PLS Model variables to be saved as
a
% .mat file.
PLS_Model_trap = struct('Date', date, 'PercentVariation', PCTVAR, 'Beta',
betamat, 'MinMax', minmax_trap);
PLS_Model_trap.NComp = ncomp_trap;

% PLS REGRESSION CARB
disp('Generating Carbonate Rock PLS Model.')
[~,~,~,~,betamat,PCTVAR] = plsregress(Xcarb,Yscaled_carb,ncomp_carb);

% Creates a structure with all of the PLS Model variables to be saved as
a
% .mat file.
PLS_Model_carb = struct('Date', date, 'PercentVariation', PCTVAR, 'Beta',
betamat, 'MinMax', minmax_carb);
PLS_Model_carb.NComp = ncomp_carb;

% PLS REGRESSION NONC
disp('Generating Non-Carbonate Rock PLS Model.')
[~,~,~,~,betamat,PCTVAR] = plsregress(Xnonc,Yscaled_nonc,ncomp_nonc);

% Creates a structure with all of the PLS Model variables to be saved as
a
% .mat file.
PLS_Model_nonc = struct('Date', date, 'PercentVariation', PCTVAR, 'Beta',
betamat, 'MinMax', minmax_nonc);
PLS_Model_nonc.NComp = ncomp_nonc;

waitbar(8.5/10,w);

% Create PLS structure that contains PLS models for base, carbonate,
% and noncarbonate all together and save. This is the file the user
% should load when testing the system as it contains all of the
% necessary PLS models.
PLS_Model_All = struct('Base', PLS_Model_base, 'Carbonate',
PLS_Model_carb, 'NonCarbonate', PLS_Model_nonc, 'Trap', PLS_Model_trap);
save_dir = check_create_dir('LAT Results\Training Data - PLS
Models',settingsSave_dir,3);
save([save_dir, '\PLS-Model-All-', TStamp, '.mat'], 'PLS_Model_All');

```



```

waitbar(10/10,w);
disp(['PLS Model saved to ', settingsSave_dir, '\LAT Results\Training Data
- PLS Models'])
disp('Model calibration complete.')
delete(w)
waitfor(msgbox(['PLS Model saved to ', settingsSave_dir, '\LAT
Results\Training Data - PLS Models'], 'Model Calibration Complete'))
end
%% TESTING MODE %%
close all;
if(strcmp(mode, 'test') || (strcmp(mode, 'testset')))
    w = waitbar(0, 'Processing testing data...', 'Name', 'Please Wait...');
    try
        frames = java.awt.Frame.getFrames();
        frames(end).setAlwaysOnTop(1);
    catch
    end
    setdata = rock_data;
    sampnum = numel(setdata);
    save_dir = check_create_dir('LAT Results\Testing Data -
Analysis', settingsSave_dir, 3);
    means=cell(sampnum+1, 25);
    chem = {'SiO2' 'Al2O3' 'Fe2O3' 'CaO' 'MgO' 'Na2O' 'P2O5' 'TiO2' 'K2O'
'MnO' 'BaO' 'SO3' 'SrO' 'CuO' 'ZrO2' 'ZnO' 'Y2O3' 'Rb2O' 'Ga2O3' 'Cl' 'Cr2O3'
'NiO' 'CeO2' 'Nb2O5'};
    means(1, 2:25)=chem;
    stddev=means;
    resultsFigure = figure('WindowStyle', 'normal', 'NumberTitle', 'Off');
    if(sampnum == 1)
        set(resultsFigure, 'Name', ['Single Test: ' resultsFigName '
Results']);
    else
        set(resultsFigure, 'Name', ['Set Test: ' resultsFigName ' Results']);
    end
    resultsTabGroup = uitabgroup(resultsFigure);
    resultsTabArray = [];
    for c = 1:sampnum
        waitbar((1/15+14/15*(c/sampnum)), w)
        rock_data = setdata{c};
        % LOAD BETA MATRIX
        dir = pwd;
        disp([setdata{c}, ':'])
        disp('Loading PLS model.')
        if(ischar(PLS))
            load(PLS);
        end
        betamat = PLS_Model_All.Base.Beta;

        % Obtain name of rock from rock_data filename.
        rock_type = rock_data(1:length(rock_data)-4);

        if(ischar(rock_data))
            disp('Loading X Data.')
            rock_data = load([settingsSave_dir '\LAT Results\Testing Data -
Conversion to mat\' TStamp '\' rock_data]);
            X = rock_data.test_rock_data;

```

```

end

% Preprocessing stage
% Should use the same techniques as in training.

[m,n]=size(X);
% Center Clipping
for i=1:m
    for j=1:n
        if X(i,j)<0
            X(i,j)=0;
        end
    end
end

% Normalizing Data to Total Light Emission
disp('Normalizing spectra to total light emission.')

% Initializing total light intensity.

    total_light_int = zeros(1,m);

for i=1:m
    for j=1:n
        total_light_int(i) = total_light_int(i) + X(i,j);
    end
end

% Initialize Xnorm
Xnorm = zeros(m,n);
for i=1:m
    for j=1:n
        Xnorm(i,j) = X(i,j)/total_light_int(i);
    end
end

% MAKE INITIAL PREDICTION
Ypredicted = [ones(size(Xnorm,1),1) Xnorm]*betamat;

% Obtain beta and minmax from carbonate or non-carbonate models based
% on carbonate threshold. Beta is used for prediction, minmax is used
% for reverse Y scaling.

% Edit: Reverse Y scaling has been changed back to just using the
Base
% min_max values rather than split based on Carbonate content.
min_max = PLS_Model_All.Base.MinMax;

numCol = size(Ypredicted,2);
for i = 1:numCol
    val_range = min_max(1,i)-min_max(2,i);
    Ypredicted(:,i) = (Ypredicted(:,i)*val_range) + min_max(2,i);

```

```

end

% Use prediction matrix to determine whether the rock is carbonate,
% non-carbonate, or trap, and then make another prediction using the
% corresponding PLS Model.

% Ratio for classification
threshratio =
mean((Ypredicted(:,1)./abs(Ypredicted(:,4))).^2.*abs(Ypredicted(:,3)));
disp(num2str(threshratio))
if (thresholds == [-1,-1])
    carbthresh=150;
    noncarbthresh=500;
else
    carbthresh=thresholds(1);
    noncarbthresh=thresholds(2);
end

if(threshratio <= carbthresh)
    betamat = PLS_Model_All.Carbonate.Beta;
    min_max = PLS_Model_All.Carbonate.MinMax;
    disp('Classified as Carbonate')
elseif (threshratio<=noncarbthresh)
    betamat = PLS_Model_All.Trap.Beta;
    min_max = PLS_Model_All.Trap.MinMax;
    disp('Classified as Trap')
else
    betamat = PLS_Model_All.NonCarbonate.Beta;
    min_max = PLS_Model_All.NonCarbonate.MinMax;
    disp('Classified as Non-Carbonate')
end

% Make new prediction based on split training decision.
Ypredicted = [ones(size(Xnorm, 1), 1) Xnorm] * betamat;

% Perform reverse Y scaling on predicted matrix.
numCol = size(Ypredicted,2);
for i = 1:numCol

    val_range = min_max(1,i)-min_max(2,i);
    %if(range == 0)
    %    Ypredicted(:,i) = 0;
    %else
    Ypredicted(:,i) = (Ypredicted(:,i)*val_range) + min_max(2,i);
    %end
    YpredLength = length(Ypredicted(:,i));
    for j=1:YpredLength
        if Ypredicted(j,i)<0
            Ypredicted(j,i)=0;
        end
    end
end

end

% MEAN AND STD. DEV. CALCULATIONS
% Initialize mean and std. dev. variables

```

```

Ymean = zeros(1,size(Ypredicted,2));
Ystd = zeros(1,size(Ypredicted,2));
Ymode = zeros(1,size(Ypredicted,2));
Ymedian = zeros(1,size(Ypredicted,2));

% Calculate mean and std. dev. for each column.
for i = 1:size(Ypredicted,2)
    Ymean(i) = mean(Ypredicted(:,i));
    Ystd(i) = std(Ypredicted(:,i));
    Ymedian(i) = median(Ypredicted(:,i));
end

% DISPLAY RESULTS IN FORMATTED TABLE
resultsTabArray(c) = uitab(resultsTabGroup, 'Title', rock_type);
Ymstd = cat(1,Ymean,Ystd,Ymedian);
t = uitable('Parent', resultsTabArray(c), 'Data', Ypredicted,
'ColumnName', chem);
set(t, 'Position', [0 80 560 315])
h = uitable('Parent', resultsTabArray(c), 'Data', Ymstd,
'ColumnName', chem, 'RowName', {'Mean', 'Std.', 'Median'});
set(h, 'Position', [0 0 560 80])
%data extraction for excel
rockname=setdata{c};
means(c+1,1)= {rockname(1:end-4)};
stddev(c+1,1)= {rockname(1:end-4)};

means(c+1,2:25)= num2cell(Ymean);
stddev(c+1,2:25)= num2cell(Ystd);

% COMPILE RESULTS STRUCTURE
Gap{1,24} = [];
lGap{1,1} = [];
ExcelRockSum{c} =
[chem;num2cell(Ypredicted);Gap;num2cell(Ymean);num2cell(Ystd)];
ERScol = size(ExcelRockSum{c},1) - 3;
ExcelRockSumLabels = {}
for lblC = 2:ERScol
    ExcelRockSumLabels{lblC,1} = ['Sample ' num2str(lblC-1)];
end
ExcelRockSumLabels = [ExcelRockSumLabels;lGap;'Mean';'Std.'];
ExcelRockSum{c} = [ExcelRockSumLabels ExcelRockSum{c}];
end
delete(w)
if exist('actxserver','file')
    w2 = waitbar(0,'Exporting to Excel...','Name','Please Wait...');
    try
        frames = java.awt.Frame.getFrames();
        frames(end).setAlwaysOnTop(1);
    catch
    end
    if(strcmp(mode,'test'))
        ExcelName = 'Single Test';
    elseif(strcmp(mode,'testset'))
        ExcelName = 'Testing Set';
    end
end

```

```

        cd(save_dir)
        warning('off','MATLAB:xlswrite:AddSheet')
        xlswrite([ExcelName ' Results Summary ' TStamp '.xls'],means,'Mean
Values')
        xlswrite([ExcelName ' Results Summary ' TStamp
'.xls'],stddev,'Standard Deviations')
        waitbar(3/10,w2)
        for xw = 1:length(ExcelRockSum)
            xlswrite([ExcelName ' Results Summary ' TStamp
'.xls'],ExcelRockSum{xw},setdata{xw}(1:end-4))
            waitbar((3/10)+ (6/10)*(xw/length(ExcelRockSum)),w2)
        end
        disp(['Prediction report spreadsheet saved to ', save_dir])
        fprintf('\n')
        objExcel = actxserver('Excel.Application');

        objExcel.Workbooks.Open(fullfile(cd,[ExcelName ' Results Summary '
TStamp '.xls']))); % Full path is necessary!
        try
            objExcel.ActiveWorkbook.Worksheets.Item(1).Delete;
        catch
        end

        try
            for cc = 1:length(ExcelRockSum)+2

invoke(objExcel.ActiveWorkbook.Worksheets.Item(length(ExcelRockSum)-cc+1),
'Activate')
                objExcel.Cells.Select;
                objExcel.Selection.Columns.AutoFit;
            end
        catch
        end

        % Save, close and clean up.
        objExcel.ActiveWorkbook.Save;
        objExcel.ActiveWorkbook.Close;
        waitbar(1,w2)
        objExcel.Quit;
        objExcel.delete;
        msgbox(['An Excel spreadsheet containing a summary of this test has
been saved in:' save_dir])
    else
        warning('ActiveX process could not be created, excel summary not
saved ')
    end
    cd(dir);
    delete(w2)
end

```